

EFFECTS OF ELECTRODEPOSITION PARAMETERS ON ZN-TIO<sub>2</sub> COATING FOR ZINC-ION  
BATTERY



A Thesis Submitted in Partial Fulfillment of the Requirements  
for the Degree of Master of Engineering in Metallurgical and Materials Engineering  
Department of Metallurgical Engineering  
FACULTY OF ENGINEERING  
Chulalongkorn University  
Academic Year 2019  
Copyright of Chulalongkorn University

ผลของตัวแปรในกระบวนการชุบด้วยไฟฟ้าต่อชั้นเคลือบ สังกะสี-ไทเทเนียมไดออกไซด์ สำหรับ  
แบตเตอรี่ชนิดซิงก์ไอออน



วิทยานิพนธ์นี้เป็นส่วนหนึ่งของการศึกษาตามหลักสูตรปริญญาวิศวกรรมศาสตรมหาบัณฑิต  
สาขาวิชาวิศวกรรมโลหการและวัสดุ ภาควิชาวิศวกรรมโลหการ  
คณะวิศวกรรมศาสตร์ จุฬาลงกรณ์มหาวิทยาลัย  
ปีการศึกษา 2562  
ลิขสิทธิ์ของจุฬาลงกรณ์มหาวิทยาลัย



กิตติมา โลลูพิมาน : ผลของตัวแปรในกระบวนการชุบด้วยไฟฟ้าต่อชั้นเคลือบ สังกะสี-ไทเทเนียมไดออกไซด์ สำหรับแบตเตอรี่ชนิดซิงก์ไอออน. ( EFFECTS OF ELECTRODEPOSITION PARAMETERS ON ZN-TIO<sub>2</sub> COATING FOR ZINC-ION BATTERY) อ.ที่ปรึกษาหลัก : ผศ. ดร.ปัญญาวัชร ว่างยาว, อ.ที่ปรึกษาร่วม : ดร.เจียเขียน ฉิน

ในปัจจุบันนักวิจัยหันมาให้ความสนใจเกี่ยวกับแบตเตอรี่ชนิดซิงก์ไอออนกันมากขึ้น เนื่องจากแบตเตอรี่ชนิดนี้มีสมบัติที่ดีในหลายด้าน เช่น การเป็นมิตรกับสิ่งแวดล้อมและมีต้นทุนในการผลิตที่ต่ำ อย่างไรก็ตาม แบตเตอรี่ชนิดนี้ก็ยังคงมีข้อเสียในเรื่องของ การเจริญเติบโตของเดนไดรท์ที่ขั้วของสังกะสีระหว่างการใช้งานไปได้ระยะหนึ่ง ดังจึงเป็นข้อจำกัดของขั้วสังกะสี ที่ไม่สามารถใช้งานได้ในระยะยาวดังเช่นแบตเตอรี่ชนิดอื่นๆ ดังนั้นในงานวิจัยนี้ได้เสนอกระบวนการชุบด้วยไฟฟ้า ที่ได้มีการเติมอนุภาคไทเทเนียมไดออกไซด์ ลงบนชั้นผิวเคลือบของสังกะสี เพื่อให้ได้วัสดุผสมสังกะสี/ไทเทเนียมไดออกไซด์ เพื่อใช้เป็นขั้วบวกในแบตเตอรี่ชนิดซิงก์ไอออน โดยทำการชุบด้วยชั้นเคลือบสังกะสีผสมไทเทเนียมไดออกไซด์ ลงบนสแตนเลสพอลย์ และนำไปใช้เป็นขั้วบวก จากนั้นทำการประกอบแบตเตอรี่ เพื่อทำการทดสอบประสิทธิภาพของขั้วสังกะสี พบว่า การรวมกลุ่มของอนุภาคไทเทเนียมไดออกไซด์ บนชั้นเคลือบสังกะสี ส่งผลให้ค่าความต่างศักย์ไฟฟ้าในระหว่างทำการทดสอบ plating and stripping นั้นลดลง และทำให้ค่าความจุจำเพาะของแบตเตอรี่เพิ่มสูงขึ้น อีกทั้งยังมีอายุการงานที่นานมากกว่าขั้วสังกะสีที่ไม่มีอนุภาคไทเทเนียมไดออกไซด์ผสมอยู่นอกจากนี้ยังได้ทำการสังเคราะห์ แมงกานีสไดออกไซด์ ซึ่งใช้เป็นขั้วลบ ด้วยวิธีไฮโดรเทอร์มอล และทำการทดสอบประสิทธิภาพของแบตเตอรี่ โดยการจำลองการใช้งาน ผลปรากฏว่าค่าความจุจำเพาะของแบตเตอรี่เพิ่มสูงขึ้น อีกทั้งยังมีอายุการงานที่ยาวนานกว่าขั้วสังกะสีที่ไม่มีอนุภาคไทเทเนียมไดออกไซด์ผสมอยู่

สาขาวิชา	วิศวกรรมโลหการและวัสดุ	ลายมือชื่อนิสิต .....
ปีการศึกษา	2562	ลายมือชื่อ อ.ที่ปรึกษาหลัก .....
		ลายมือชื่อ อ.ที่ปรึกษาร่วม .....

# # 6070126621 : MAJOR METALLURGICAL AND MATERIALS ENGINEERING

KEYWORD: Zn-ion battery, Zn anode, Zn electrodeposition, electrodeposition, plating-stripping, specific capacity, cycle ability, Titanium dioxide nanoparticle

Kittima Lolupiman : EFFECTS OF ELECTRODEPOSITION PARAMETERS ON ZN-TiO<sub>2</sub> COATING FOR ZINC-ION BATTERY. Advisor: Asst. Prof. PANYAWAT WANGYAO, Ph.D. Co-advisor: Dr. JIAQIAN QIN, Ph.D.

This research work has an aim to modify and develop to obtain environmentally friendly Zinc ion battery (ZIB) with low cost. Usually, the limit of Zn ion battery is occurred by dendrite growth during cycling of Zn anode leading to shorter service lifetime. Therefore, in this present work had an idea to modify electrodeposition process by adding TiO<sub>2</sub> nano particles into coated Zn layers. This composite deposits were used as the anode materials of ZIBs. The only Zn and Zn/TiO<sub>2</sub> composite coatings were deposited on the stainless-steel foil as modified anodes. The plating and stripping tests of symmetric cells reveal that the agglomeration of TiO<sub>2</sub> with Zn coatings would reduce the overpotential curves between plating and stripping processes. The galvanostatic charge-discharge tests reveal that the modified Zn/TiO<sub>2</sub>//MnO<sub>2</sub> batteries exhibit higher rate ability and longer service lifetime than those of Zn//MnO<sub>2</sub> batteries. Furthermore, increasing both current density and concentration of TiO<sub>2</sub> in the electrolyte during electroplating results in more proper morphology of composite deposit of zinc electrode, which provides higher performances and longer lifetime of battery.

Field of Study: Metallurgical and Materials Engineering Student's Signature .....

Academic Year: 2019

Advisor's Signature .....

Co-advisor's Signature .....

## ACKNOWLEDGEMENTS

First and foremost, I would like to express my deepest gratitude to my thesis advisor Assistant Professor Dr. Panyawat Wangyao and Co-Advisor, Dr. Jiaqian Qin for their continuous support and guidance. Both advisors motivate, encourage and steer me in the right direction whenever I had problems during my study.

I am grateful to my thesis committee Professor Dr. Gobboon Lothongkum, Associate Professor Dr. Seksak Asavavisithchai and Assistant Professor Dr. Tanaporn Rojhirunsakool for valuable advice and comments.

I would also like to thank my colleagues from the Energy Storage lab at MMRI, CU and all my friends for their support and suggestions.

I would like to acknowledge the financial support from the Energy Conservation Promotion Fund from and the Energy Policy and Planning Office, Ministry of Energy, and TRF-IRN Program granted to the International Research Network on Electroplating Technology (IRN61W0002) and Thailand Research Fund (RSA6080017).

Kittima Lolupiman

## TABLE OF CONTENTS

	Page
ABSTRACT (THAI) .....	iii
ABSTRACT (ENGLISH) .....	iv
ACKNOWLEDGEMENTS .....	v
TABLE OF CONTENTS .....	vi
LIST OF TABLES .....	x
LIST OF FIGURES .....	xii
Chapter 1 Introduction .....	1
1.1 Background .....	1
1.2 Objectives .....	3
1.3 Scopes .....	3
Chapter 2 Literature Review .....	4
2.1 Energy Storage Technology .....	4
2.2 Battery Technology .....	5
2.2.1 Primary Battery .....	5
2.2.2 Secondary Battery .....	6
2.3 Zinc ion batteries (ZIBs) .....	6
2.3.1 Charge-Storage Mechanism .....	8
2.3.2 Electrolyte for Zinc Ion Batteries (ZIBs) .....	9
2.3.3 Cathode Materials .....	9
2.3.4 Anode for Zinc Ion Batteries .....	10
Chapter 3 Experimental Procedures .....	17

3.1 Battery Components.....	17
3.1.1 Anode.....	17
3.1.1.1 Preparation of Zn-TiO <sub>2</sub> composite.....	17
3.1.1.2 TiO <sub>2</sub> powder.....	17
3.1.2 Cathode.....	19
3.1.3 Separator.....	19
3.1.4 Electrolyte.....	19
3.2 A Coin Cell Assembly (CR2032).....	19
3.3 Characterization.....	20
3.3.1 Scanning electron microscope with energy dispersive spectroscopy.....	20
(SEM-EDS).....	20
3.3.2 X-ray Powder Diffraction (XRD).....	20
3.3.3 LAND battery.....	20
3.3.4 Potentiostatic.....	20
Chapter 4 Results and Discussions.....	22
4.1 Microstructure Characterization.....	22
4.1.1 Morphology and microstructure.....	22
4.1.1.1 The Zn without TiO <sub>2</sub> .....	22
4.1.1.2 The Zn electrodeposition with TiO <sub>2</sub> 1 g/L.....	25
4.1.1.3 The Zn electrodeposition with TiO <sub>2</sub> 3 g/L.....	29
4.1.1.4 The Zn electrodeposition with TiO <sub>2</sub> 5 g/L.....	32
4.1.1.5 The Zn electrodeposition with TiO <sub>2</sub> 10 g/L.....	36
4.2 Zn Plating and Stripping.....	40
4.2.1 The Zn without TiO <sub>2</sub> .....	41



4.2.2 The Zn with TiO <sub>2</sub> 1g/L.....	42
4.2.3 The Zn with TiO <sub>2</sub> 3g/L.....	43
4.2.4 The Zn with TiO <sub>2</sub> 5g/L.....	44
4.2.4 The Zn with TiO <sub>2</sub> 10g/L.....	45
4.3 Potentiostat.....	46
4.3.1 Potentiostat (Cyclic voltammetry, CV).....	46
4.3.1.1 The Zn without TiO <sub>2</sub> .....	46
4.3.1.2 The Zn with TiO <sub>2</sub> 10 g/L.....	47
4.3.2 Potentiostatic (The electrochemical impedance spectroscopy, EIS).....	48
4.4 Battery performance (Rate ability).....	49
4.4.1 The Zn without TiO <sub>2</sub> .....	49
4.4.2 The Zn with TiO <sub>2</sub> 1 g/L.....	54
4.4.3 The Zn with TiO <sub>2</sub> 3 g/L.....	59
4.4.4 The Zn with TiO <sub>2</sub> 5 g/L.....	64
4.4.5 The Zn with TiO <sub>2</sub> 10 g/L.....	69
4.5 Battery performance (cyclic ability).....	74
4.5.1 The Zn without TiO <sub>2</sub> .....	74
4.5.2 The Zn with TiO <sub>2</sub> 1 g/L.....	75
4.5.3 The Zn with TiO <sub>2</sub> 3 g/L.....	76
4.5.4 The Zn with TiO <sub>2</sub> 5 g/L.....	77
4.5.5 The Zn with TiO <sub>2</sub> 10 g/L.....	78
4.6 Microstructure Characterization after battery performance testing.....	79
4.6.1 Morphology and microstructure of Zn without TiO <sub>2</sub> .....	79
4.6.2 Morphology and microstructure of Zn with TiO <sub>2</sub> 10 g/L.....	80

Chapter 5 Conclusions.....	81
5.1 Zn without TiO <sub>2</sub> .....	81
5.2 Zn with TiO <sub>2</sub> 1 g/L.....	83
5.3 Zn with TiO <sub>2</sub> 3 g/L.....	84
5.4 Zn with TiO <sub>2</sub> 5 g/L.....	86
5.5 Zn with TiO <sub>2</sub> 10 g/L.....	88
REFERENCES .....	90
VITA.....	93



## LIST OF TABLES

	Page
Table 1 Bath composition .....	14
Table 2 Experimental conditions .....	18
Table 3 Research Timeline .....	21
Table 4 Open circuit voltage of the Zn without TiO <sub>2</sub> .....	50
Table 5 The initial discharge specific capacity with current density at 50 mA/g of the Zn without TiO <sub>2</sub> .....	51
Table 6 The initial discharge specific capacity at various current densities of 50, 100, 200, 500, and 1000 mA/g of the Zn without TiO <sub>2</sub> .....	53
Table 7 Open circuit voltage of the Zn with TiO <sub>2</sub> 1 g/L .....	55
Table 8 The initial discharge specific capacity with current density at 50 mA/g of the Zn with TiO <sub>2</sub> 1 g/L .....	56
Table 9 The initial discharge specific capacity at various current densities of 50, 100, 200, 500, and 1000 mA/g of the Zn with TiO <sub>2</sub> 1 g/L.....	58
Table 10 Open circuit voltage of the Zn with TiO <sub>2</sub> 3 g/L .....	60
Table 11 The initial discharge specific capacity with current density at 50 mA/g of the Zn with TiO <sub>2</sub> 3 g/L.....	61
Table 12 The initial discharge specific capacity at various current densities of 50, 100, 200, 500, and 1000 mA/g of the Zn with TiO <sub>2</sub> 3 g/L.....	63
Table 13 Open circuit voltage of the Zn with TiO <sub>2</sub> 5 g/L .....	65
Table 14 The initial discharge specific capacity with current density at 50 mA/g of the Zn with TiO <sub>2</sub> 5 g/L.....	66
Table 15 The initial discharge specific capacity at various current densities of 50, 100, 200, 500, and 1000 mA/g of the Zn with TiO <sub>2</sub> 5 g/L.....	68

Table 16	Open circuit voltage of the Zn with TiO <sub>2</sub> 10 g/L.....	70
Table 17	The initial discharge specific capacity with current density at 50 mA/g of the Zn with TiO <sub>2</sub> 10 g/L.....	71
Table 18	The initial discharge specific capacity at various current densities of 50, 100, 200, 500, and 1000 mA/g of the Zn with TiO <sub>2</sub> 10 g/L.....	73
Table 19	Morphology of Zn without TiO <sub>2</sub> .....	81
Table 20	The battery performances of the Zn without TiO <sub>2</sub> (1).....	82
Table 21	The battery performances of the Zn without TiO <sub>2</sub> (2).....	82
Table 22	Morphology of Zn with TiO <sub>2</sub> 1 g/L.....	83
Table 23	The battery performances of the Zn with TiO <sub>2</sub> 1 g/L (1).....	83
Table 24	The battery performances of the Zn with TiO <sub>2</sub> 1 g/L (2).....	84
Table 25	Morphology of Zn with TiO <sub>2</sub> 3 g/L.....	84
Table 26	The battery performances of the Zn with TiO <sub>2</sub> 3 g/L (1).....	85
Table 27	The battery performances of the Zn with TiO <sub>2</sub> 3 g/L (2).....	85
Table 28	Morphology of Zn with TiO <sub>2</sub> 5 g/L.....	86
Table 29	The battery performances of the Zn with TiO <sub>2</sub> 5 g/L (1).....	87
Table 30	The battery performances of the Zn with TiO <sub>2</sub> 5 g/L (2).....	87
Table 31	Morphology of Zn with TiO <sub>2</sub> 10 g/L.....	88
Table 32	The battery performances of the Zn with TiO <sub>2</sub> 10 g/L (1).....	89
Table 33	The battery performances of the Zn with TiO <sub>2</sub> 10 g/L (2).....	89

## LIST OF FIGURES

	Page
Figure 1 Operating voltage versus specific capacity for Zn anode .....	2
Figure 2 Types of energy storage system.....	4
Figure 3 (left) Cross section of a zinc-carbon dry cell and (right) Alkaline batteries.....	5
Figure 4 The Zinc ion batteries (ZIBs) parts .....	7
Figure 5 Schematic illustrate the charge-transfer mechanism of zinc ion battery.....	8
Figure 6 Schematics of zinc ion battery [15] .....	9
Figure 7 Electrodeposition setup .....	10
Figure 8 FESEM images of (a) Zn plate, (b) Cu plate, and Zn deposits at different current densities .....	11
Figure 9 SEM images of synthesized anode with and without organic additives and commercialized zinc.....	12
Figure 10 SEM image of the surface (a) Zn-TiO <sub>2</sub> 3 g/L, (b) 5 g/L, (c) 10 g/L, and (d) Degussa .....	13
Figure 11 SEM micrographs of the surface of Zn after 48 h immersion in 0.2 g/L (NH <sub>4</sub> ) <sub>2</sub> SO <sub>4</sub> .....	13
Figure 12 SEM micrographs of the surface of Zn-TiO <sub>2</sub> films from different baths.....	14
Figure 13 Layer thicknesses of electrodeposited layers .....	15
Figure 14 SEM images of surfaces after anodic polarization A) pure zinc coating.....	15
Figure 15 TiO <sub>2</sub> nano-powder (P25, Degussa TiO <sub>2</sub> ).....	17
Figure 16 A Coin Cell Assembly (CR2032) .....	19
Figure 17 The Zn electrodeposition without TiO <sub>2</sub> at current density of 0.01 A/cm <sup>2</sup> ..	22
Figure 18 The Zn electrodeposition without TiO <sub>2</sub> at current density of 0.02 A/cm <sup>2</sup> ..	23

Figure 19 The Zn electrodeposition without TiO <sub>2</sub> at current density of 0.03 A/cm <sup>2</sup> ..	23
Figure 20 The Zn electrodeposition without TiO <sub>2</sub> at current density of 0.04 A/cm <sup>2</sup> ..	23
Figure 21 EDS representative spectra of Zn without TiO <sub>2</sub> at current density 0.01 A/cm <sup>2</sup> .....	24
Figure 22 The wt% of Zn and O at different current densities .....	25
Figure 23 The Zn electrodeposition with TiO <sub>2</sub> 1 g/L at current density of 0.01 A/cm <sup>2</sup> .....	26
Figure 24 The Zn electrodeposition with TiO <sub>2</sub> 1 g/L at current density of 0.02 A/cm <sup>2</sup> .....	26
Figure 25 The Zn electrodeposition with TiO <sub>2</sub> 1 g/L at current density of 0.03 A/cm <sup>2</sup> .....	27
Figure 26 The Zn electrodeposition with TiO <sub>2</sub> 1 g/L at current density of 0.04 A/cm <sup>2</sup> .....	27
Figure 27 EDS representative spectra of Zn with TiO <sub>2</sub> 1 g/L at current density of 0.01 A/cm <sup>2</sup> .....	28
Figure 28 The wt% of Zn, O, and TiO <sub>2</sub> at different current densities.....	28
Figure 29 The Zn electrodeposition with TiO <sub>2</sub> 3 g/L at current density of 0.01 A/cm <sup>2</sup> .....	30
Figure 30 The Zn electrodeposition with TiO <sub>2</sub> 3 g/L at current density of 0.02 A/cm <sup>2</sup> .....	30
Figure 31 The Zn electrodeposition with TiO <sub>2</sub> 3 g/L at current density of 0.03 A/cm <sup>2</sup> .....	30
Figure 32 The Zn electrodeposition with TiO <sub>2</sub> 3 g/L at current density of 0.04 A/cm <sup>2</sup> .....	31
Figure 33 EDS representative spectra of Zn with TiO <sub>2</sub> 3 g/L at current density of 0.01 A/cm <sup>2</sup> .....	31

Figure 34 The wt% of Zn, O, and TiO <sub>2</sub> at different current densities.....	32
Figure 35 The Zn electrodeposition with TiO <sub>2</sub> 5 g/L at current density of 0.01 A/cm <sup>2</sup> .....	33
Figure 36 The Zn electrodeposition with TiO <sub>2</sub> 5 g/L at current density of 0.02 A/cm <sup>2</sup> .....	33
Figure 37 The Zn electrodeposition with TiO <sub>2</sub> 5 g/L at current density of 0.03 A/cm <sup>2</sup> .....	34
Figure 38 The Zn electrodeposition with TiO <sub>2</sub> 5 g/L at current density of 0.04 A/cm <sup>2</sup> .....	34
Figure 39 EDS representative spectra of Zn with TiO <sub>2</sub> 5 g/L at current density of 0.01 A/cm <sup>2</sup> .....	35
Figure 40 The wt% of Zn, O, and TiO <sub>2</sub> at different current densities.....	36
Figure 41 The Zn electrodeposition with TiO <sub>2</sub> 10 g/L at current density of 0.01 A/cm <sup>2</sup> .....	37
Figure 42 The Zn electrodeposition with TiO <sub>2</sub> 10 g/L at current density of 0.02 A/cm <sup>2</sup> .....	37
Figure 43 The Zn electrodeposition with TiO <sub>2</sub> 10 g/L at current density of 0.03 A/cm <sup>2</sup> .....	37
Figure 44 The Zn electrodeposition with TiO <sub>2</sub> 10 g/L at current density of 0.04 A/cm <sup>2</sup> .....	38
Figure 45 EDS representative spectra of Zn with TiO <sub>2</sub> 10 g/L at current density of 0.01 A/cm <sup>2</sup> .....	38
Figure 46 The wt% of Zn, O, and TiO <sub>2</sub> at different current densities.....	39
Figure 47 Polarization voltage during cycle of samples Zn without TiO <sub>2</sub> at different current densities a) 0.01 b) 0.02, c) 0.03, and d) 0.04 A/cm <sup>2</sup> .....	41
Figure 48 Polarization voltage during cycle of samples Zn with TiO <sub>2</sub> 1g/L at different current densities a) 0.01 b) 0.02, c) 0.03, and d) 0.04 A/cm <sup>2</sup> .....	42

Figure 49 Polarization voltage during cycle of samples Zn with TiO <sub>2</sub> 3g/L at different current densities a) 0.01 b) 0.02, c) 0.03, and d) 0.04 A/cm <sup>2</sup> .....	43
Figure 50 Polarization voltage during cycle of samples Zn with TiO <sub>2</sub> 5g/L at different current densities a) 0.01 b) 0.02, c) 0.03, and d) 0.04 A/cm <sup>2</sup> .....	44
Figure 51 Polarization voltage during cycle of samples Zn with TiO <sub>2</sub> 10g/L at different current densities a) 0.01 b) 0.02, c) 0.03, and d) 0.04 A/cm <sup>2</sup> .....	45
Figure 52 Cyclic voltammetry of Zn without TiO <sub>2</sub> at all current densities .....	46
Figure 53 Cyclic voltammetry of Zn with TiO <sub>2</sub> 10g/L at all current densities .....	47
Figure 54 EIS of the Zn without TiO <sub>2</sub> .....	48
Figure 55 EIS of the Zn with TiO <sub>2</sub> 10 g/L.....	48
Figure 56 Rate ability of the Zn without TiO <sub>2</sub> at different current densities .....	49
Figure 57 Charge-discharge profiles at 50 mA/g in 1 <sup>st</sup> -5 <sup>th</sup> cycles of the Zn without TiO <sub>2</sub> at different current densities.....	50
Figure 58 Charge-discharge profiles at various current densities of 50, 100, 200, 500, and 1000 mA/g of the Zn without TiO <sub>2</sub> at different current densities.....	52
Figure 59 Rate ability of the Zn with TiO <sub>2</sub> 1 g/L at different current densities.....	54
Figure 60 Charge-discharge profiles at 50 mA/g in 1 <sup>st</sup> -5 <sup>th</sup> cycles of the Zn with TiO <sub>2</sub> 1 g/L at different current densities.....	55
Figure 61 Charge-discharge profiles at various current densities of 50, 100, 200, 500, and 1000 mA/g of the Zn with TiO <sub>2</sub> 1 g/L at different current densities.....	57
Figure 62 Rate ability of the Zn with TiO <sub>2</sub> 3 g/L at different current densities.....	59
Figure 63 Charge-discharge profiles at 50 mA/g in 1 <sup>st</sup> -5 <sup>th</sup> cycles of the Zn with TiO <sub>2</sub> 3 g/L at different current densities .....	60
Figure 64 Charge-discharge profiles at various current densities of 50, 100, 200, 500, and 1000 mA/g of the Zn with TiO <sub>2</sub> 3 g/L at different current densities.....	62
Figure 65 Rate ability of the Zn with TiO <sub>2</sub> 5 g/L at different current density.....	64



Figure 66 Charge-discharge profiles at 50 mA/g in 1 <sup>st</sup> -5 <sup>th</sup> cycles of the Zn with TiO <sub>2</sub> 5 g/L at different current densities .....	65
Figure 67 Charge-discharge profiles at various current densities of 50, 100, 200, 500, and 1000 mA/g of the Zn with TiO <sub>2</sub> 5 g/L at different current densities.....	67
Figure 68 Rate ability of the Zn with TiO <sub>2</sub> 10 g/L at different current densities.....	69
Figure 69 Charge-discharge profiles at 50 mA/g in 1 <sup>st</sup> -5 <sup>th</sup> cycles of the Zn with TiO <sub>2</sub> 10 g/L at different current densities.....	70
Figure 70 Charge-discharge profiles at various current densities of 50, 100, 200, 500, and 1000 mA/g of the Zn with TiO <sub>2</sub> 10 g/L at different current densities .....	72
Figure 71 Cyclic ability of the Zn without TiO <sub>2</sub> .....	74
Figure 72 Cyclic ability of the Zn with TiO <sub>2</sub> 1 g/L.....	75
Figure 73 Cyclic ability of the Zn with TiO <sub>2</sub> 3 g/L.....	76
Figure 74 Cyclic ability of the Zn with TiO <sub>2</sub> 5 g/L.....	77
Figure 75 Cyclic ability of the Zn with TiO <sub>2</sub> 10 g/L.....	78
Figure 76 The Zn electrode sample of Zn without TiO <sub>2</sub> .....	79
Figure 77 The Zn electrode sample of Zn with TiO <sub>2</sub> 10g/L.....	80

# Chapter 1

## Introduction

### 1.1 Background

Energy storage systems are used to store electricity from renewable resources, such as solar energy, water energy, wind energy, and biomass [1]. Energy storage technologies can greatly enhance the efficiency of electrical supply which leads to further progress in development of sustainable energy. Battery, one of the most popular types of electrical energy storage, is an essential component in various applications, such as portable electronic devices and electric vehicles [2, 3].

Battery can be classified into two different types, primary battery and secondary battery [4]. For primary battery, the electrochemical reaction cannot be reversed and so it cannot be recharged. The secondary battery uses electrochemical cells whose chemical reactions can be reversed and recharged. The charge and discharge process can be performed many times depending on the type of battery. Various types of rechargeable batteries are nickel-cadmium (Ni-Cd), nickel-metal hydride (Ni-MH), lead acid (LAB), lithium-ion batteries (LIBs), and zinc ion batteries (ZIBs).

Although many battery types are already commercial, they still have limitations. Lithium ion battery (LIBs), the most successful secondary battery technology up to date, is widely used for electrical energy storage due to its high energy density and long lifespan. However, in grid-scale electrochemical energy storage, lithium ion battery has many problems such as high cost, poisonous chemical and limited supplies of materials [5]. These lead to the development of battery technology which were able to reduce the mentioned disadvantage but also maintain or further improve the benefits of current Lithium ion battery.

Alternative battery has been developed recently. Zinc ion batteries (ZIBs) is a system which consists of zinc anode and an intercalation cathode in aqueous electrolytes. ZIBs has  $Zn^{2+}$  that is a multivalent in aqueous electrolytes.

Among various types of battery, the batteries that use zinc electrode are very interesting as zinc is abundant, non-toxic, stable, environmental friendly and

recyclable [3]. These can solve the limitation of LIBs. Zinc electrodes have good theoretical capacity, 820 mAh/g [6], suitable as LIBs alternative. It also has a unique good reversibility property, the plating and stripping cycle at anode, which should lead to longer lifespan [7]. However, zinc, from its metallurgical properties, always has a corrosion resistant problem. This will reduce the lifespan of ZIBs because there is an increasing chance of short circuit as dendrite grows on the surface of the electrode [8].

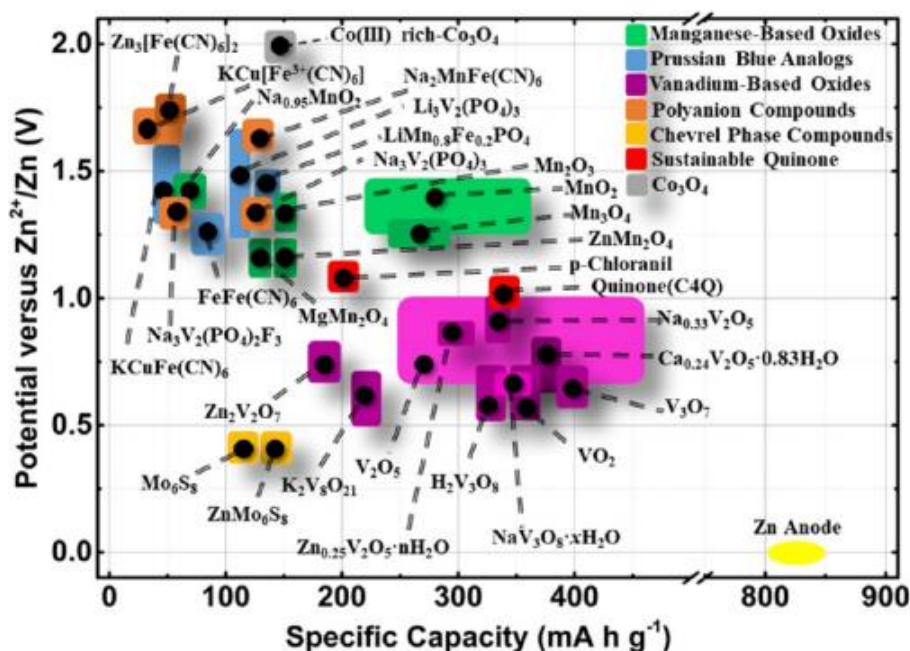


Figure 1 Operating voltage versus specific capacity for Zn anode and various cathode materials.

The studies of ZIBs emphasize on the development of new intercalation cathodes and anode. Figure 1 shown among various cathodes for ZIBs, manganese dioxide (MnO<sub>2</sub>) is one of the most promising cathodes for ZIBs because it has high theoretical specific capacity of 616 mAh/g [2].

Although manganese-based oxides are abundant, non-toxic and environment friendly, this does not solve the main problem of ZIBs, dendrite growth. In order to improve the lifespan of ZIBs, further improvement of anode must be done.

The recent work shows that synthesis of novel zinc anodes via electroplating mitigates issues of corrosion, dendrite growth, and hydrogen evolution [8].

In many cases, metal matrix composite coatings can be prepared by co-electrodepositing of microparticle and nanoparticle metal as secondary phase, such as  $\text{SiO}_2$ ,  $\text{AlO}_2$ ,  $\text{ZrO}_2$ , and  $\text{TiO}_2$  particles. The combination of zinc and secondary phase material will form a zinc protective layers with superior corrosion resistance property [9, 10]. Therefore, this research will synthesize zinc anodes via electrodeposition incorporation of titanium dioxide ( $\text{TiO}_2$ ) to mitigate issues of corrosion and dendrite formation, resulting in better battery performance of ZIBs.

## 1.2 Objectives

1.2.1 To prepare zinc with titanium dioxide ( $\text{TiO}_2$ ) particles for anode of zinc ion batteries via electrodeposition

1.2.2 To study the effect of electrodeposition parameters on the microstructure of zinc anode and battery performance.

## 1.3 Scopes

This research focuses on preparation of zinc anode via electrodeposition by adding titanium dioxide nanoparticle ( $\text{TiO}_2$ ) in zinc electroplating solution. The effect of concentration of titanium dioxide (0, 1, 3, 5, and 10 g/L), the current density (0.01, 0.02, 0.03, and 0.04  $\text{A}/\text{cm}^2$ ) and time (30 mins) were studied. The morphology and phase composition were analyzed by scanning electron microscope (SEM) and X-ray diffraction (XRD), respectively. The coin cell (CR2032) was assembled for electrochemical properties (The electrochemical impedance spectroscopy, EIS and cyclic voltammetry, CV) and battery performance (specific capacitance and cycle stability).

## Chapter 2

### Literature Review

#### 2.1 Energy Storage Technology

Energy storage systems are used to store various forms of energy. Energy storage works by capturing electricity produced from renewable and non-renewable sources such as solar power, wind power, and tidal power [2]. Grid energy storage or large-scale energy storage is a collection of methods used to store electrical energy on a large scale within an electrical power grid [6]. Energy storage methods may be classified into different groups as shown in Figure 2 [11].

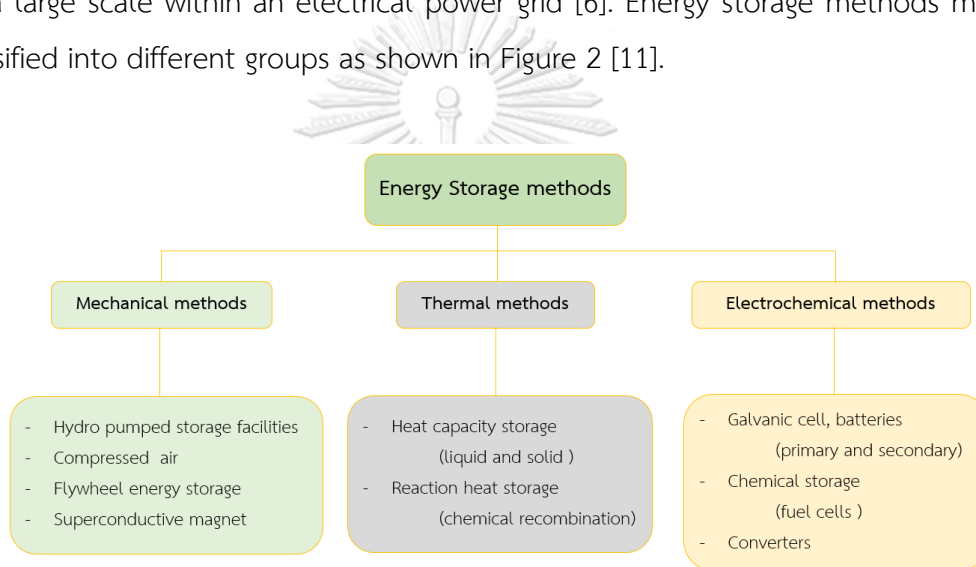


Figure 2 Types of energy storage system

Electrochemical energy storage devices, such as rechargeable batteries, are critical for overcoming the worldwide energy challenge because of their high energy density and long cycle life. Aqueous rechargeable batteries are a promising class of batteries for grid-scale electrochemical energy storage because of their low-cost, high operational safety, and environmental friendly [7].

## 2.2 Battery Technology

The battery technology is an alternative use for energy storage. Generally, batteries can be classified into different types.

### 2.2.1 Primary Battery

Primary battery is a battery that can be used once and cannot be recharged. The electrochemical reaction is irreversible. Chemical energy is converted into electrical energy when current is drawn from it [12]. In general, primary batteries always have high specific energy but low load current. Examples of primary battery are zinc-carbon batteries and alkaline batteries. The cross section of a zinc-carbon dry cell and alkaline batteries are shown in Figure 3.

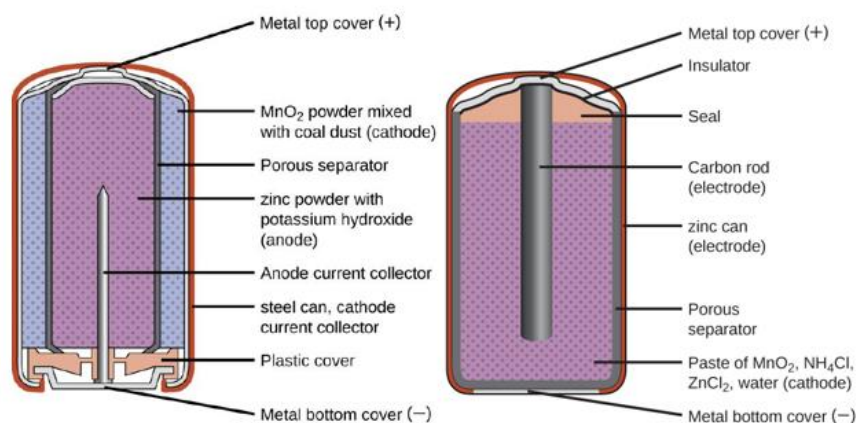


Figure 3 (left) Cross section of a zinc-carbon dry cell and (right) Alkaline batteries

The difference between zinc-carbon batteries and alkaline batteries is the electrolyte. Zinc-carbon batteries normally use ammonium chloride (NH<sub>4</sub>Cl) or zinc chloride (ZnCl<sub>2</sub>) while alkaline batteries use potassium hydroxide (KOH). The alkaline battery is preferred due to its high energy density and long lifespan. The disadvantage of primary battery devices is to low current usage.

### 2.2.2 Secondary Battery

Secondary battery is battery with electrochemical cells whose chemical reaction is reversible and rechargeable after the energy is used up. The cycle for charging and discharging process depends on the battery type. Secondary battery devices are used to power portable electronic devices such as smartphones and gadgets in electric vehicle. Although initial cost of acquiring rechargeable batteries is much higher than the primary batteries, they are the most long-term and cost-effectiveness.

Secondary battery can be further classified into several other types based on their chemistry. This is very important because the chemistries can affect to specific energy and cycle life. Examples of secondary battery are lead-acid battery, nickel-cadmium battery (Ni-Cd), nickel-metal hydride battery (Ni-MH) [4], and intercalation based batteries (monovalent metal-ion ( $\text{Li}^+$ ) and multivalent metal-ion ( $\text{Ca}^{2+}$ ,  $\text{Mg}^{2+}$ ,  $\text{Al}^{3+}$ , and  $\text{Zn}^{2+}$ )) [13]. In this work, the study of Zn-ion battery was focused.

Lithium-ion batteries (LIBs) are the most popular rechargeable batteries and used widely in electrical devices because then can provide a large amount current and long lifespan. However, there are some problems such as the safety concerns about flammable organic electrolytes, high cost and limited supplies of lithium [5].

New battery chemistry and design are required for rechargeable batteries with high capacity and fast charge/discharge capability as well as safety concerns and environmental friendliness.

### 2.3 Zinc ion batteries (ZIBs)

Zinc-ion batteries (ZIBs) with mild neutral pH (or slightly acidic) electrolyte are promising for grid-scale energy storage. Since Volta et al. employed metallic zinc (Zn) in the first battery in 1799, Zn anode has been regarded as an ideal negative electrode in various Zn-based batteries, such as Zn-Mn, Zn-air and Ni-Zn batteries because Zn has high capacity, relatively low redox potential, low cost, and high safety [2, 3, 6]. Although ZIBs has many advantages, problem like corrosion of zinc anode could occurred.

Metal corrosion contributes to a decrease in capacity over time. The corrosion on the metal surface leads to the loss of active metal at the surface for electrochemical reactions [14].

A high corrosion rate causes the battery to lose its capacity at a faster rate and eventually fail. Another problem is a formation of dendrites. Dendrite is formed during zinc ion deposition which decreases the coulombic efficiency [8]. As this unbalanced zinc deposition continues, the dendrite starts to grow at the region of high deposition, and also on the other side of the electrode, hence, creating a short-circuit [8, 15]. Short-circuits in batteries result in overheating, fire, and explosions.

The zinc ion batteries (ZIBs) consists of 5 parts: 1) zinc anode (e.g., zinc foil, zinc nanoparticle electrodeposited on a porous substrate), 2) electrolyte (e.g.,  $\text{ZnSO}_4$ ,  $\text{ZnCl}_2$  and  $\text{Zn}(\text{CF}_3\text{SO}_3)_2$ ), 3) cathode materials (e.g., manganese-based and vanadium-based), 4) current collector (e.g., stainless steel foil, titanium foil, carbon-coated steel and graphite foil), and 5) separator (e.g., porous cellulose, glass microfiber filter paper) as shown in Figure 4 [2].

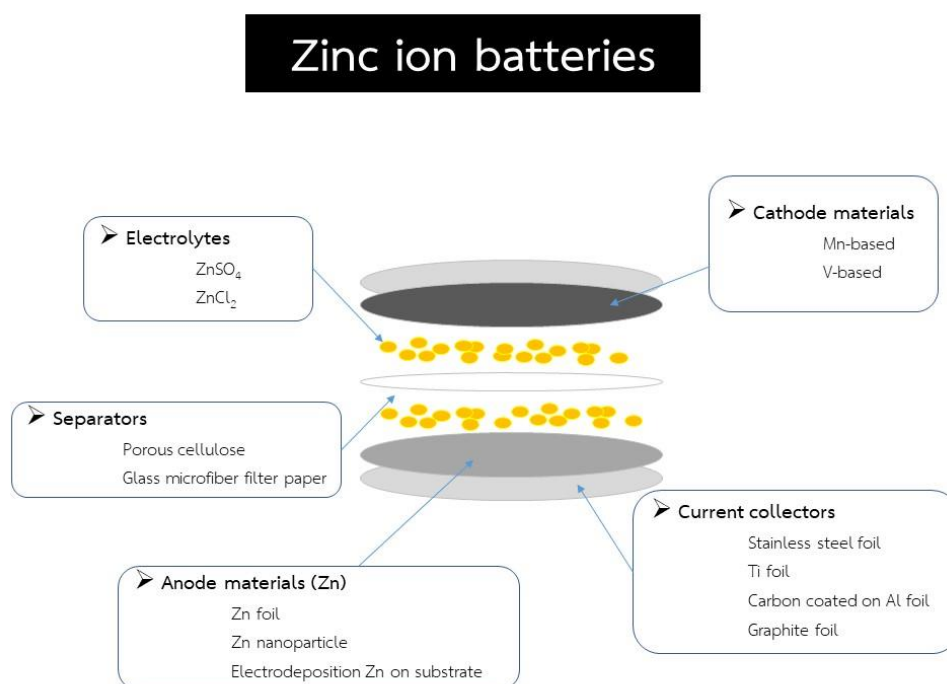
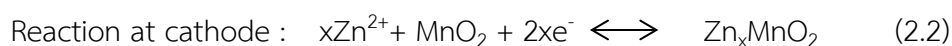


Figure 4 The Zinc ion batteries (ZIBs) parts



### 2.3.1 Charge-Storage Mechanism

According to recent researches, Manganese-based on zinc ion batteries (ZIBs) have the same charge-storage mechanism as other metal-ion batteries (MIBs), which the reaction can be written as



During discharging, zinc on the anode surface was oxidized to  $\text{Zn}^{2+}$  and intercalated into  $\text{MnO}_2$  that host material. Initially, manganese in manganese dioxide has oxidation number +4, ( $\text{Mn}^{4+}$ ). After the insertion of zinc-ion the oxidation number of Manganese decrease to +2, ( $\text{Mn}^{2+}$ ). The charge-storage mechanism as shown in Figure 5.

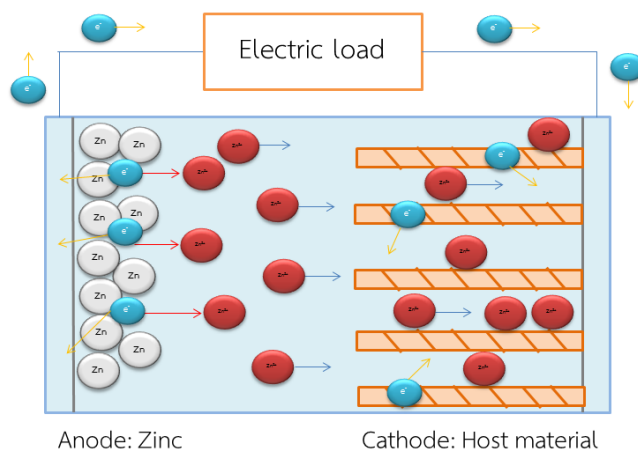


Figure 5 Schematic illustrate the charge-transfer mechanism of zinc ion battery

The amount of charge transfer from this process can be theoretically calculated as 616 mAh/g. From previous reports, the measured specific capacity of this system is only about 200 mAh/g which depends on the crystal structure of manganese dioxide  $\text{MnO}_2$ , ( $\alpha$ ,  $\gamma$ ,  $\beta$ ,  $\delta$ ,  $\lambda$ , and  $\epsilon$  phase) [2, 7].

### 2.3.2 Electrolyte for Zinc Ion Batteries (ZIBs)

Aqueous electrolyte is cheap, non-toxic, and provides a better stability for both anode and cathode. Furthermore, a neutral or mildly acidic aqueous electrolyte also mitigates corrosion and dendrite formation, but too strong acidic electrolyte can corrode both zinc anode and current collector. Up to now, zinc salts, such as  $\text{ZnSO}_4$ ,  $\text{Zn}(\text{CF}_3\text{SO}_3)_2$ ,  $\text{Zn}(\text{NO}_3)_2$ , and  $\text{ZnCl}_2$ , have been widely investigated as ZIB electrolytes. Among these,  $\text{ZnSO}_4$  and  $\text{Zn}(\text{CF}_3\text{SO}_3)_2$  are the most commonly use because of their stability and compatibility with the electrodes.  $\text{Zn}(\text{CF}_3\text{SO}_3)_2$  is significantly more expensive than  $\text{ZnSO}_4$  [3]. In this work,  $\text{ZnSO}_4$  is chosen as electrolyte due to all the mentioned benefits.

### 2.3.3 Cathode Materials

Manganese-based and vanadium-based cathode are usually cathode in zinc ion batteries. The performance of a  $\text{MnO}_2$  cathode depends on its crystal structure. In 1988, Takayuki Shoji et al. [16] The first reported a rechargeable aqueous  $\text{Zn-MnO}_2$  battery using  $\text{ZnSO}_4$  aqueous electrolyte. Chengjun Xu, et al [17] presented a power type battery that safe and environmentally friendly. Zinc ion batteries composes of a zinc anode, an  $\alpha$ - $\text{MnO}_2$  cathode and a mild  $\text{ZnSO}_4$  or  $\text{Zn}(\text{NO}_3)_2$  aqueous as electrolyte, as shown in schematics of zinc ion batteries in Figure 6.

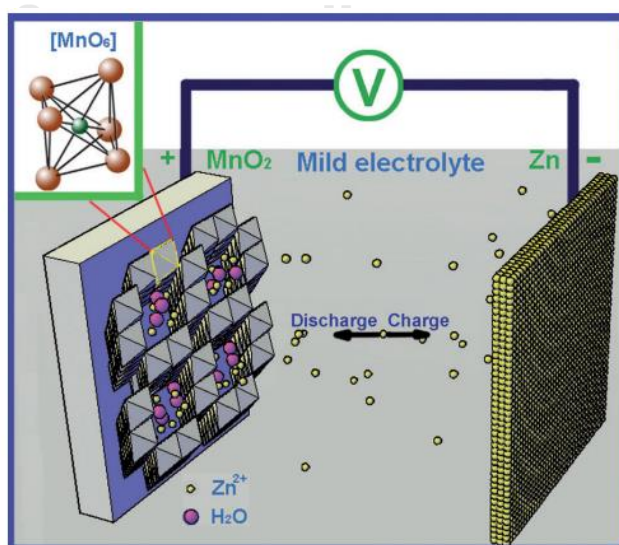


Figure 6 Schematics of zinc ion battery [15]

Up to now, cathode materials for zinc ion batteries are manganese-based oxides [18, 19], vanadium-based oxides [20], Prussian blue analogues [21], and chevrel phase compounds [22].

But  $\text{MnO}_2$  are the most commonly use because various  $\text{MnO}_2$  structures, showing good battery performance, low cost, and less toxic. This work used  $\text{MnO}_2$ -base as a cathode of zinc ion batteries.

#### 2.3.4 Anode for Zinc Ion Batteries

Zinc ion batteries usually use pure zinc metal as an anode. Zinc foil is the most widely used anode due to its simplicity and low cost [2]. However, choosing of anode material should concern about dendrite formation and the corrosion of the zinc anode. Many methods that improve the performance of zinc was proposed, such as the usage of zinc alloy powders, the synthesis of fiber, gel formed zinc the addition of polymer additives [23], and electrodeposition [8, 24, 25].

Electrodeposition is a method that does not required any advance equipment but has the advantage of controlling shape and grain size [24].

The baht is set up of zinc electrodeposition, as shown in Figure 7. The incorporation of a dispersed second phase material (micro or nano particles) into the metal matrix during the electrodeposition process makes it possible to adjust the properties of the coating layer for a variety of applications. It can be further enhanced by adding specific types of particle which will mitigate the corrosion and dendrite formation.

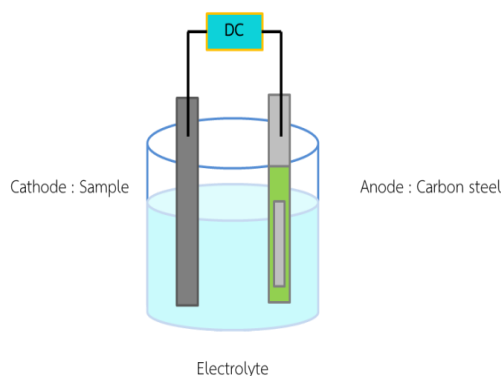


Figure 7 Electrodeposition setup

Nurhaswani Alias and Ahmad Azmin Mohamad [26] studied about the electrodeposition process of zinc on copper plate surface in a Zn sulfate ( $\text{ZnSO}_4$ ). At low current density,  $0.01 \text{ A/cm}^2$ , a thin deposited layer of Zn was formed but there was not clear detail about the structure. When the current density was increased to  $0.02 \text{ A/cm}^2$ , the morphology changed to a hexagonal-like crystalline structure. However, the nucleation and growth of metallic zinc were detected at  $0.04$  to  $0.1 \text{ A/cm}^2$ . At  $0.1 \text{ A/cm}^2$  the morphology changed to a flake-like structure as shown in Figure 8.

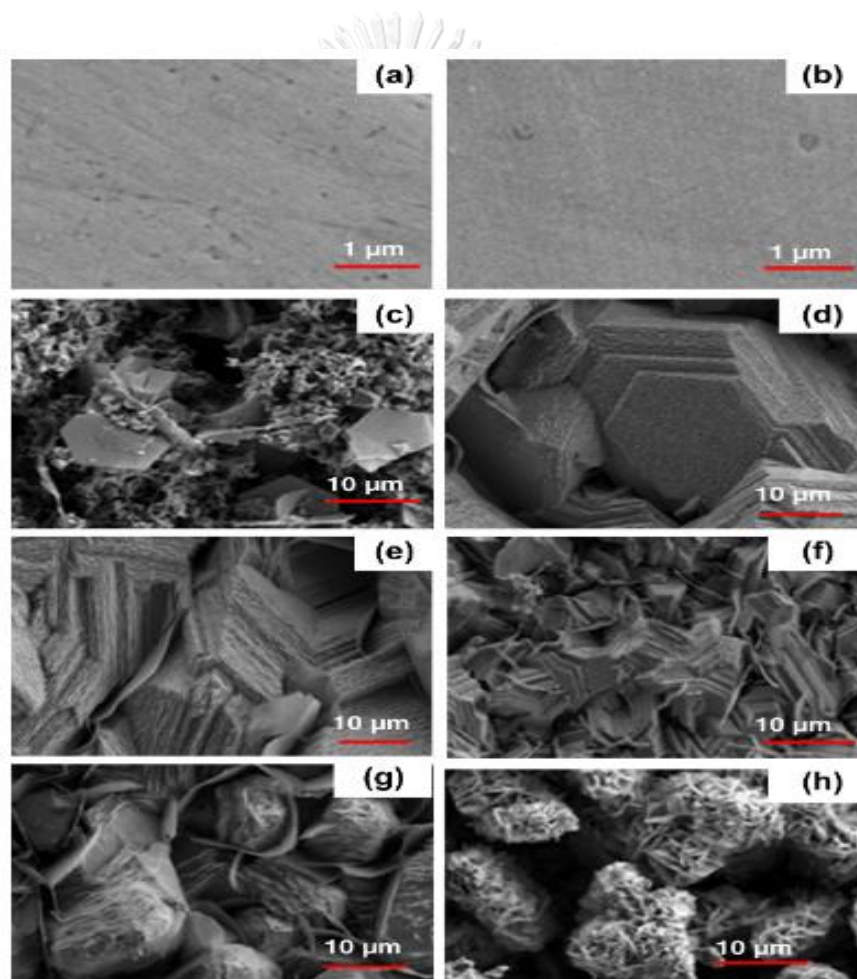


Figure 8 FESEM images of (a) Zn plate, (b) Cu plate, and Zn deposits at different current densities

Kyung Eun et al. [8] added organic and inorganic additive into electrodeposition process to reduce the corrosion and dendrite formation. The selected organic additives were cetyl trimethylammonium bromide (CTAB), thiourea, sodium dodecyl sulfate (SDS), polyethylene glycol 8000 (PEG), and the inorganic additives were indium (II) sulfate, tin (IV) oxide, and boric acid. The morphology, as shown in Figure 9, the result is performed better than the commercial zinc anode, its low corrosion rate, low dendrite formation, low float current, and high capacity retention after 1000 cycles.

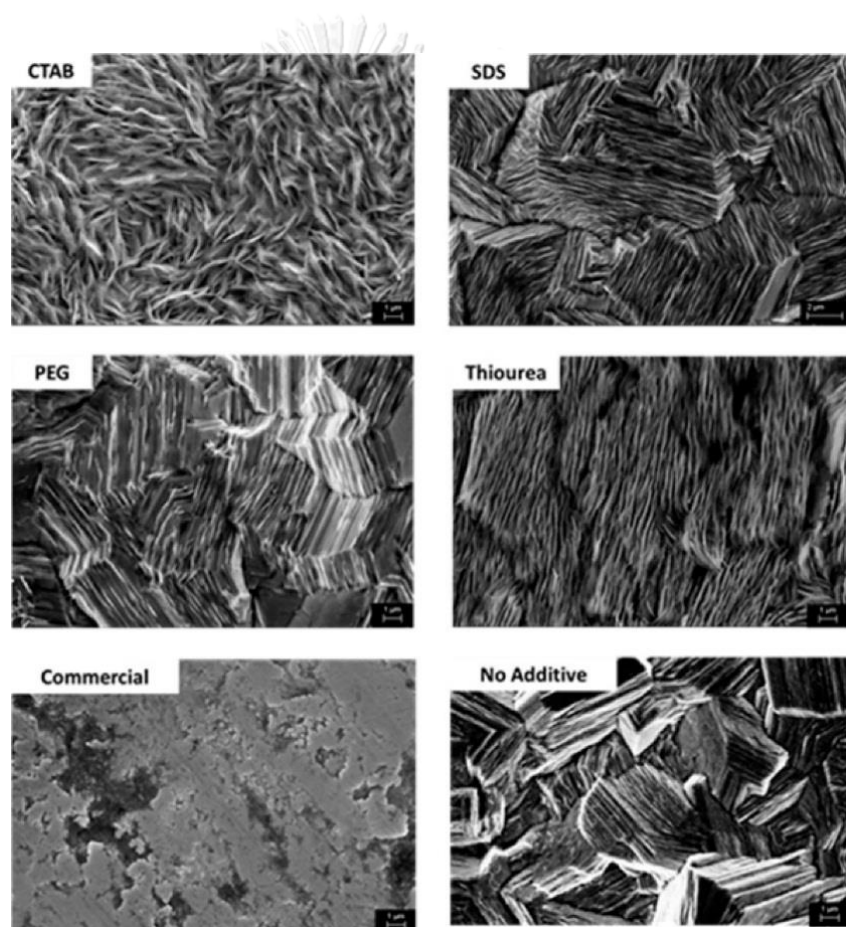


Figure 9 SEM images of synthesized anode with and without organic additives and commercialized zinc.

S. Lee et al. [9] investigated the effect of the additives ( $\text{Al}_2\text{O}_3$ ,  $\text{Bi}_2\text{O}_3$ , and  $\text{In}_2\text{O}_3$ ) on the zinc electrode in the zinc-air batteries. Among three additives, aluminum oxide showed the lowest hydrogen gas evolution and corrosion.

New composite coatings with metallic matrix can be done by electrodeposition. A variety of spherical shaped, has successfully incorporated into zinc deposition [35]. From many research works, adding ceramic nanoparticles, such as  $\text{AlO}_2$ ,  $\text{ZrO}_2$ ,  $\text{SiO}_2$ , and  $\text{TiO}_2$ , into the electrodeposition process gave a better corrosion resistance [9]. Among the ceramic particle,  $\text{TiO}_2$  is a great choice due to its semiconducting properties and also improves a corrosion resistance properties [10].

Adriana Vlasa et al. studied about corrosion behavior of Zn- $\text{TiO}_2$  nanocomposite coatings. The concentrations of  $\text{TiO}_2$  nanoparticles in the plating bath were 3, 5 and 10 g/L, respectively. The morphology is shown in Figure 10 [27].

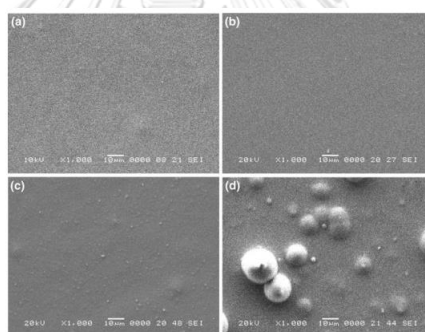


Figure 10 SEM image of the surface (a) Zn- $\text{TiO}_2$  3 g/L, (b) 5 g/L, (c) 10 g/L, and (d) Degussa

After corrosion test, The morphology is shown in Figure 11 [27] the composite coatings exhibit higher corrosion resistance than pure Zn coatings.

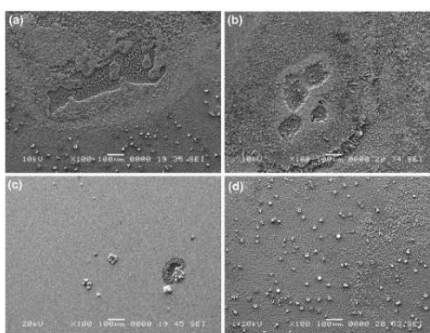


Figure 11 SEM micrographs of the surface of Zn after 48 h immersion in 0.2 g/L  $(\text{NH}_4)_2\text{SO}_4$ .

J. Fustes et al. [28] studied about Zn-TiO<sub>2</sub> nanocomposite films by pulsed electrodeposition from zinc sulfate solution and the concentration of TiO<sub>2</sub> in the bath were 1.0, 10 and 16 g/L. The bath pH was adjusted to 4 by adding a diluted solution of H<sub>2</sub>SO<sub>4</sub>. From this method, a disperse TiO<sub>2</sub> nanoparticles was successfully as shown in Figure 12 and grain size decreases as the of nanoparticles increases.

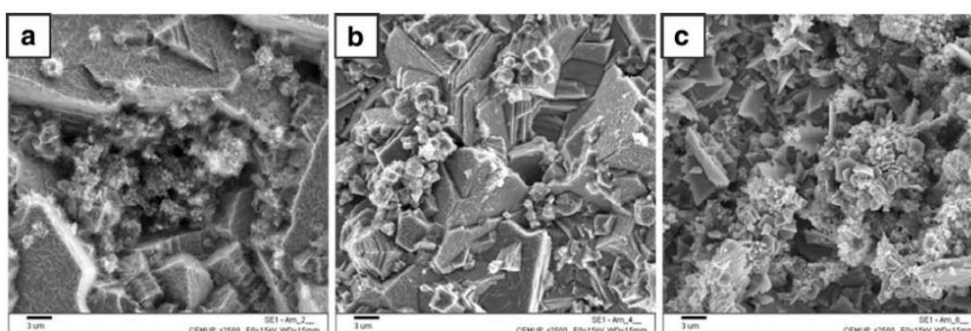


Figure 12 SEM micrographs of the surface of Zn-TiO<sub>2</sub> films from different baths

Table 1 Bath composition

Compound	Concentration (g/L)
ZnSO <sub>4</sub> ·7H <sub>2</sub> O	200
Na <sub>2</sub> SO <sub>4</sub>	15
ZnCl <sub>2</sub>	35
TiO <sub>2</sub>	5,10,20
pH	4.85
Temperature	25°C
cathode potentials	-1600
	-1900
	-2100
Electrodeposition time	5,10,15 min
Magnetic stirring	300 rpm

L.Benea et al. [29] studied about the development of electrodeposited Zn/nano-TiO<sub>2</sub> composite coatings with enhanced corrosion resistance. The coatings were prepared on low-carbon steel by electro co-deposition technique and the electroplating bath was prepared with the bath composition as shown in Table 1.



Figure 13 as shows the thickness of the layer increased with the increase of the required cathodic potential for pure zinc layers and nanocomposite layers. At the same deposition time, nanocomposite coatings have slightly higher thickness than that of pure zinc, thus confirming the inclusion of  $\text{TiO}_2$  nanoparticles in the zinc matrix.

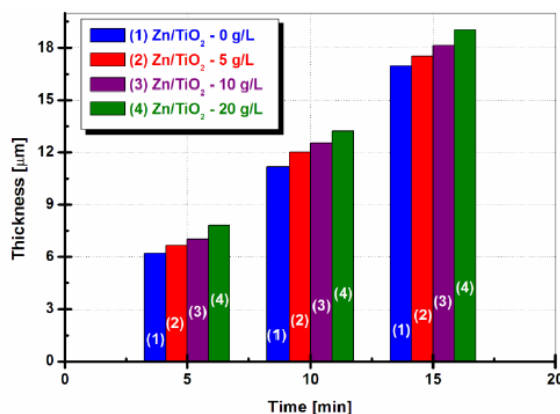


Figure 13 Layer thicknesses of electrodeposited layers

B.M. Praveen et al. [10] studied about pure zinc and Zn-TiO<sub>2</sub> coatings electrodeposited from sulfate bath. The result showed that the grain size of the composite coated sample was smaller when compared with the pure zinc coating. The coated specimens were kept for about 10–15 mins in the 3.5% NaCl solution prior to anodic polarization test. For pure zinc coating (Figure 14A), zinc was etched from the surface continuously while for Zn-TiO<sub>2</sub> composite coating (Figure 14B), the zinc was etched away slowly leaving TiO<sub>2</sub> on the metal surface. This hindered further dissolution of zinc metal.

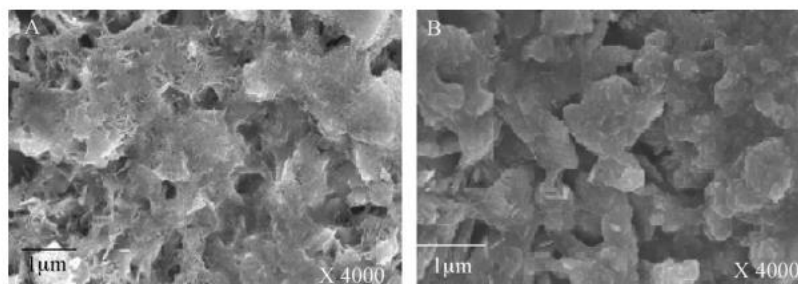


Figure 14 SEM images of surfaces after anodic polarization A) pure zinc coating and B) Zn-TiO<sub>2</sub> composite coating



From many research works, ceramic nanoparticles were added into the electrodeposition process to have nanocomposite materials as layers on top of other materials. These types of ceramic particles could be  $\text{Al}_2\text{O}_3$ ,  $\text{ZrO}_2$ ,  $\text{TiO}_2$ ,  $\text{SiO}_2$ , which had higher corrosion resistance. Among the ceramic particles,  $\text{TiO}_2$  was attractive for the generation of composite zinc coatings as the semiconductor properties of  $\text{TiO}_2$ , which could reinforce with zinc electroplate to enhance the corrosion resistance.

Thus, this research will prepare zinc anode via electrodeposition by adding titanium dioxide nanoparticle in zinc sulfate ( $\text{ZnSO}_4$ ) bath. The concentration of titanium dioxide were 0, 1, 3, 5, and 10 g/L, the current density were 0.01, 0.02, 0.03, and 0.04  $\text{A}/\text{cm}^2$  and time for electrodeposition is 30 mins.



## Chapter 3

### Experimental Procedures

#### 3.1 Battery Components

In this work, the electrodes are fabricated but this work focuses on the modification of the anode by varying several parameters.

##### 3.1.1 Anode

The anode used in this work is Zn-TiO<sub>2</sub> composite.

##### 3.1.1.1 Preparation of Zn-TiO<sub>2</sub> composite

The Zn-TiO<sub>2</sub> composite is prepared by using electrodeposition technique. Carbon steel plate is used as an anode and stainless steel is used as a cathode. Stainless steel size 5 cm x 5 cm was used as a substrate. The substrate was pretreated by degreasing in NaOH for 3 mins and activated in 5% HCl for 5 mins. The electroplating solution was prepared by dissolving 100g of zinc sulfate (ZnSO<sub>4</sub>) in 500 mL of distilled water. Then add 40g of sodium sulfate (NaSO<sub>4</sub>), 20g of sodium chloride (NaCl), 8g of boric acid (H<sub>3</sub>BO<sub>3</sub>), and titanium dioxide (TiO<sub>2</sub>) powder into the solution, respectively. The solution was stirred for 24 hours until a clear solution is obtained. The processing parameters is shown consistency in Table 2. After plating, the samples were dried in oven at 80°C for 24 hours. Then the sample was cut in a circular shape with a diameter of 14 mm.

##### 3.1.1.2 TiO<sub>2</sub> powder

In this research used TiO<sub>2</sub> nano-powder (P25, Degussa TiO<sub>2</sub>) has the particle size less than 21nm. The scanning electron microscope (SEM) was used to study the morphology of TiO<sub>2</sub> the result shown in Figure 15.

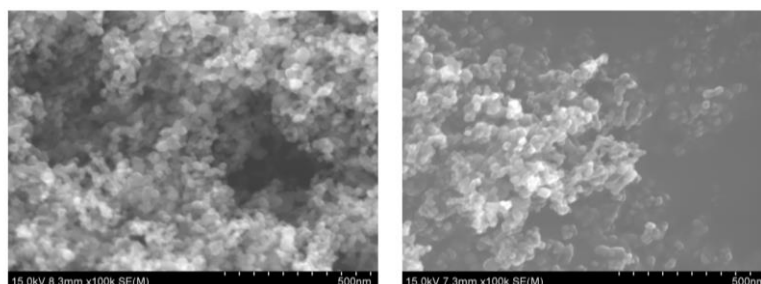


*Figure 15 TiO<sub>2</sub> nano-powder (P25, Degussa TiO<sub>2</sub>)*

Table 2 Experimental conditions

Bath	Concentration of TiO <sub>2</sub> (g/L)	Current density (A/cm <sup>2</sup> )	Time (mins)
1	0	0.01	30
	0	0.02	30
	0	0.03	30
	0	0.04	30
2	1	0.01	30
	1	0.02	30
	1	0.03	30
	1	0.04	30
3	3	0.01	30
	3	0.02	30
	3	0.03	30
	3	0.04	30
4	5	0.01	30
	5	0.02	30
	5	0.03	30
	5	0.04	30
5	10	0.01	30
	10	0.02	30
	10	0.03	30
	10	0.04	30

### 3.1.2 Cathode

The cathode used in this work is manganese dioxide ( $\text{MnO}_2$ ).  $\text{MnO}_2$  is prepared by mixing 70 wt.% of  $\text{MnO}_2$ , 20 wt.% of conduction carbon and 1 wt.% of polyvinylidene fluoride (PVDF) in dimethyl formamide (DMF) and sonicate the slurry for 60 minutes. Then consistency continue stirring the slurry for 30 minutes and coated the mixed slurry on carbon coated aluminium foil by coating machine and dry in vacuum oven at  $70^\circ\text{C}$  for 24 hours. After the sample was dried, cut it in a circular shape with a diameter of 14 mm.

### 3.1.3 Separator

The separator used in this work is glass microfiber filter because of very small and highly porous structure.

### 3.1.4 Electrolyte

The electrolyte used is a mixture of 2M zinc sulfate 0.05M and manganese sulfate dissolved in distilled water was the electrolyte of the battery cell.

## 3.2 A Coin Cell Assembly (CR2032)

Figure 16 shows how a coin cell is assembled. First, put the Zn anode and 2 pieces of glass microfiber filter into the anode case, respectively and drop  $50\ \mu\text{L}$  of electrolyte on the glass microfiber filter. Next, place  $\text{MnO}_2$  cathode and drop  $50\ \mu\text{L}$  of electrolyte. Then, adjust the thickness by using support and spring and close the cell with a cathode case. Finally, compress the cell with a load of  $80\ \text{kg}/\text{cm}^2$ .

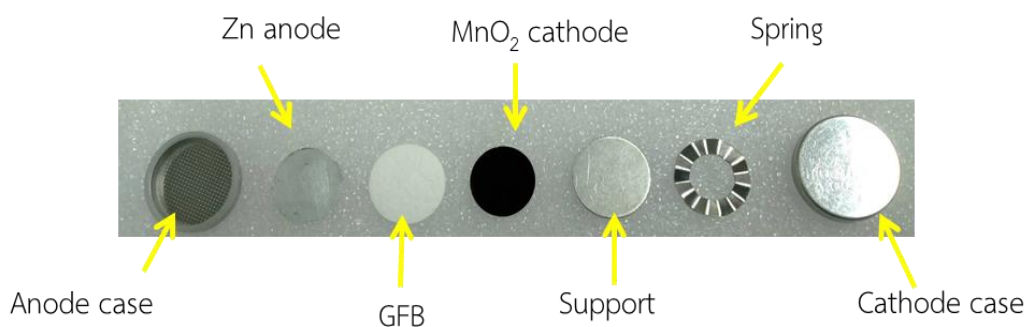


Figure 16 A Coin Cell Assembly (CR2032)

### 3.3 Characterization

Several techniques were used to characterize the components of the battery cell.

#### 3.3.1 Scanning electron microscope with energy dispersive spectroscopy (SEM-EDS)

The scanning electron microscope (SEM) is used to study morphology and microstructure of the electrodes. EDS is used to determine the chemical composition and elemental analysis.

#### 3.3.2 X-ray Powder Diffraction (XRD)

X-ray diffractometry is used to analyze the crystal structure of the material.

#### 3.3.3 LAND battery

LAND battery is used to test the performance of the battery (capacity, energy density, power, and cycle life). LAND battery can be used to determine the current density, specific capacity, energy density and coulombic efficiency.

#### 3.3.4 Potentiostatic

Galvanostatic charge-discharge test, cyclic voltammetry (CV), and electrochemical impedance spectroscopy (EIS) are the methods used to analyze the performance of the battery. Galvanostatic charge-discharge method studies the cell performance and cyclability. Cyclic voltammetry investigates the redox reaction characteristic of the electrode. In addition, the internal resistance of the cell and the charge-transfer resistance can be determined from the EIS method. The obtained results can be used to determine the current density, specific capacity, energy density and coulombic efficiency via equation 3.1, 3.2, and 3.3 respectively.

$$\text{current density} = \frac{I}{M_{ac}} \quad (3.1)$$

When  $I$  = current

$M$  = weight of cathode

The capacity of the cathode is determined by measuring the total charge delivered from the cathode upon the charging or discharging and can be calculated as followed

$$\text{specific capacity} = \frac{I}{M_{ac}} \int_{t_0}^{t_f} T dT \quad (3.2)$$

When  $I$  = current

$M$  = weight of cathode

$T$  = time

The percentage of discharging capacity compared with the charging capacity is called coulombic efficiency, and can be calculated as followed

$$\text{coulombic efficiency} = \frac{\text{discharge capacity}}{\text{charge capacity}} \times 100 \quad (3.3)$$

Table 3 Research Timeline

Year	2018			2019											
Month	10	11	12	1	2	3	4	5	6	7	8	9	10	11	12
Literature review	← →														
Propose proposal						← →									
Prepare chemical								← →							
Experimental									← →						
Testing										← →					
Analysis and conclusion											← →				
Write the result											← →				
Progressive														← →	

## Chapter 4

### Results and Discussions

#### 4.1 Microstructure Characterization

##### 4.1.1 Morphology and microstructure

##### 4.1.1.1 The Zn without $TiO_2$

The Zn without  $TiO_2$  sample was prepared by using electrodeposition technique and was deposited with different current densities (0.01, 0.02, 0.03, and 0.04  $A/cm^2$ ). Carbon steel plate used as an anode and stainless steel was used as a cathode. Stainless steel size of 5 cm x 5 cm was used as a substrate to deposit zinc coatings. After the electrodeposition of Zn, the scanning electron microscope (SEM) was used to study the morphology and microstructure of the electrodes. EDS was used to determine the chemical composition and elemental analysis.

The results are shown in Figures 17-20. The Zn particles were deposited with different current densities (0.01, 0.02, 0.03, and 0.04  $A/cm^2$ ). The produced coarse-grained deposits have non-uniform morphology particularly at low current densities, 0.01  $A/cm^2$  and the size of deposited particles is the smallest as  $\sim 2.2 \mu m$ . While at higher current densities (0.02-0.04  $A/cm^2$ ), the particle sizes are about  $\sim 4 \mu m$ , which are bigger than those of low current density.

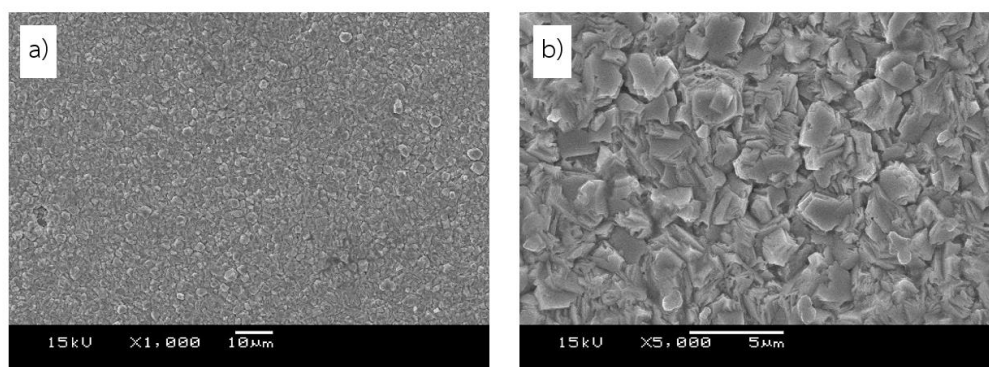


Figure 17 The Zn electrodeposition without  $TiO_2$  at current density of 0.01  $A/cm^2$  1000X and (b) 5000X

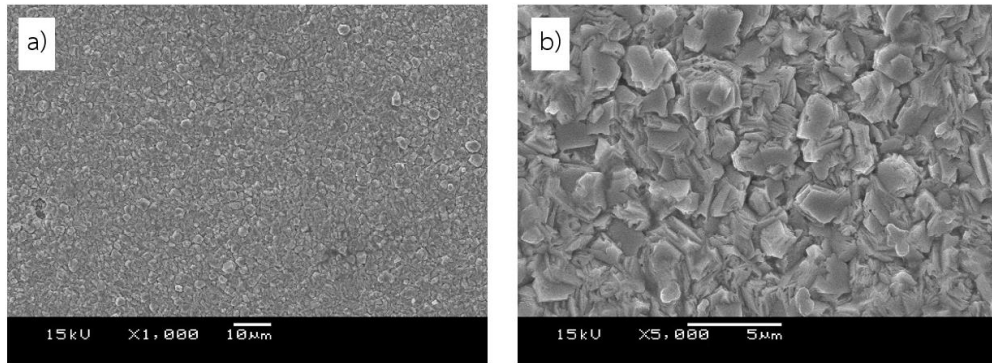


Figure 18 The Zn electrodeposition without  $\text{TiO}_2$  at current density of  $0.02 \text{ A/cm}^2$   
(a) 1000X and (b) 5000X

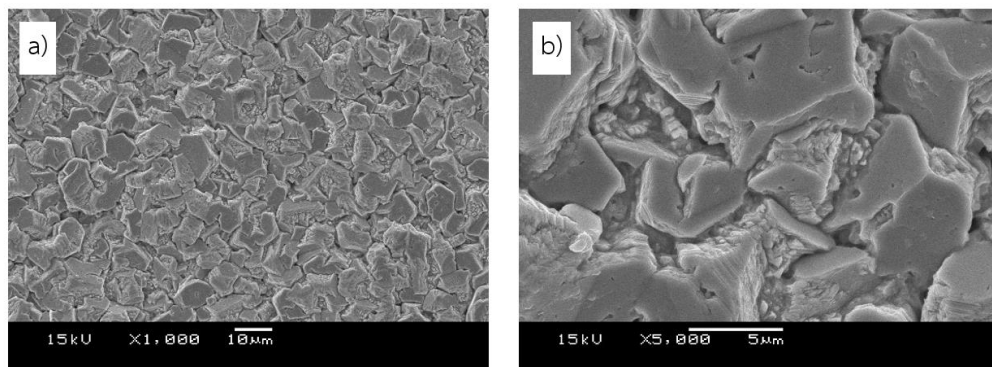


Figure 19 The Zn electrodeposition without  $\text{TiO}_2$  at current density of  $0.03 \text{ A/cm}^2$   
(a) 1000X and (b) 5000X

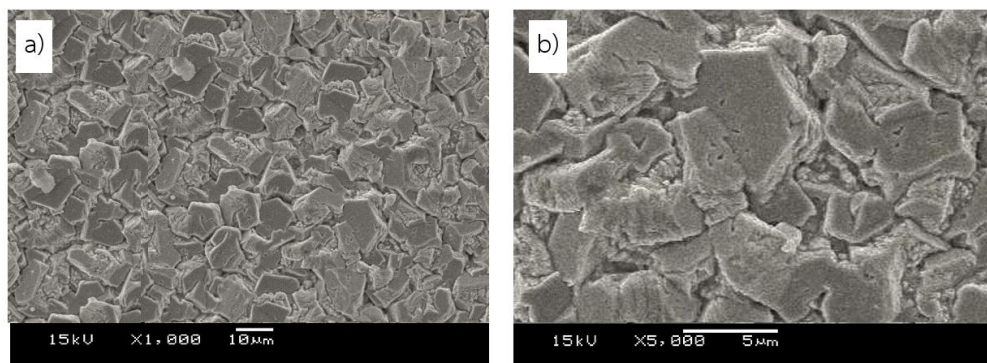
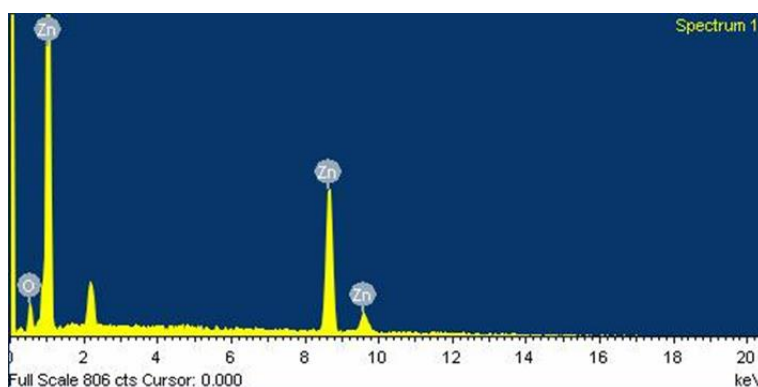


Figure 20 The Zn electrodeposition without  $\text{TiO}_2$  at current density of  $0.04 \text{ A/cm}^2$   
(a) 1000X and (b) 5000X



During the electrodeposition process the crystal size was controlled by the formation of the crystal growth rate. Fine-grained deposits are generally obtained with a faster formation of nucleation sites as result of heterogeneous nucleation with bigger grain size.

Energy Dispersive X-ray Spectrometer (EDS) with mapping analysis method was used to determine the chemical composition and elemental analysis. The EDS result of sample with current density of  $0.01 \text{ A/cm}^2$  is shown in Figure 21.



*Figure 21 EDS representative spectra of Zn without  $\text{TiO}_2$  at current density  $0.01 \text{ A/cm}^2$*

Generally, the coating layer properties are directly related to the received microstructure of the metal. In this work, at low current density of  $0.01 \text{ A/cm}^2$ , sample consists of 89.6 wt% zinc and 10.4 wt% oxygen but at higher current densities  $0.02$ ,  $0.03$ , and  $0.04 \text{ A/cm}^2$ , the percent weight of Zn increases when deposited current densities increases. In this case, the current density affected to the morphology by providing more Zn deposition and increasing with bigger grain size. The wt% of zinc and oxygen of all samples are shown in Figure 22.

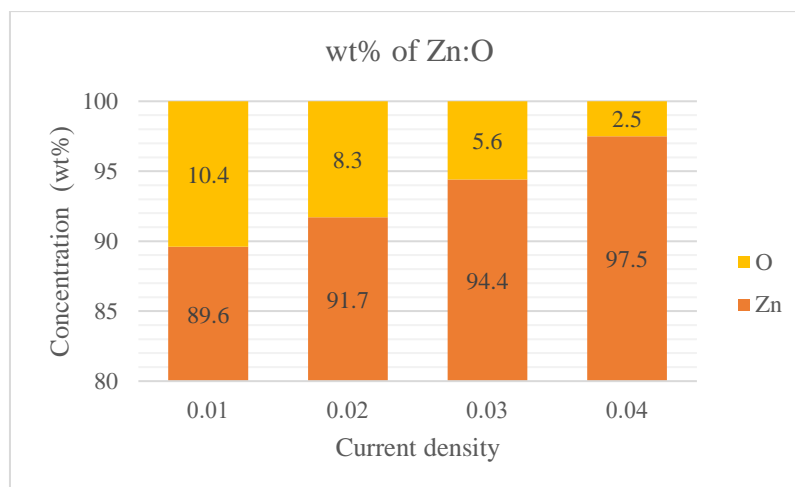


Figure 22 The wt% of Zn and O at different current densities

#### 4.1.1.2 The Zn electrodeposition with $\text{TiO}_2$ 1 g/L

The Zn - $\text{TiO}_2$  composite layer was prepared by using electrodeposition technique, which deposited with different current densities (0.01, 0.02, 0.03, and 0.04  $\text{A}/\text{cm}^2$ ). In the baht for electrodeposition with 1g of  $\text{TiO}_2$  addition, Carbon steel plate was used as an anode and stainless steel was used as a cathode. Stainless steel size of 5 cm x 5 cm was used as a substrate to deposit zinc coatings. After the electrodeposition of zinc, the scanning electron microscope (SEM) was used to study the morphology and microstructure of the electrodes.

Zn- $\text{TiO}_2$  composite layers with significant differences in the morphology were obtained by varying current density. The results are shown in Figures 23-26. At low current density of 0.01  $\text{A}/\text{cm}^2$ , it was found that surface layer consists of a non-uniform crystal grain distribution and the deposited particle size is the smallest  $\sim 3.2$   $\mu\text{m}$ . While at higher current densities (0.02-0.03  $\text{A}/\text{cm}^2$ ), it was found that surface layer consisted of homogeneous crystals with randomly distributed particle sizes of Zn- $\text{TiO}_2$  composite coatings,  $\sim 3.5$  to 4.4  $\mu\text{m}$ . For the highest current density of 0.04  $\text{A}/\text{cm}^2$  it was found that surface layer consisted of shape layer of zinc as flake morphology with the particle size  $\sim 4.8$   $\mu\text{m}$ . Samples with all current densities show the  $\text{TiO}_2$  agglomeration with small sizes, less amount, and non-uniform distribution of  $\text{TiO}_2$  nanoparticles on the Zn surface.

According to the previous research [29], the amount of incorporated metal oxide particles in Zn electrodeposits has generally been low dispersion stability because the high ionic strength on the coating surface layer consists of less amount and non-uniform distribution of  $\text{TiO}_2$  nanoparticles. During the electrodeposition process the crystal size was controlled by the formation of the crystal growth rate. Fine-grained deposits are generally obtained with a faster formation of nucleation sites as result of heterogeneous nucleation. The bigger grain size was obtained when the current density for depositing was increasing.

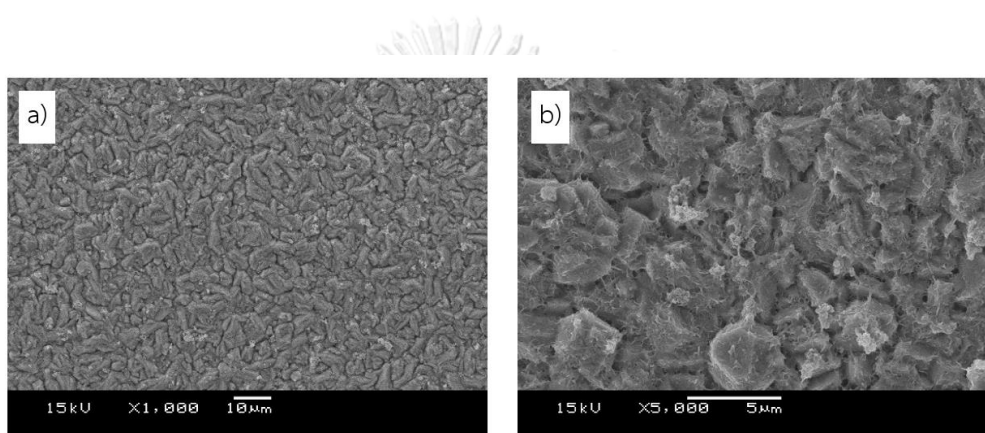


Figure 23 The Zn electrodeposition with  $\text{TiO}_2$  1 g/L at current density of  $0.01 \text{ A/cm}^2$

(a) 1000X and (b) 5000X

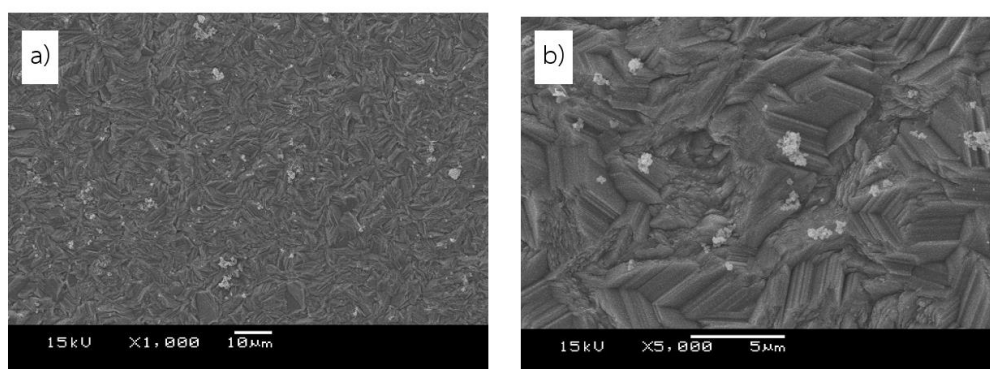


Figure 24 The Zn electrodeposition with  $\text{TiO}_2$  1 g/L at current density of  $0.02 \text{ A/cm}^2$

(a) 1000X and (b) 5000X

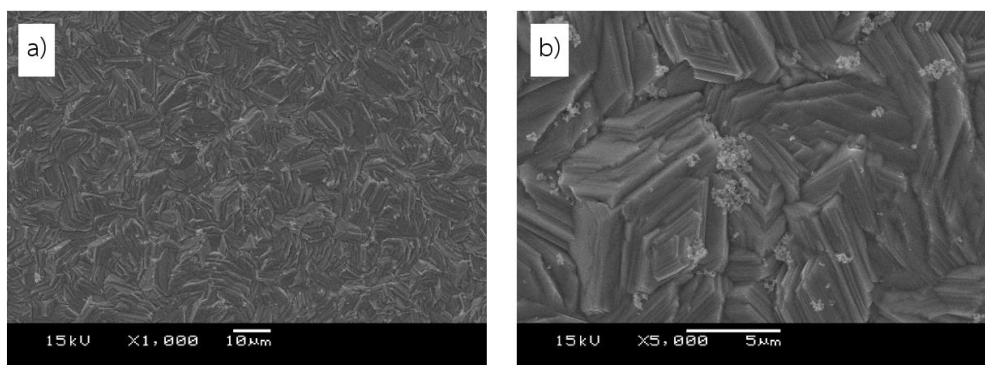


Figure 25 The Zn electrodeposition with  $\text{TiO}_2$  1 g/L at current density of  $0.03 \text{ A/cm}^2$   
(a) 1000X and (b) 5000X

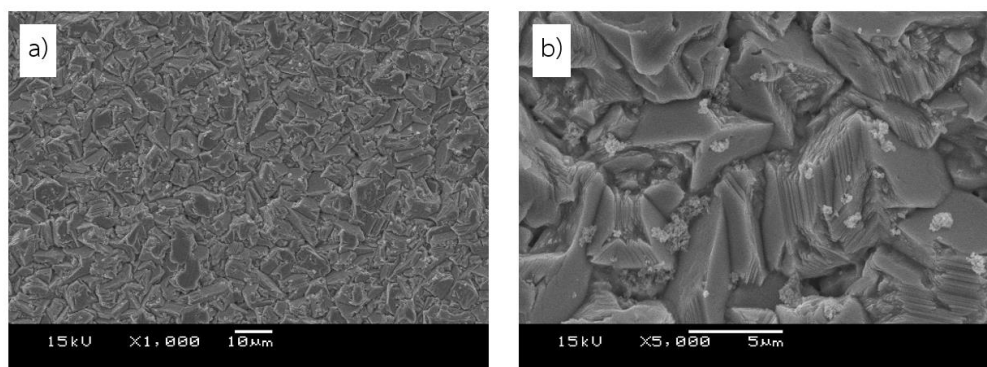


Figure 26 The Zn electrodeposition with  $\text{TiO}_2$  1 g/L at current density of  $0.04 \text{ A/cm}^2$   
(a) 1000X and (b) 5000X

Energy Dispersive X-ray Spectrometer (EDS) with mapping analysis method was used to determine the chemical composition and elemental analysis. The EDS result of sample with current density of  $0.01 \text{ A/cm}^2$  is shown in Figure 27.

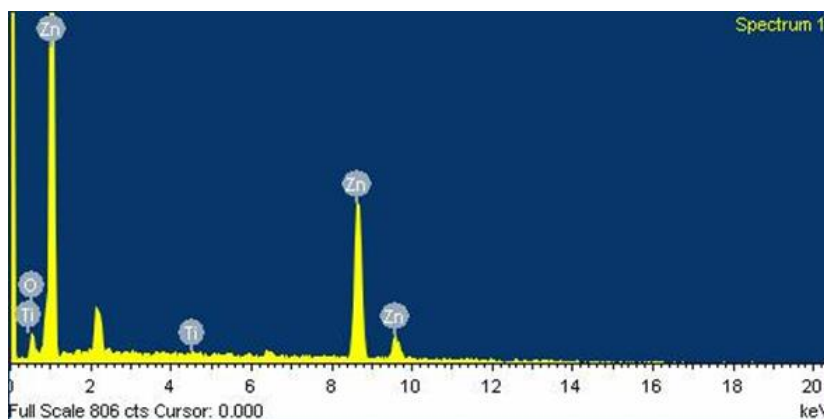


Figure 27 EDS representative spectra of Zn with  $\text{TiO}_2$  1 g/L at current density of  $0.01 \text{ A/cm}^2$

Generally, the composite layer properties directly relate to the amounts of incorporated particles, their uniform distribution within the metal matrix as well as the obtained resulted morphology of the metal. In this work all samples with current densities, ( $0.01$ ,  $0.02$ ,  $0.03$ , and  $0.04 \text{ A/cm}^2$ ) consist of 93-95 wt% zinc, 5 wt% oxygen and 0.2wt% titanium. Therefore, in this case, the current density increasing did not affect to wt% of  $\text{TiO}_2$ . The wt% zinc, titanium, and oxygen of all samples are shown in Figure 28. The samples with  $\text{TiO}_2$  on the coated surface would affect to Zn electrode and properties, which the performances of the obtained battery will be shown in another section.

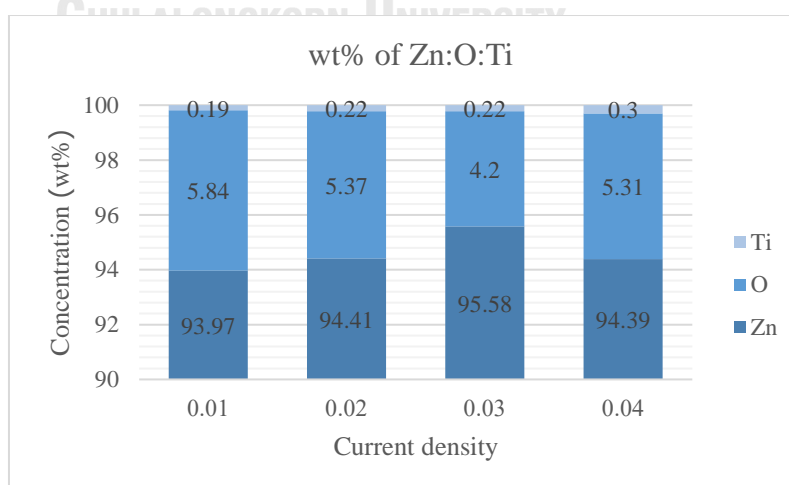


Figure 28 The wt% of Zn, O, and  $\text{TiO}_2$  at different current densities

#### 4.1.1.3 The Zn electrodeposition with $\text{TiO}_2$ 3 g/L

The Zn - $\text{TiO}_2$  composite layers were prepared by using electrodeposition technique, which deposited with different current densities (0.01, 0.02, 0.03, and 0.04  $\text{A}/\text{cm}^2$ ). In the bath for electrodeposition, 3 g of  $\text{TiO}_2$  was added, Carbon steel plate was used as an anode and stainless steel was used as a cathode. Stainless steel size of 5 cm x 5 cm was used as a substrate to deposit zinc coatings. After the electrodeposition of zinc, the scanning electron microscope (SEM) was used to study the morphology and microstructure of the electrodes.

Zn- $\text{TiO}_2$  composite layers with significant different morphologies were obtained by varying current density. At low current densities, (0.01-0.02  $\text{A}/\text{cm}^2$ ), samples were found that surface layer with the crystals are homogeneous with randomly size-distribution. The Zn crystal layer is in flake-like structure with the size of  $\sim 3.7$  to 5  $\mu\text{m}$  in Zn- $\text{TiO}_2$  composite coatings, as shown in Figures 29-30. During the electrodeposition process the crystal size was controlled by the formation of the crystal growth rate. Fine-grained deposits are generally obtained with a faster formation of nucleation sites as result of heterogeneous nucleation. The bigger grain size is received when the current density for deposition increasing. For samples with higher current densities (0.03-0.04  $\text{A}/\text{cm}^2$ ), it was found that surface layer consisting of homogeneous crystals and random size-distribution with tending to form hexagonal platelets, as shown in Figures 31-32. The particle size is in range of  $\sim 8$  to 10  $\mu\text{m}$  and the deposits transform to a multilayer structure.

All sample surfaces with different current densities consist of  $\text{TiO}_2$  agglomeration with small sizes, less amount, and non-uniform distribution of  $\text{TiO}_2$  nanoparticles on the Zn surface. According to the previous research [29], the amount of incorporated metal oxide particles in Zn electrodeposits has generally been low dispersion stability due to the high ionic strength.



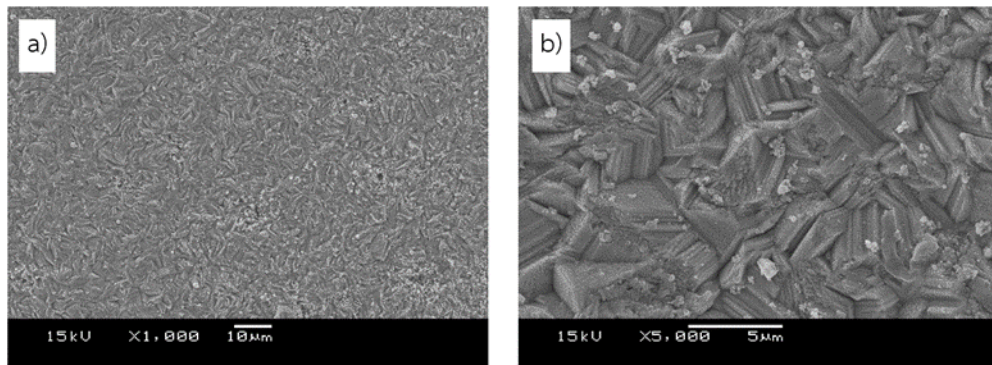


Figure 29 The Zn electrodeposition with  $\text{TiO}_2$  3 g/L at current density of  $0.01 \text{ A/cm}^2$

(a) 1000X and (b) 5000X

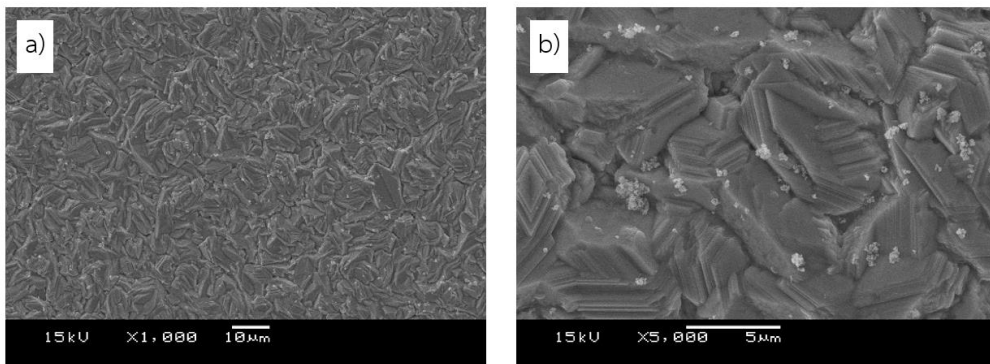


Figure 30 The Zn electrodeposition with  $\text{TiO}_2$  3 g/L at current density of  $0.02 \text{ A/cm}^2$

(a) 1000X and (b) 5000X

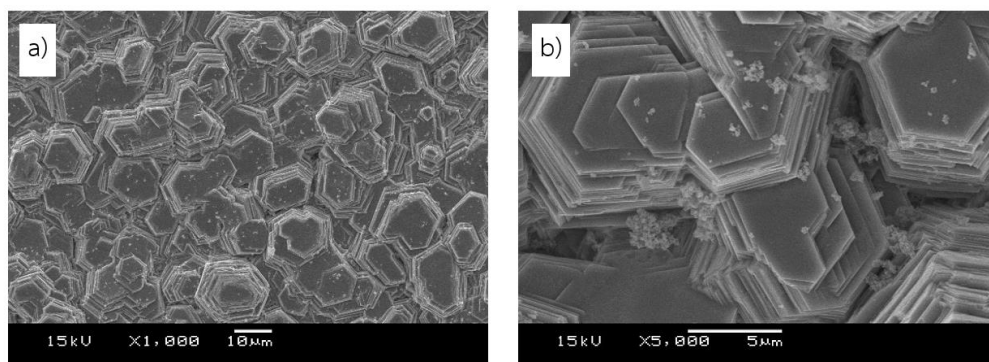


Figure 31 The Zn electrodeposition with  $\text{TiO}_2$  3 g/L at current density of  $0.03 \text{ A/cm}^2$

(a) 1000X and (b) 5000X

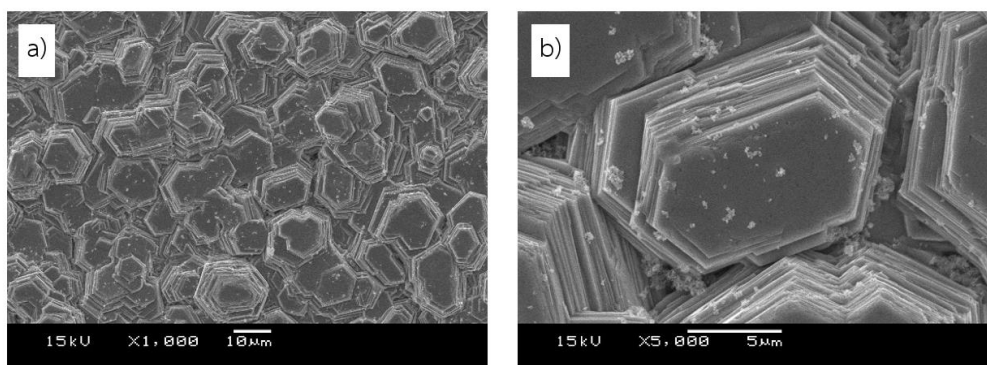


Figure 32 The Zn electrodeposition with  $\text{TiO}_2$  3 g/L at current density of  $0.04 \text{ A/cm}^2$   
(a) 1000X and (b) 5000X

Energy Dispersive X-ray Spectrometer (EDS) with mapping analysis method was used to determine the chemical composition and elemental analysis. The EDS result of sample with current density of  $0.01 \text{ A/cm}^2$  is shown in Figure 33.

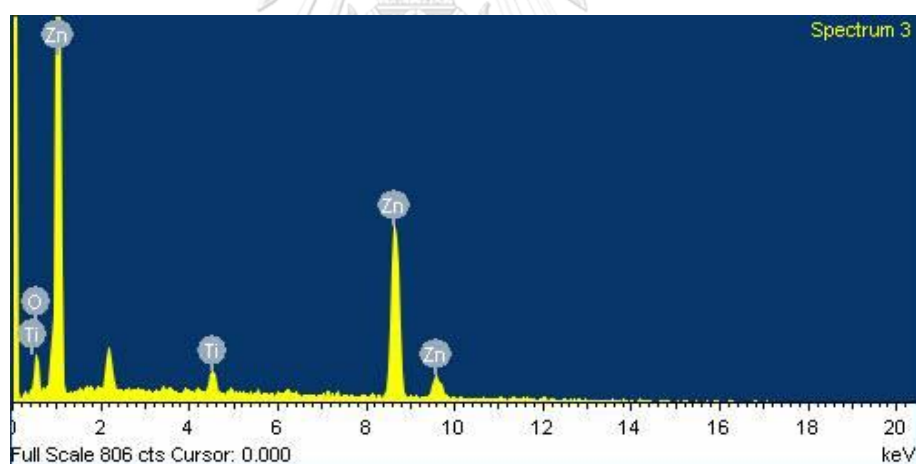


Figure 33 EDS representative spectra of Zn with  $\text{TiO}_2$  3 g/L  
at current density of  $0.01 \text{ A/cm}^2$

Generally, the composite layer properties directly relate to the amounts of incorporated particles, their uniform distribution within the metal matrix as well as the obtained morphology of the metal. In this work all samples with different current densities ( $0.01$ ,  $0.02$ ,  $0.03$ , and  $0.04 \text{ A/cm}^2$ ) consist of 95 wt% zinc, 4 wt% oxygen and 0.5 wt% titanium. Therefore, in this case, the wt% titanium increased slightly when



the current density for electroplating increased. However, all tested current densities are not big different in values. Therefore, they did not provide any insignificant effect on wt% of the elements. The wt% zinc, titanium and oxygen of all sample are shown in Figure 33. The samples with  $\text{TiO}_2$  on the coated surface would affect to Zn electrode, and properties, which the performances of the battery will be shown in another section.



Figure 34 The wt% of Zn, O, and  $\text{TiO}_2$  at different current densities

#### 4.1.1.4 The Zn electrodeposition with $\text{TiO}_2$ 5 g/L

The Zn - $\text{TiO}_2$  composite layer was prepared by using electrodeposition technique, which deposited with different current densities (0.01, 0.02, 0.03, and 0.04  $\text{A/cm}^2$ ). In the baht for electrodeposition with 5g of  $\text{TiO}_2$  addition carbon steel plate was used as an anode and stainless steel was used as a cathode. Stainless steel size 5 cm x 5 cm was used as a substrate to deposit zinc coatings. After the electrodeposition of zinc, the scanning electron microscope (SEM) was used to study the morphology and microstructure of the electrodes.

Zn- $\text{TiO}_2$  composite layers with significant different morphologies were obtained by varying current density. All samples with different current densities, (0.01, 0.02, 0.03, and 0.04  $\text{A/cm}^2$ ) consist of coated microstructure with the randomly

size-distributed crystals. The crystal shape layer transformed to a multilayer structure in Zn-TiO<sub>2</sub> composite coatings, as shown in Figures 35-38 with particle size of ~5.6 to 7 μm. During the electrodeposition process the crystal size was controlled by the formation of the crystal growth rate. Fine-grained deposits are generally obtained with a faster formation of nucleation sites as result of heterogeneous nucleation. The bigger grain size was obtained when the current density for depositing was increased.

All sample surfaces with different current densities consist of TiO<sub>2</sub> agglomeration with small sizes, less amount, and non-uniform distribution of TiO<sub>2</sub> particles on the Zn surface. According to the previous research [29], the amount of incorporated metal oxide particles in Zn electrodeposits has generally been low dispersion stability due to the high ionic strength.

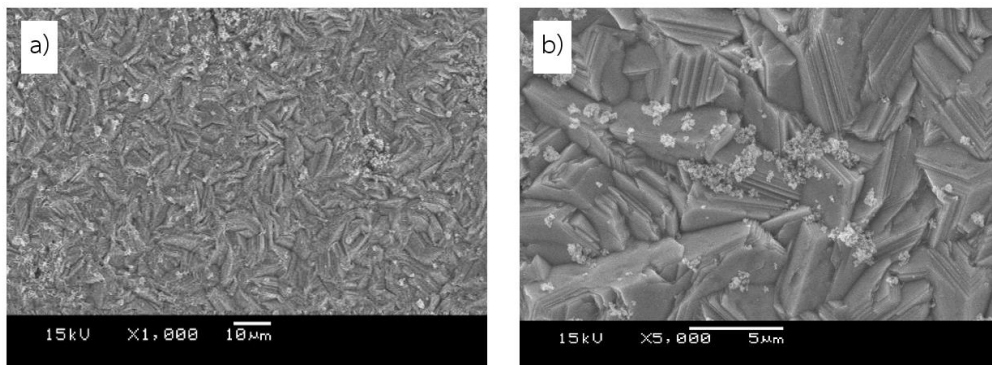


Figure 35 The Zn electrodeposition with TiO<sub>2</sub> 5 g/L at current density of 0.01 A/cm<sup>2</sup>  
(a) 1000X and (b) 5000X

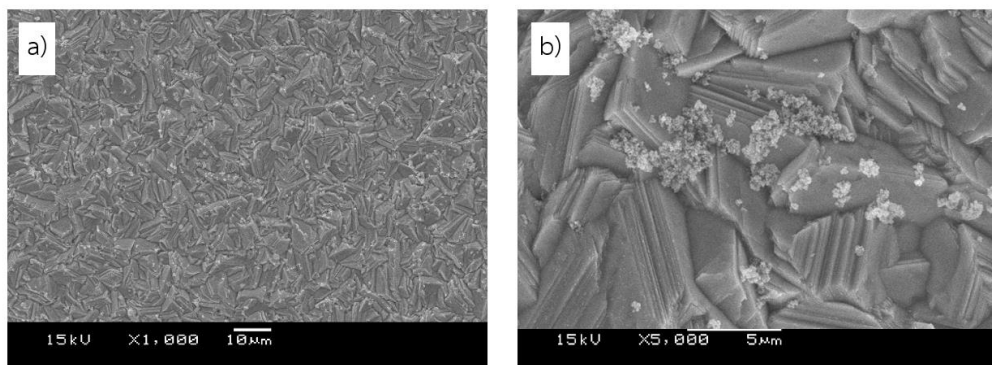


Figure 36 The Zn electrodeposition with TiO<sub>2</sub> 5 g/L at current density of 0.02 A/cm<sup>2</sup>  
(a) 1000X and (b) 5000X

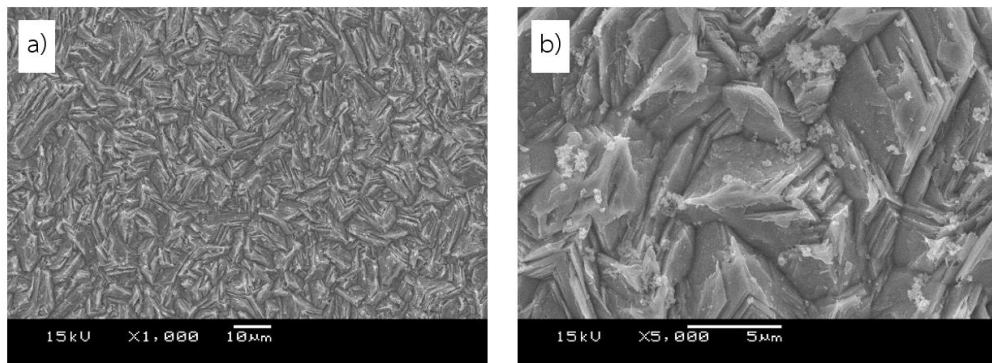


Figure 37 The Zn electrodeposition with  $\text{TiO}_2$  5 g/L at current density of  $0.03 \text{ A/cm}^2$   
(a) 1000X and (b) 5000X

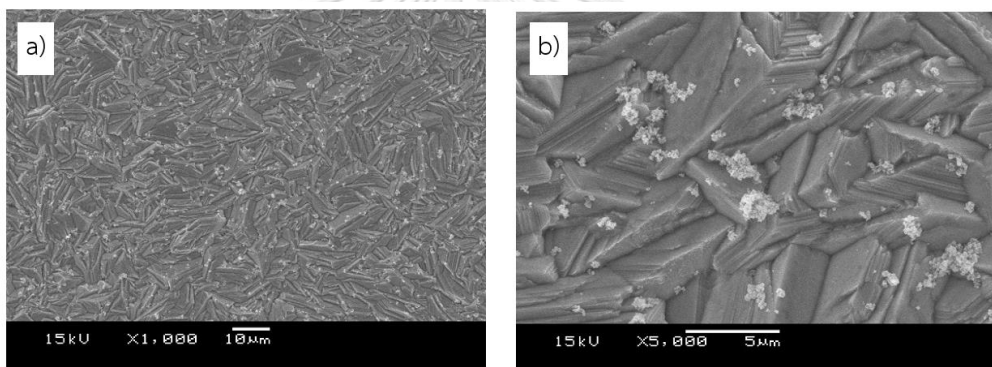
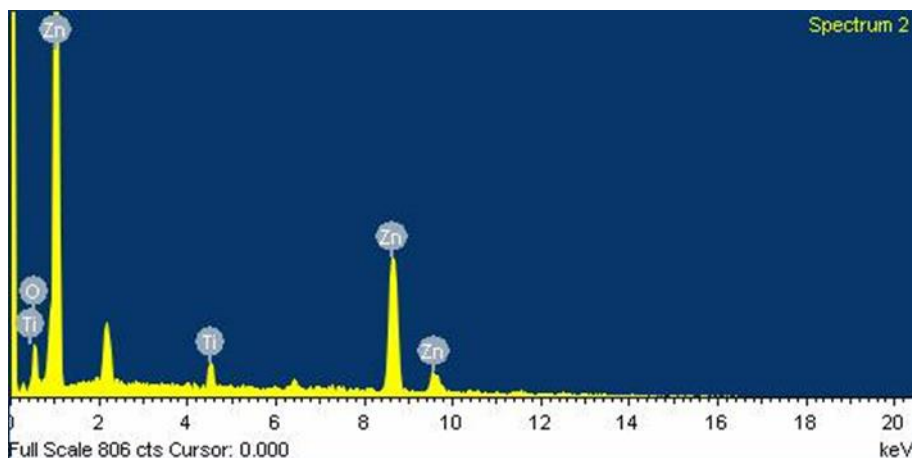


Figure 38 The Zn electrodeposition with  $\text{TiO}_2$  5 g/L at current density of  $0.04 \text{ A/cm}^2$   
(a) 1000X and (b) 5000X

Energy Dispersive X-ray Spectrometer (EDS) with mapping analysis method was used to determine the chemical composition and elemental analysis. The EDS result of sample with current density of  $0.01 \text{ A/cm}^2$  is shown in Figure 39.



*Figure 39 EDS representative spectra of Zn with  $\text{TiO}_2$  5 g/L at current density of  $0.01 \text{ A/cm}^2$*

Generally, the composite layer properties directly relate to the amounts of incorporated particles, their uniform distribution within the metal matrix as well as the obtained morphology of the metal. In this work all samples with different current densities ( $0.01$ ,  $0.02$ ,  $0.03$ , and  $0.04 \text{ A/cm}^2$ ) consist of 95 wt% zinc, 3-5 wt% oxygen and 0.8 wt% titanium. Therefore, in this case, the wt% titanium increased slightly when the current density for electroplating increased. However, all tested current densities are not big different in values. Therefore, they did not provide any insignificant effect on wt% of the elements. The wt% zinc, titanium and oxygen of all samples are shown in Figure 40. The samples with  $\text{TiO}_2$  on the coated surface would affect to Zn electrode and properties, which the performances of the battery will be shown in another section.



Figure 40 The wt% of Zn, O, and TiO<sub>2</sub> at different current densities

#### 4.1.1.5 The Zn electrodeposition with TiO<sub>2</sub> 10 g/L

The Zn -TiO<sub>2</sub> composite layer was prepared by using electrodeposition technique, which deposited with different current densities (0.01, 0.02, 0.03, and 0.04 A/cm<sup>2</sup>). In the bath for electrodeposition, with 10g of TiO<sub>2</sub> addition, carbon steel plate was used as an anode and stainless steel was used as a cathode. Stainless steel size of 5 cm x 5 cm was used as a substrate to deposit zinc coatings. After the electrodeposition of zinc, the scanning electron microscope (SEM) was used to study the morphology and microstructure of the electrodes.

Zn-TiO<sub>2</sub> composite layers with significant different morphologies were obtained by varying current density. All samples with different current densities (0.01, 0.02, 0.03, and 0.04 A/cm<sup>2</sup>) show the coated microstructure with the randomly size-distributed crystals. The crystals stacked and transformed to a multilayer structure in Zn-TiO<sub>2</sub> composite coatings as shown in Figures 41-44 with the particle size of ~5.4 to 8.37. During the electrodeposition process the crystal size was controlled by the formation of the crystal growth rate. Fine-grained deposits are generally obtained with a faster formation of nucleation sites as result of heterogeneous nucleation. The bigger grain size was increased when the current density for deposited was increased. The samples with all current densities exhibit uniform distribution of TiO<sub>2</sub> nanoparticles on the Zn surface.

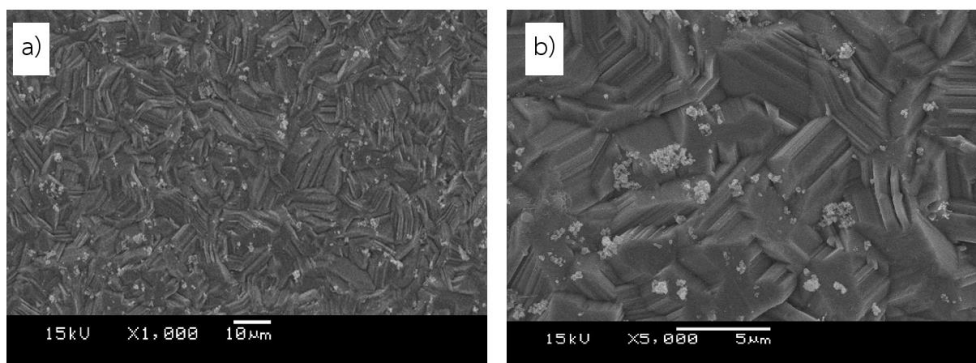


Figure 41 The Zn electrodeposition with  $\text{TiO}_2$  10 g/L at current density of  $0.01 \text{ A/cm}^2$   
(a) 1000X and (b) 5000X

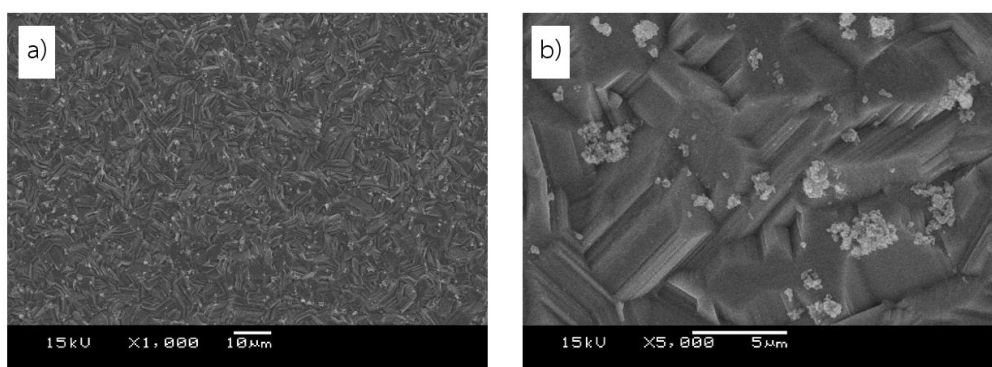


Figure 42 The Zn electrodeposition with  $\text{TiO}_2$  10 g/L at current density of  $0.02 \text{ A/cm}^2$   
(a) 1000X and (b) 5000X

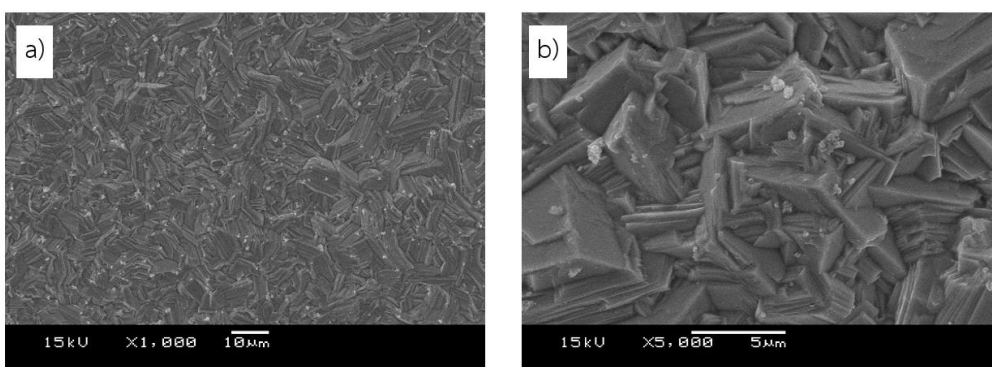


Figure 43 The Zn electrodeposition with  $\text{TiO}_2$  10 g/L at current density of  $0.03 \text{ A/cm}^2$   
(a) 1000X and (b) 5000X

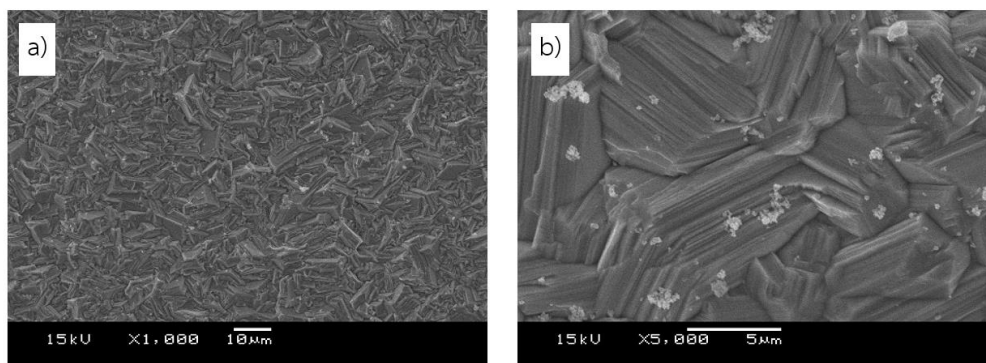


Figure 44 The Zn electrodeposition with  $\text{TiO}_2$  10 g/L at current density of  $0.04 \text{ A/cm}^2$   
(a) 1000X and (b) 5000X

Energy Dispersive X-ray Spectrometer (EDS) with mapping analysis method was used to determine the chemical composition and elemental analysis. The EDS result of sample with current density of  $0.01 \text{ A/cm}^2$  is shown in Figure 45.

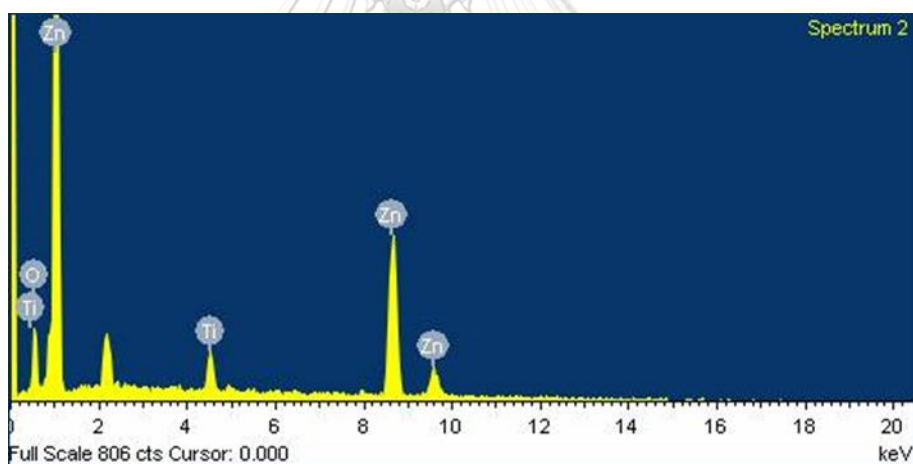


Figure 45 EDS representative spectra of Zn with  $\text{TiO}_2$  10 g/L  
at current density of  $0.01 \text{ A/cm}^2$

Generally, the composite layer properties directly relate to the amounts of incorporated particles, their uniform distribution within the metal matrix as well as the obtained morphology of the metal. In this work, all samples with different current densities (0.01, 0.02, 0.03, and 0.04 A/cm<sup>2</sup>) consist of 90 wt% zinc, 8 wt% oxygen and 2 wt% titanium. Therefore, in this case, the wt% titanium increased slightly when the current density for electroplating increased. However, all tested current densities are not big different in values. Therefore, they did not provide any insignificant effect on wt% of the elements. The wt% zinc, titanium and oxygen of all samples are shown in Figure 46. The samples with TiO<sub>2</sub> on the coated surface would affect to Zn electrode and properties, which the performances of the battery will be shown in another section.

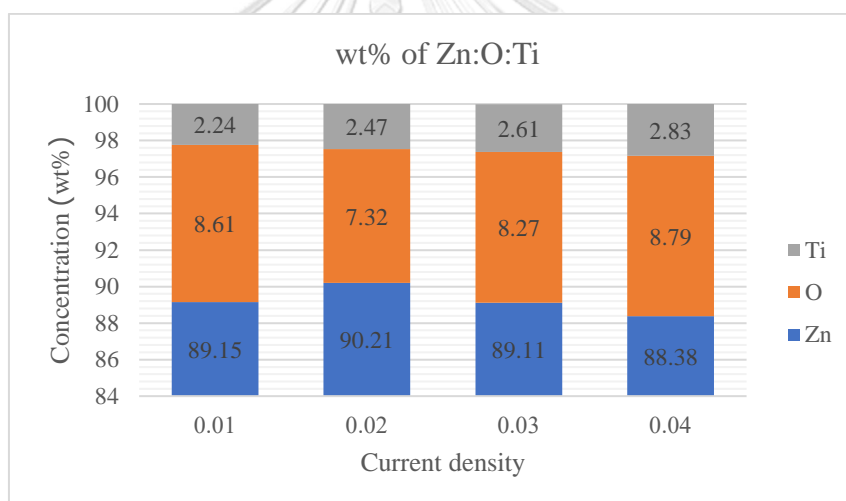
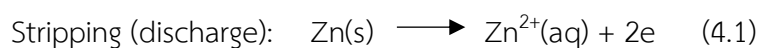


Figure 46 The wt% of Zn, O, and TiO<sub>2</sub> at different current densities



## 4.2 Zn Plating and Stripping

The reversible Zn plating/stripping becomes possible to a certain extent. Thus, recharging the battery becomes much easier by means of the following reactions.



The different metal surfaces exhibit different kinetic overpotentials for surface reactions. According to the previous research, the actual potential at which hydrogen gas evolved is significantly lowered and make the possibility for Zn to deposited instead and affecting to the performances of the battery.

The reversible plating/stripping of Zn is one of the most important aspects of the Zn electrode for ZIBs and another important is electrolyte (2M ZnSO<sub>4</sub>+0.5M MnSO<sub>4</sub>), which was chosen for this study. The long-term cycling behavior of the Zn electrode was examined using a Zn||Zn cell in 2M ZnSO<sub>4</sub>+0.5M MnSO<sub>4</sub>. Zn electrodes were used as positive and negative electrodes. The cells were tested for 500 cycles at 0.5 mA/cm<sup>2</sup> for 15 min at each cycle.

#### 4.2.1 The Zn without $\text{TiO}_2$

Figure 47 shows polarization voltage during cycling. At each current density (0.01, 0.02, 0.03, 0.04  $\text{A}/\text{cm}^2$ ), the polarization voltage was bounded by the maximum and minimum voltages of  $-0.06$  to  $+0.06$  V. Furthermore, the voltages did increase upon the cycling indicating that Zn had passivation layer which took place on the Zn surface. Therefore, Zn plating and stripping were unstable until the end of testing at 500 cycles (about 250 hours). This might be due to that there was some corrosion or dendrite formation on the Zn electrode surface.

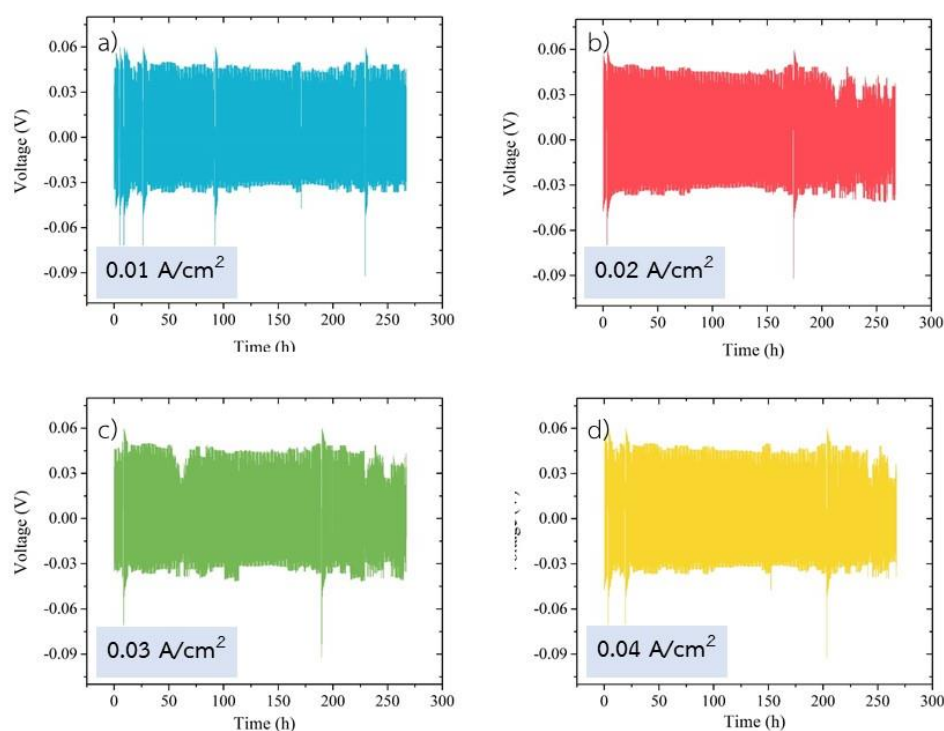


Figure 47 Polarization voltage during cycle of samples Zn without  $\text{TiO}_2$  at different current densities a) 0.01 b) 0.02, c) 0.03, and d) 0.04  $\text{A}/\text{cm}^2$

#### 4.2.2 The Zn with $\text{TiO}_2$ 1g/L

Figure 48 shows polarization voltage during cycling, at low current densities (0.01, 0.02, 0.03  $\text{A}/\text{cm}^2$ ), the polarization voltage was bounded by the maximum and minimum voltages of  $-0.05$  to  $+0.05$  V. The sample deposited at current density of  $0.02\text{A}/\text{cm}^2$  can stable at this polarization voltage until 250 hours. At the highest current density ( $0.04\text{ A}/\text{cm}^2$ ), the polarization voltage was bounded by the maximum and minimum voltages of  $-0.06$  to  $+0.06$  V. The voltages did slightly increase upon the cycling indicating that Zn had passivation layer takes place on the Zn surface. Therefore, Zn plating and stripping were unstable until the end of testing at 500 cycles (about 250 hours).

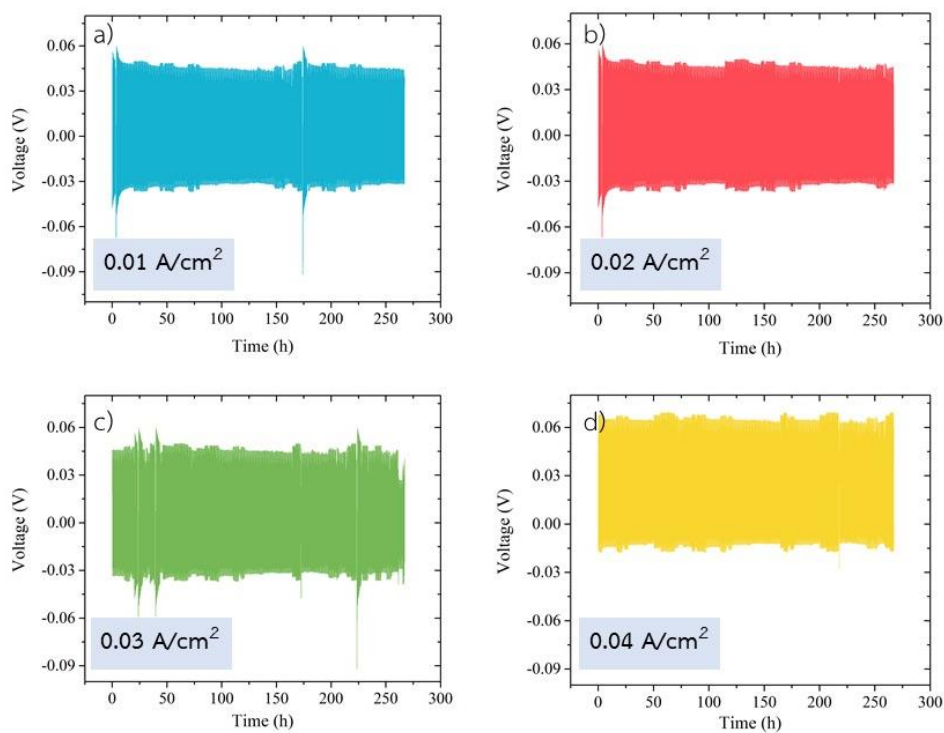


Figure 48 Polarization voltage during cycle of samples Zn with  $\text{TiO}_2$  1g/L at different current densities a) 0.01 b) 0.02, c) 0.03, and d)  $0.04\text{ A}/\text{cm}^2$

#### 4.2.3 The Zn with TiO<sub>2</sub> 3g/L

Figure 49 shows polarization voltage during cycling, at the lowest current density (0.01 A/cm<sup>2</sup>), the polarization voltage at this current density was bounded by the maximum and minimum voltages of -0.05 to +0.05 V. It increased from initial testing -0.03 to +0.03 V. However, at current density of 0.02 A/cm<sup>2</sup>, the polarization voltage was bounded by the maximum and minimum voltages of -0.04 to +0.04 V and stable at this polarization voltage until 250 hours. At current density of 0.03 A/cm<sup>2</sup> the polarization voltage at this current density was bounded by the maximum and minimum voltages of -0.05 to +0.05 V. It also increased from initial testing. At the highest current density (0.04 A/cm<sup>2</sup>), the polarization voltage was bounded by the maximum and minimum voltages of -0.05 to +0.05 V and unstable until the end of testing. In this case with all current densities for depositing Zn electrode, it can be continued for testing up to 500 cycles, which are longer cycle testing than those of samples deposited with TiO<sub>2</sub> 1 g/L. This might be due to that TiO<sub>2</sub> on the surface can suppress dendrite formation and reduce a corrosion rate.

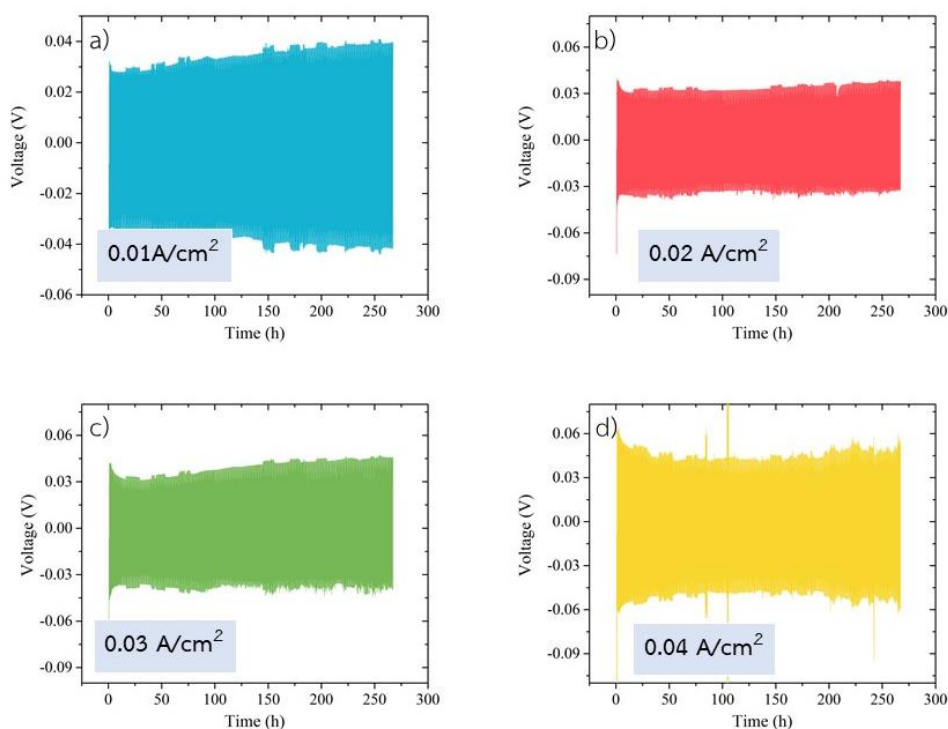


Figure 49 Polarization voltage during cycle of samples Zn with TiO<sub>2</sub> 3g/L at different current densities a) 0.01 b) 0.02, c) 0.03, and d) 0.04 A/cm<sup>2</sup>

#### 4.2.4 The Zn with TiO<sub>2</sub> 5g/L

Figure 50 shows polarization voltage during cycling, at the lowest current density (0.01 A/cm<sup>2</sup>), the polarization voltage at this current density was bounded by the maximum and minimum voltages of -0.05 to +0.05 V. It decreased after testing for 70 hours. The polarization voltage is in the range of -0.04 to +0.04 V. However, at higher current densities (0.02-0.03 A/cm<sup>2</sup>), The polarization voltage was bounded by the maximum and minimum voltages of -0.03 to +0.03 V. Also, the voltages were a slightly increased upon the longer cycling indicating that no passivation layer took place on the Zn surface. Therefore, Zn plating and stripping were stable until the end of testing at 500 cycles (about 250 hours). The highest current density (0.04 A/cm<sup>2</sup>), the polarization voltage was bounded by the maximum and minimum voltages of -0.04 to +0.04 V. After testing for 150 hours, it increased to -0.05 to +0.05 V. In this case with all current densities for depositing Zn electrode can be continued for testing up to 500 cycles. This might be due to that TiO<sub>2</sub> on the surface can suppress dendrite formation and reduce a corrosion rate as well as affect to the performances of the battery, which will be shown in another section.

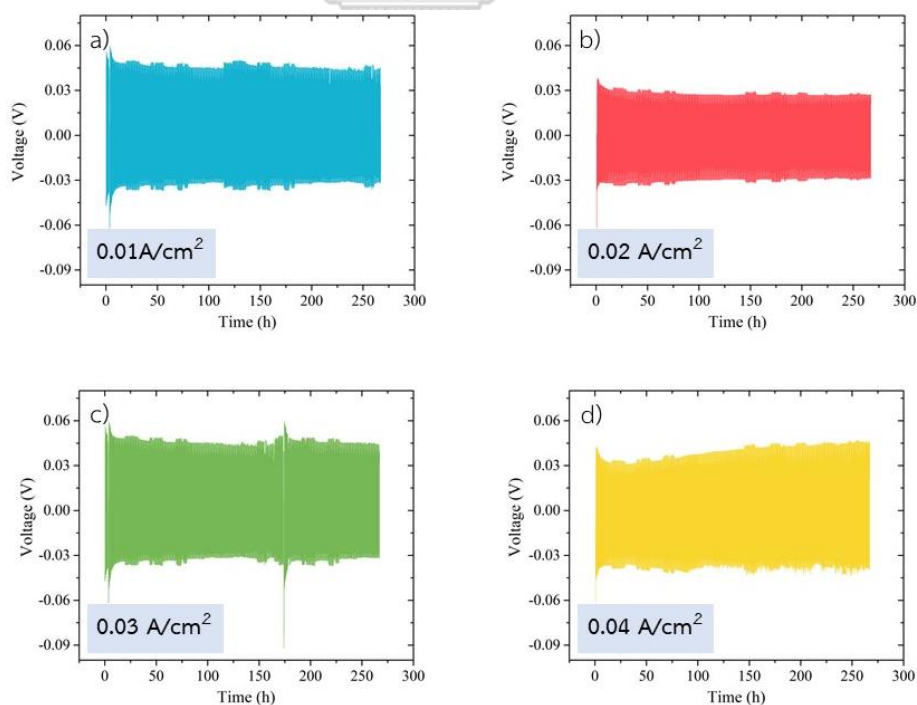


Figure 50 Polarization voltage during cycle of samples Zn with TiO<sub>2</sub> 5g/L at different current densities a) 0.01 b) 0.02, c) 0.03, and d) 0.04 A/cm<sup>2</sup>

#### 4.2.4 The Zn with TiO<sub>2</sub> 10g/L

Figure 51 shows polarization voltage during cycling, at current densities (0.01, 0.02, 0.03 A/cm<sup>2</sup>), the polarization voltage at each current density was bounded by the maximum and minimum voltages of -0.03 to +0.03 V. The voltages did not increase upon the longer cycling indicating that no passivation layer took place on the Zn surface. The highest current density (0.04 A/cm<sup>2</sup>) the polarization voltage was bounded by the maximum and minimum voltages of -0.04 to +0.04 V, with slightly increased voltages. In this with case of all samples, the Zn plating and stripping were stable until the end of testing at 500 cycle (about 250 hours). This was due to that the TiO<sub>2</sub> on the surface can suppress dendrite formation and reduce a corrosion rate as well as affect to the performances of the battery, which will be shown in another section.

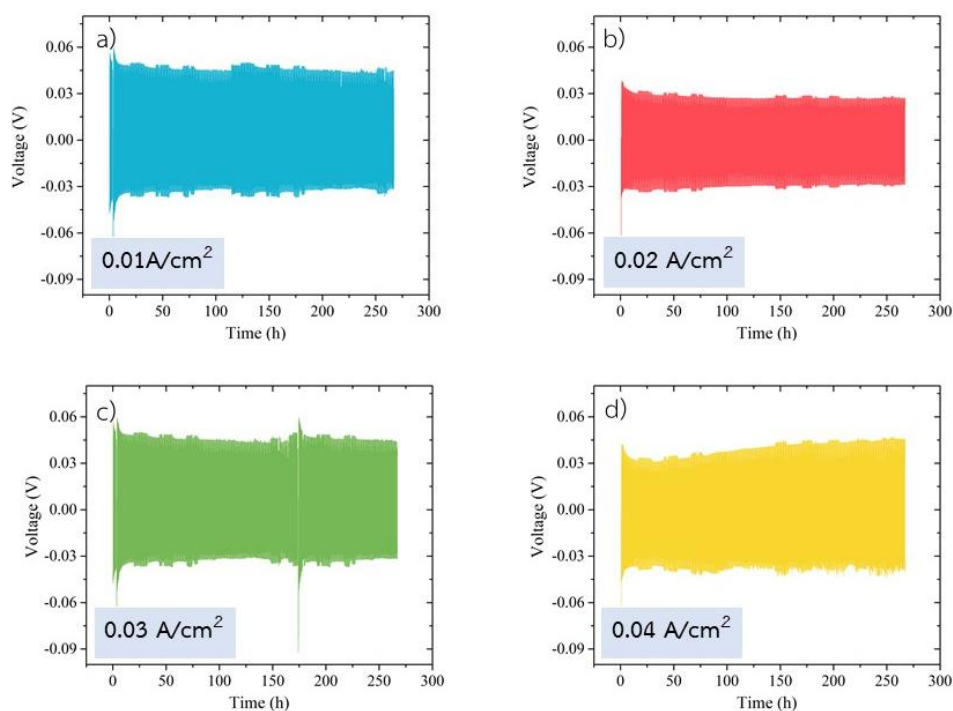


Figure 51 Polarization voltage during cycle of samples Zn with TiO<sub>2</sub> 10g/L at different current densities a) 0.01 b) 0.02, c) 0.03, and d) 0.04 A/cm<sup>2</sup>

### 4.3 Potentiostat

#### 4.3.1 Potentiostat (Cyclic voltammetry, CV)

The cyclic voltammetry of the  $\text{MnO}_2$  electrode was prepared for the cell as a battery by using the two-electrode configuration where the negative (Zn) electrode and the positive ( $\text{MnO}_2$ ) electrode were connected as the counter and the working electrodes, respectively. The counter electrode was used as the reference electrode. Testing for 3 cycles with the potential range from 1.0 to 2.0 V with a scanning rate of 0.5 mV/s was performed for each sample to check the charge-transfer characteristic of the  $\text{MnO}_2$  electrode.

##### 4.3.1.1 The Zn without $\text{TiO}_2$

Figure 52, all current densities for deposited Zn electrode show that the reduction reaction points are close has started the open-circuit potential from 1.67 V. This may be a result of the insertion of  $\text{Zn}^{2+}$  into the  $\text{MnO}_2$  (Charge process). The oxidation peak occurred at 1.5 V, which can be referred to the  $\text{Zn}^{2+}$  extraction from the  $\text{MnO}_2$  (Discharge process). According to the previous research [26]. This behaviour of the present work has reduction-oxidation reaction in the similar range.

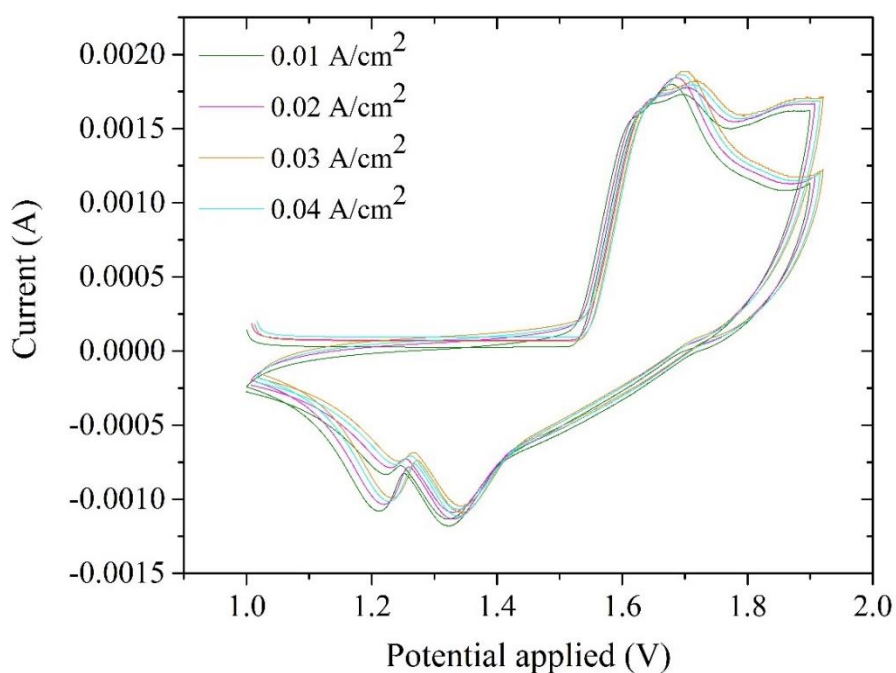


Figure 52 Cyclic voltammetry of Zn without  $\text{TiO}_2$  at all current densities



#### 4.3.1.2 The Zn with $\text{TiO}_2$ 10 g/L

Figure 53 shows the reduction reaction points has started the open-circuit potential from 1.69 V. This may be a result of the insertion of  $\text{Zn}^{2+}$  into the  $\text{MnO}_2$  (Charge process). The oxidation peak occurred at 1.58 V, which can be referred to the  $\text{Zn}^{2+}$  extraction from the  $\text{MnO}_2$  (Discharge process). According to the previous research [26]. This behaviour of the present work has reduction-oxidation reaction in the similar range.

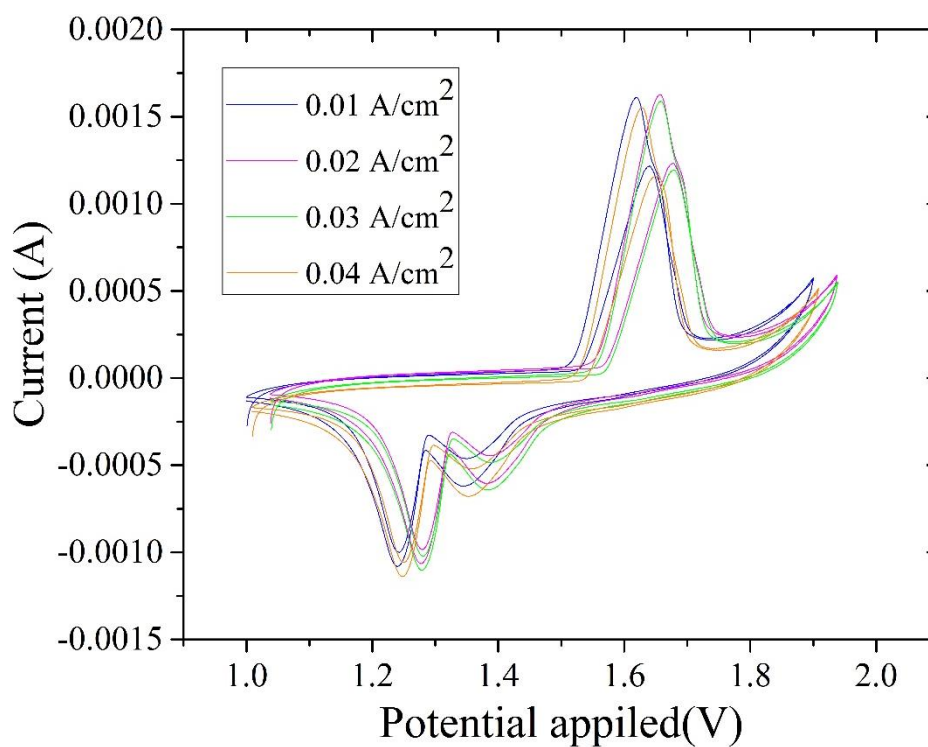


Figure 53 Cyclic voltammetry of Zn with  $\text{TiO}_2$  10g/L at all current densities



### 4.3.2 Potentiostatic (The electrochemical impedance spectroscopy, EIS)

To investigate the change in the charge-transfer characteristic of the battery, EIS Nyquist plots were performed using the two electrodes configuration with potentiostatic EIS mode in the frequency range of 100 kHz to 10mHz and amplitude potential of 10mV. Figures 54 and 55 show the EIS Nyquist plots of the Zn without  $\text{TiO}_2$  and with  $\text{TiO}_2$  10 g/L, respectively in the fully charged and discharged electrode at the 10 cycles. The results show that the Zn with  $\text{TiO}_2$  10 g/L has smaller impedance and lower charge-transfer resistance compared with those of the Zn without  $\text{TiO}_2$  at all current densities for deposited Zn electrode. Thus, the lower resistance can provide the higher performances of the battery.

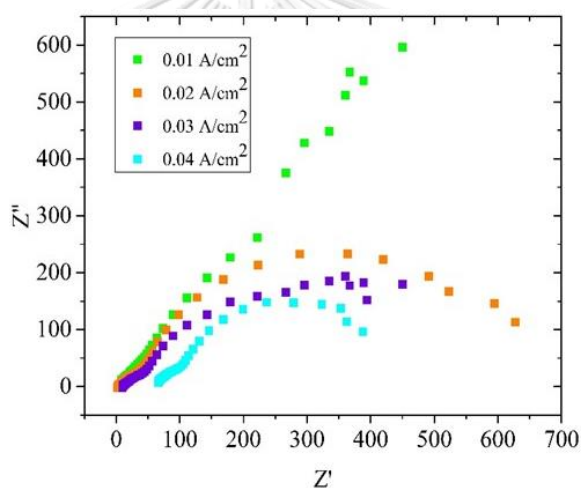


Figure 54 EIS of the Zn without  $\text{TiO}_2$

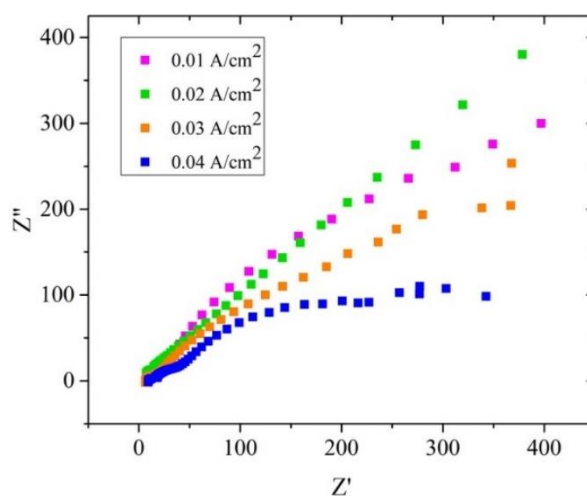


Figure 55 EIS of the Zn with  $\text{TiO}_2$  10 g/L

#### 4.4 Battery performance (Rate ability)

The batteries exhibit an open-circuit voltage of about 1.35-1.68 V as prepared. The rate ability test was conducted by discharging the battery until it reaching to the lower cutoff voltage of 0.6 V. Then charging was continued until it reaching to a higher cutoff voltage of 1.7 V. The cell was tested at different current densities of 50, 100, 200, 500, and 1000 mA/g  $\text{MnO}_2$  for 5 cycles at each current density.

##### 4.4.1 The Zn without $\text{TiO}_2$

Figures 56 a), b), c), and d) show the rate ability of the Zn without  $\text{TiO}_2$  with current densities of 0.01, 0.02, 0.03, and 0.04  $\text{A}/\text{cm}^2$ , respectively, illustrating the rate ability of the battery from the 1<sup>st</sup> cycle to the 25<sup>th</sup> cycle. The charge & discharge specific capacity and columbic efficiency of all samples are shown in the figures. The columbic efficiency of Zn without  $\text{TiO}_2$  of all current densities are about 90-98% and operate with higher stability.

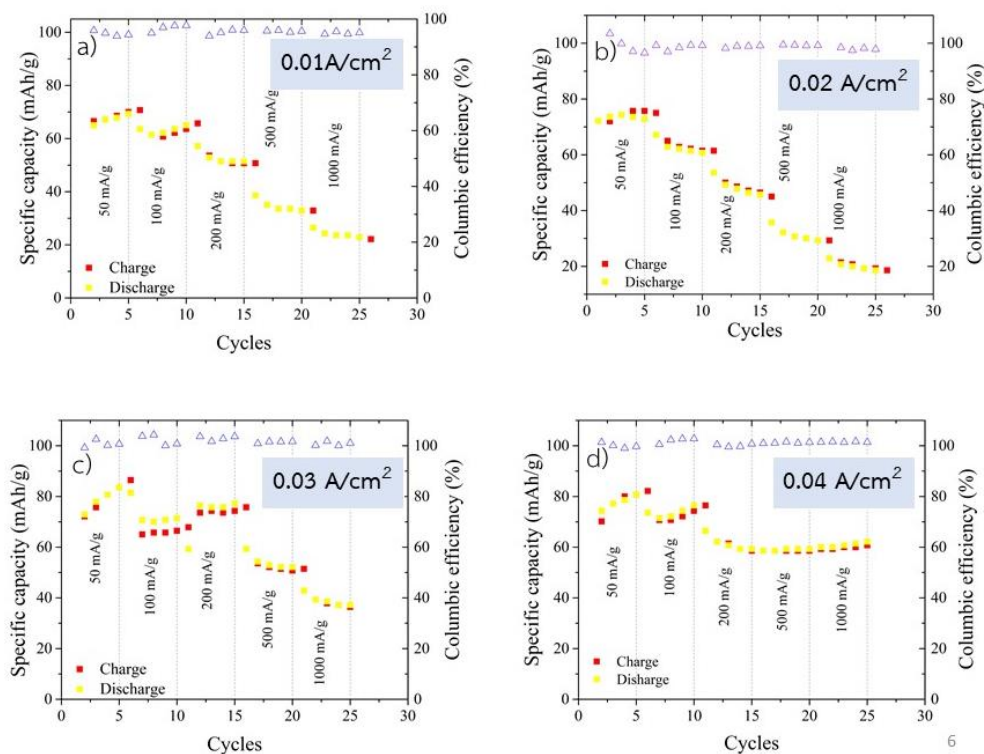


Figure 56 Rate ability of the Zn without  $\text{TiO}_2$  at different current densities

Figure 57 shows charge-discharge profile of Zn without  $\text{TiO}_2$  with current densities of 0.01, 0.02, 0.03, and 0.04  $\text{A}/\text{cm}^2$ , respectively. The coin cells were tested at current density at  $50\text{mA}/\text{g}$  in 1<sup>st</sup>-5<sup>th</sup> cycle under the lower and upper cut-off voltage between 0.6-1.7V. The results show open circuit voltage of freshly fabricated cells in table 4 and discharge specific capacity in table 5.

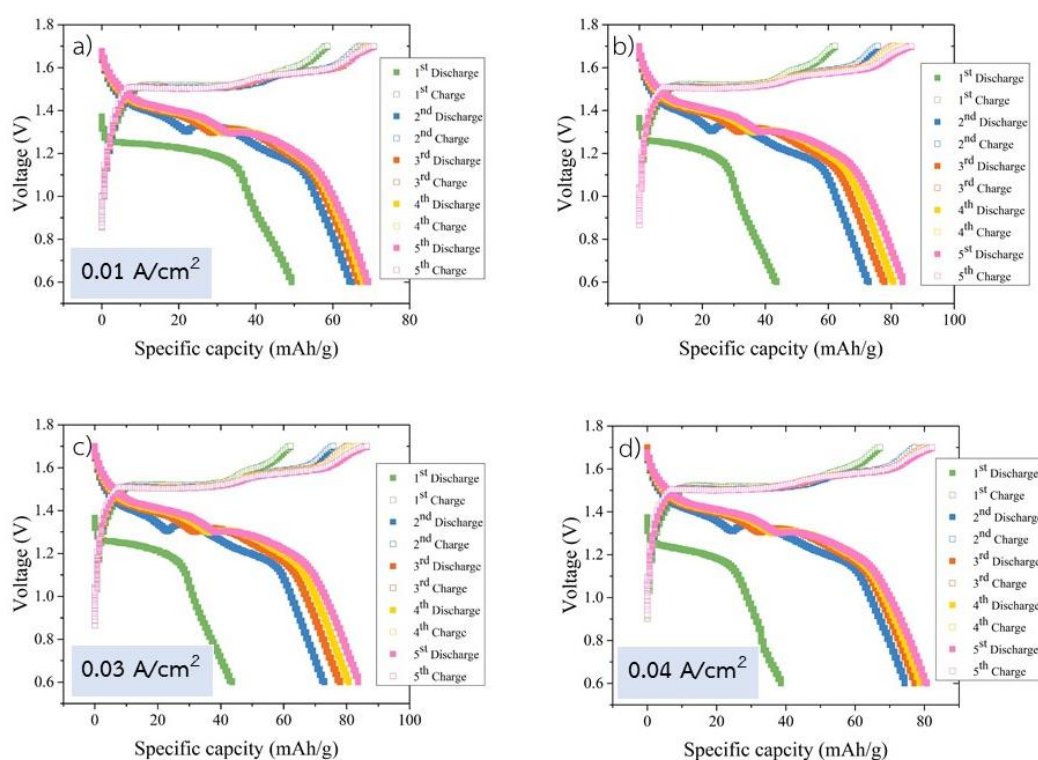


Figure 57 Charge-discharge profiles at  $50\text{ mA}/\text{g}$  in 1<sup>st</sup>-5<sup>th</sup> cycles of the Zn without  $\text{TiO}_2$  at different current densities

The battery exhibited an open-circuit voltage of the Zn without  $\text{TiO}_2$  about 1.37-1.38 V as prepared. The voltage of coin cell will increase when the current density for electroplating increase but not very different as shown in table 4.

Table 4 Open circuit voltage of the Zn without  $\text{TiO}_2$

	Zn deposited with different current densities			
	0.01 $\text{A}/\text{cm}^2$	0.02 $\text{A}/\text{cm}^2$	0.03 $\text{A}/\text{cm}^2$	0.04 $\text{A}/\text{cm}^2$
Open circuit voltage	1.3725 V	1.3818 V	1.3654 V	1.3741 V

The discharge specific capacities of Zn without  $\text{TiO}_2$  of all current densities were tested at current density at  $50\text{mA/g}$  in  $1^{\text{st}}\text{-}5^{\text{th}}$  cycle, as the result shows in table 5. The specific capacity increased slightly at  $2^{\text{nd}}\text{-}5^{\text{th}}$  cycle due to electrolyte can be better adsorbed into the  $\text{MnO}_2$  cathode. When comparing with different current densities, the specific capacity increased slightly when the current density for electroplating is increased but it shows insignificant difference because the morphologies were similar.

Table 5 The initial discharge specific capacity with current density at  $50\text{ mA/g}$  of the Zn without  $\text{TiO}_2$

Cycles	Zn deposited with different current densities			
	$0.01\text{ A/cm}^2$	$0.02\text{ A/cm}^2$	$0.03\text{ A/cm}^2$	$0.04\text{ A/cm}^2$
$1^{\text{st}}$	51.4419	43.2654	41.4593	39.7443
$2^{\text{nd}}$	65.9532	72.14286	72.85714	74.28571
$3^{\text{rd}}$	67.14286	73.57143	74.85714	77.14286
$4^{\text{th}}$	67.85714	74.28571	77.71429	78.57143
$5^{\text{th}}$	69.28571	73.57143	83.57143	84.71429

Figure 58 shows charge-discharge profile in  $1^{\text{st}}$  cycle of Zn without  $\text{TiO}_2$  with all current densities. The coin cells were tested at various current densities of 50, 100, 200, 500, and 1000  $\text{mA/g}$  under the lower and upper cut-off voltage between 0.6-1.7V. The obtained resulted are shown in table 6.

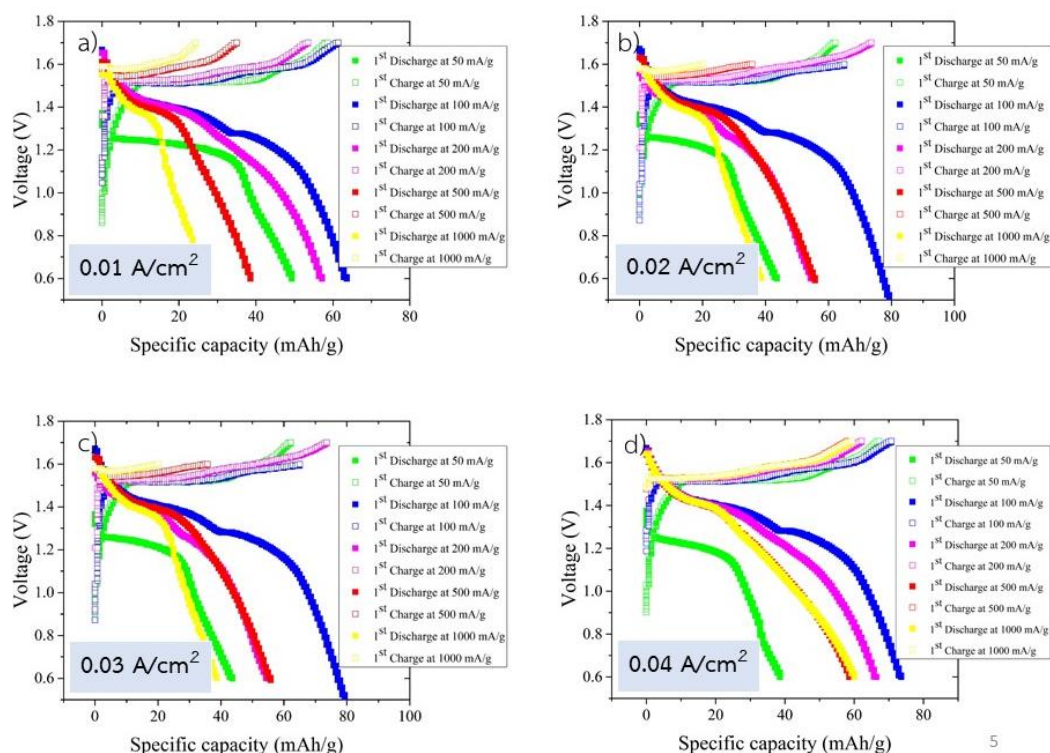


Figure 58 Charge-discharge profiles at various current densities of 50, 100, 200, 500, and 1000 mA/g of the Zn without  $\text{TiO}_2$  at different current densities

Table 6 shows the discharge specific capacities of Zn without  $\text{TiO}_2$  with all current densities. They tested at various current densities of 50, 100, 200, 500, and 1000 mA/g, respectively. When current densities were increased for testing at 6<sup>th</sup>-25<sup>th</sup> cycles, lower specific capacities than those of 1<sup>st</sup>-5<sup>th</sup> cycles were obtained due to the  $\text{MnO}_2$  cathode has ZnO on the surface. Therefore, electrolyte was reduced by being adsorbed into the  $\text{MnO}_2$  cathode. On the other hand, when comparing with current density for depositing, it was found that the specific capacities were increased slightly when the current densities for electroplating were increased. They show insignificant results due to morphology of Zn electrode with non-uniform crystal of Zn layer and similar current densities.

Table 6 The initial discharge specific capacity at various current densities of 50, 100, 200, 500, and 1000 mA/g of the Zn without TiO<sub>2</sub>

Cycles	Zn deposited with different current densities			
	0.01 A/cm <sup>2</sup>	0.02 A/cm <sup>2</sup>	0.03 A/cm <sup>2</sup>	0.04 A/cm <sup>2</sup>
1 <sup>st</sup> (50 mA/g)	51	43.26	41.4	39.74
6 <sup>th</sup> (100 mA/g)	63.57143	72.85714	81.42857	73.57143
11 <sup>th</sup> (200 mA/g)	57.14286	60.71429	59.28571	66.42857
16 <sup>th</sup> (500 mA/g)	38.57143	45.71429	59.28571	58.57143
21 <sup>st</sup> (1000 mA/g)	26.42857	29.28571	40.85714	60

From the rate ability of the Zn without TiO<sub>2</sub> with all current densities (0.01-0.04 A/cm<sup>2</sup>) shows that increasing the current density for electroplating also increases slightly the specific capacity. This was due to that morphology of Zn electrode at higher current density has higher wt% of Zn, which Zn<sup>+</sup> could insert into MnO<sub>2</sub> more than that of the lower current density with non-uniform crystal of Zn layer with similar current density. Therefore, there was insignificant effect to the specific capacity. The columbic efficiencies of all samples are of 90-98% and operate with higher stability. The battery efficiency depends not only on the morphology of Zn deposits but also on the type used of electrolyte.



#### 4.4.2 The Zn with TiO<sub>2</sub> 1 g/L

Figures 59 a), b), c), and d) show the rate ability of the Zn with TiO<sub>2</sub> 1 g/L with current densities of 0.01, 0.02, 0.03, and 0.04 A/cm<sup>2</sup>, respectively, illustrating the rate ability of the battery from the 1<sup>st</sup> cycle to the 25<sup>th</sup> cycle. The charge & discharge specific capacity and columbic efficiency of all samples are shown in the figures. The columbic efficiency of Zn with TiO<sub>2</sub> 1 g/L of all current densities are about 93-98% and operate with higher stability.

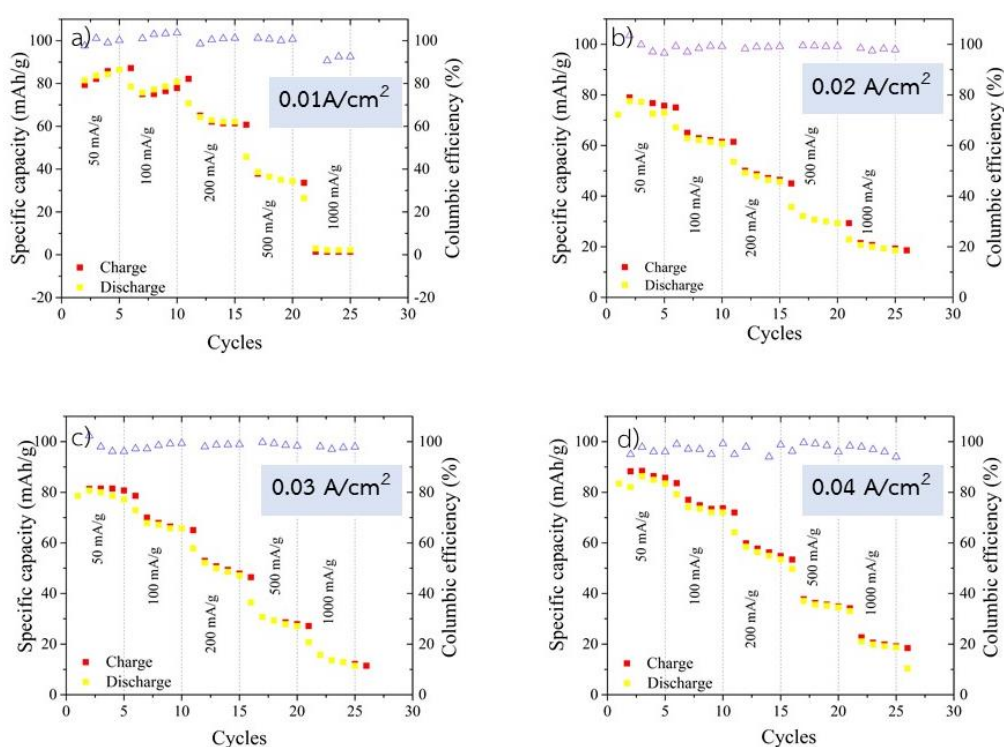


Figure 59 Rate ability of the Zn with TiO<sub>2</sub> 1 g/L at different current densities

Figure 60 shows charge-discharge profile of Zn with TiO<sub>2</sub> 1 g/L with current densities of 0.01, 0.02, 0.03, and 0.04 A/cm<sup>2</sup>, respectively. The coin cells were tested at current density at 50mA/g in 1<sup>st</sup>-5<sup>th</sup> cycle under the lower and upper cut-off voltage between 0.6-1.7V. The results show open circuit voltage of freshly fabricated cells in table 7 and discharge specific capacity in table 8.

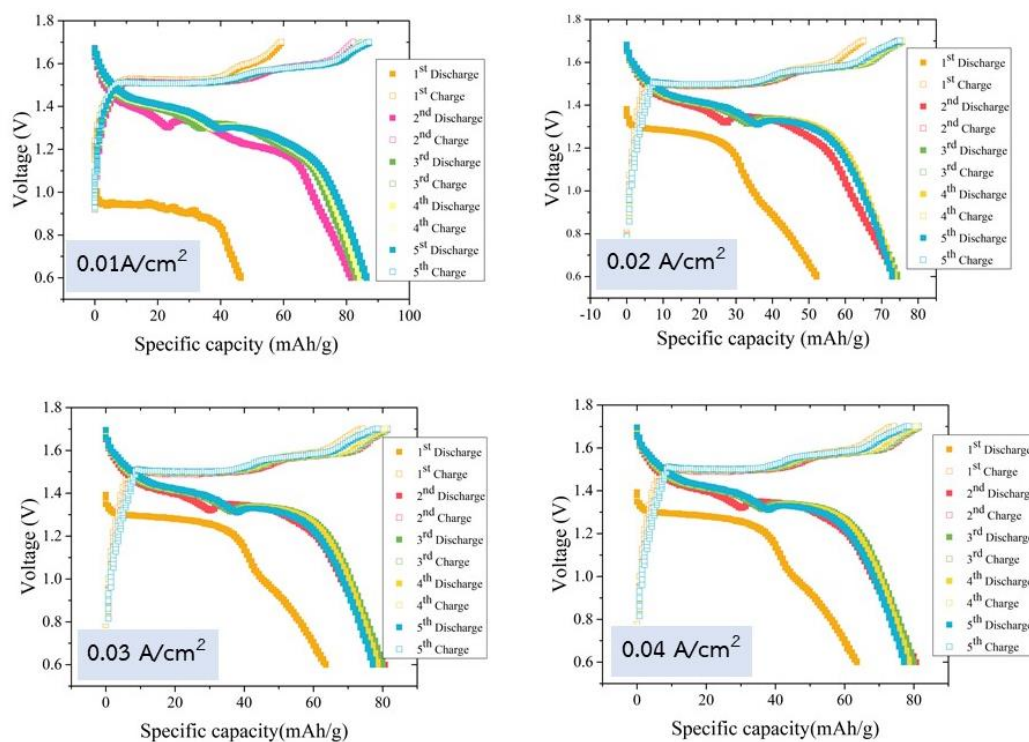


Figure 60 Charge-discharge profiles at 50 mA/g in 1<sup>st</sup>-5<sup>th</sup> cycles of the Zn with TiO<sub>2</sub> 1 g/L at different current densities

The battery provides an open-circuit voltage of the Zn with TiO<sub>2</sub> 1 g/L about 1.0-1.38 V as prepared. The voltage of coin cell will increase when the current density for electroplating increase but not very different as shown in table 7.

Table 7 Open circuit voltage of the Zn with TiO<sub>2</sub> 1 g/L

	Zn deposited with different current densities			
	0.01 A/cm <sup>2</sup>	0.02 A/cm <sup>2</sup>	0.03 A/cm <sup>2</sup>	0.04 A/cm <sup>2</sup>
Open circuit voltage	1.0868	1.3814	1.3799	1.3801



The discharge specific capacity of Zn with  $\text{TiO}_2$  1 g/L with all current densities were tested at current densities at 50mA/g in 1<sup>st</sup>-5<sup>th</sup> cycle, the result shows in table 8. The specific capacity increased slightly at 2<sup>nd</sup>-5<sup>th</sup> cycle due to electrolyte can be better adsorbed into the  $\text{MnO}_2$  cathode. When comparing results of different current densities, the specific capacity increased slightly when the current density for electroplating increased but not very different because the morphology was similar.

Table 8 The initial discharge specific capacity with current density at 50 mA/g of the Zn with  $\text{TiO}_2$  1 g/L

Cycles	Zn deposited with different current density			
	0.01 A/cm <sup>2</sup>	0.02 A/cm <sup>2</sup>	0.03 A/cm <sup>2</sup>	0.04 A/cm <sup>2</sup>
1 <sup>st</sup>	46.88432	54.14286	68.57143	63.45143
2 <sup>nd</sup>	81.42857	77.57143	81.71429	78.03629
3 <sup>rd</sup>	83.57143	77.28571	80	79.322
4 <sup>th</sup>	84.28571	72.57143	78.57143	80.89343
5 <sup>th</sup>	86.42857	72.85714	77.14286	84.46486

Figure 61 shows charge-discharge profile in 1<sup>st</sup> cycle of Zn with  $\text{TiO}_2$  1 g/L all current densities. The coin cells were tested at various current densities of 50, 100, 200, 500, and 1000 mA/g under the lower and upper cut-off voltage between 0.6-1.7V. The obtained results are shown in table 9.

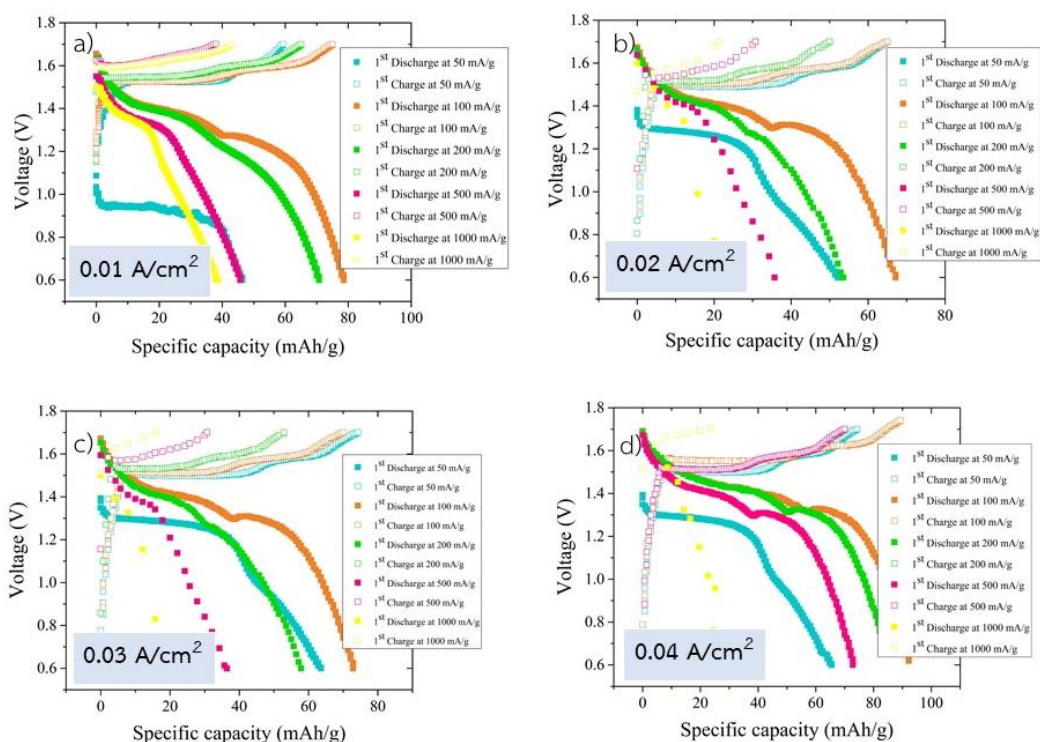


Figure 61 Charge-discharge profiles at various current densities of 50, 100, 200, 500, and 1000 mA/g of the Zn with  $\text{TiO}_2$  1 g/L at different current densities

Table 9 shows the discharge specific capacities of Zn with  $\text{TiO}_2$  1 g/L of all current densities. They were tested at various current densities of 50, 100, 200, 500, and 1000 mA/g, respectively. When current densities for testing increased, it was found that at 6<sup>th</sup>-25<sup>th</sup> cycles they have lower specific capacities than those of 1<sup>st</sup>-5<sup>th</sup> cycle due to that the  $\text{MnO}_2$  cathode has ZnO on the surface. Therefore, electrolyte could be reduced by being adsorbed into the  $\text{MnO}_2$  cathode. On the other hand, when comparing with this current density for depositing, it was found that the specific capacity increased slightly when the current density for electroplating increased but not very different due to morphology of Zn electrode, which was found less amount with non-uniform distribution of  $\text{TiO}_2$  nanoparticles on the Zn surface and current densities not very different.

Table 9 The initial discharge specific capacity at various current densities of 50, 100, 200, 500, and 1000 mA/g of the Zn with TiO<sub>2</sub> 1 g/L

Cycles	Zn deposited with different current densities			
	0.01 A/cm <sup>2</sup>	0.02 A/cm <sup>2</sup>	0.03 A/cm <sup>2</sup>	0.04 A/cm <sup>2</sup>
1 <sup>st</sup> (50 mA/g)	46.88432	54.14286	68.57143	63.45143
6 <sup>th</sup> (100 mA/g)	78.57143	67.14286	72.85714	92.17914
11 <sup>th</sup> (200 mA/g)	70.71429	53.57143	57.85714	84.17914
16 <sup>th</sup> (500 mA/g)	45.71429	35.71429	36.42857	73.75057
21 <sup>st</sup> (1000 mA/g)	26.42857	22.85714	20.71429	33.03629

From the rate ability of the Zn with TiO<sub>2</sub> 1 g/L with all current densities (0.01-0.04 A/cm<sup>2</sup>) shows that increasing the current density for electroplating also increases slightly the specific capacity. This was due to that morphology of Zn electrode. At higher current density with higher wt% of Zn which Zn<sup>+</sup> could insert into MnO<sub>2</sub> more than that of the lower current density. Less and non-uniform distribution of TiO<sub>2</sub> nanoparticle on the Zn surface of electrode were observed, where current densities are not very different. Therefore, this could not provide any significant effect on the specific capacity. The columbic efficiencies of all samples are of 90-98% and operate with higher stability. The battery efficiency depends not only on the morphology of Zn deposits but also on the type used of electrolyte.

#### 4.4.3 The Zn with $\text{TiO}_2$ 3 g/L

Figures 62 a), b), c), and d) show the rate ability of the Zn with  $\text{TiO}_2$  3 g/L with current densities of 0.01, 0.02, 0.03, and 0.04  $\text{A}/\text{cm}^2$ , respectively, illustrating the rate ability of the battery from the 1<sup>st</sup> cycle to the 25<sup>th</sup> cycle. The figures also present charge & discharge specific capacity and columbic efficiency of all samples as shown in the figures. The columbic efficiencies of Zn with  $\text{TiO}_2$  3 g/L of all current densities are about 95-98% and operate with higher stability.

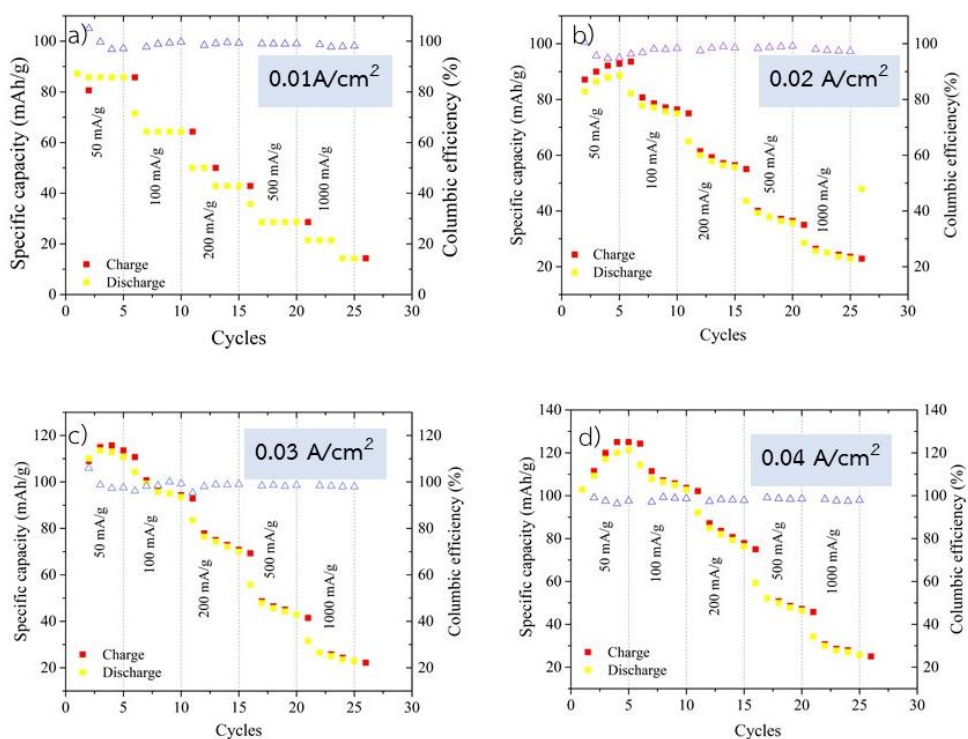


Figure 62 Rate ability of the Zn with  $\text{TiO}_2$  3 g/L at different current densities

Figure 63 shows charge-discharge profile of Zn with  $\text{TiO}_2$  3 g/L with current densities of 0.01, 0.02, 0.03, and 0.04  $\text{A}/\text{cm}^2$ , respectively. The coin cells were tested at current density at 50mA/g in 1<sup>st</sup>-5<sup>th</sup> cycle under the lower and upper cut-off voltage between 0.6-1.7 V. The obtained results show open circuit voltage of freshly fabricated cells in table 10 and discharge specific capacity in table 11.

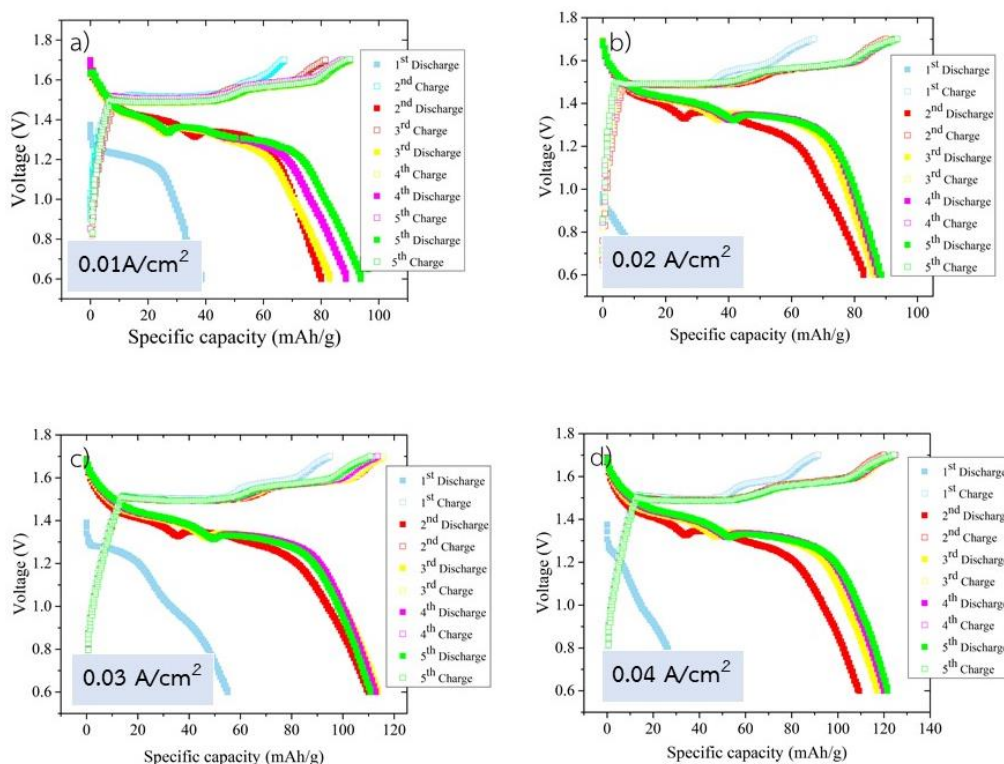


Figure 63 Charge-discharge profiles at 50 mA/g in 1<sup>st</sup>-5<sup>th</sup> cycles of the Zn with TiO<sub>2</sub> 3 g/L at different current densities

The battery provides an open-circuit voltage of the Zn with TiO<sub>2</sub> 3 g/L about 1.1-1.39 V as prepared. The voltage of coin cell increases when the current density for electroplating increases but not very different as shown in table 10.

Table 10 Open circuit voltage of the Zn with TiO<sub>2</sub> 3 g/L

	Zn deposited with different current densities			
	0.01 A/cm <sup>2</sup>	0.02 A/cm <sup>2</sup>	0.03 A/cm <sup>2</sup>	0.04 A/cm <sup>2</sup>
Open circuit voltage	1.3811	1.1163	1.3907	1.3

The discharge specific capacity of Zn with  $\text{TiO}_2$  3 g/L of all current densities were tested at current densities at 50mA/g in 1<sup>st</sup>-5<sup>th</sup> cycle, the result shows in table11. The specific capacity increased slightly at 2<sup>nd</sup>-5<sup>th</sup> cycle due to electrolyte can be better adsorbed into the  $\text{MnO}_2$  cathode. When comparing with different current densities for deposition, the specific capacity increased when the current density for electroplating increased because the morphology of the Zn crystal tended to form hexagonal platelets and transform to a multilayer structure that has small amount and non-uniform distribution  $\text{TiO}_2$  nanoparticles on the Zn surface.

Table 11 The initial discharge specific capacity with current density at 50 mA/g of the Zn with  $\text{TiO}_2$  3 g/L

Cycles	Zn deposited with different current densities			
	0.01 A/cm <sup>2</sup>	0.02 A/cm <sup>2</sup>	0.03 A/cm <sup>2</sup>	0.04 A/cm <sup>2</sup>
1 <sup>st</sup>	39.14286	18.47342	57.8773	32.85714
2 <sup>nd</sup>	79.71429	82.85714	110	109.28571
3 <sup>rd</sup>	81.71429	86.42857	113.57143	117.14286
4 <sup>th</sup>	84.71429	87.85714	112.85714	120
5 <sup>th</sup>	92.71429	88.57143	110.71429	121.42857

Figure 64 shows charge-discharge profile in 1<sup>st</sup> cycle of Zn with  $\text{TiO}_2$  1 g/L all current densities. The coin cells were tested at various current densities of 50, 100, 200, 500, and 1000 mA/g under the lower and upper cut-off voltage between 0.6-1.7V. The obtained results are shown in table 12.



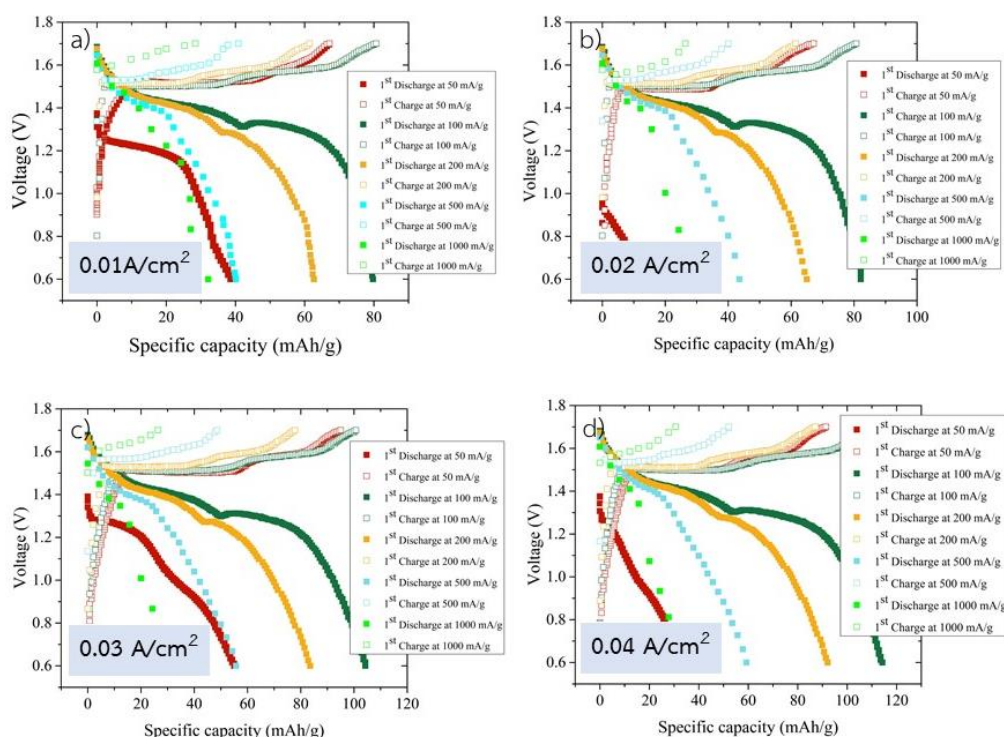


Figure 64 Charge-discharge profiles at various current densities of 50, 100, 200, 500, and 1000 mA/g of the Zn with  $\text{TiO}_2$  3 g/L at different current densities

Table 12 shows the discharge specific capacities of Zn with  $\text{TiO}_2$  3 g/L of all current densities, which were tested at various current densities of 50, 100, 200, 500, and 1000 mA/g, respectively. When increasing current density for testing, it was found that at 6<sup>th</sup>-25<sup>th</sup> cycles provided lower specific capacities than 1<sup>st</sup>-5<sup>th</sup> cycles due to that the  $\text{MnO}_2$  cathode had ZnO on the surface. Therefore, electrolyte could be reduced by being adsorbed into the  $\text{MnO}_2$  cathode. On the other hand, when comparing with this current density for depositing, it was found that the specific capacity increased slightly when the current density for electroplating increased but not very different due to that the morphology of the Zn crystal tended to form hexagonal platelets and transformed to a multilayer structure with small amount and non-uniform distribution  $\text{TiO}_2$  of nanoparticles on the Zn surface.

Table 12 The initial discharge specific capacity at various current densities of 50, 100, 200, 500, and 1000 mA/g of the Zn with TiO<sub>2</sub> 3 g/L

Cycles	Zn deposited with different current densities			
	0.01 A/cm <sup>2</sup>	0.02 A/cm <sup>2</sup>	0.03 A/cm <sup>2</sup>	0.04 A/cm <sup>2</sup>
1 <sup>st</sup> (50 mA/g)	39.14286	18.47342	57.8773	32.85714
6 <sup>th</sup> (100 mA/g)	81.42857	82.14286	104.28571	114.28571
11 <sup>th</sup> (200 mA/g)	62	65	83.57143	92.14286
16 <sup>th</sup> (500 mA/g)	40.71429	43.57143	55.71429	59.28571
21 <sup>st</sup> (1000 mA/g)	28.42857	28.57143	31.42857	34.28571

From the rate ability of the Zn with TiO<sub>2</sub> 3 g/L of all current densities (0.01-0.04 A/cm<sup>2</sup>) shows that increasing the current density for electroplating also increases slightly the specific capacity. This was due to that morphology of Zn electrode. At higher current density with higher wt% of Zn, which Zn<sup>+</sup> could insert into MnO<sub>2</sub> more than that of the lower current density. The Zn crystal has layer of zinc like flake structure and tended to form hexagonal platelets and the Zn deposits transform to a multilayer structure were small amount and non-uniform distribution TiO<sub>2</sub> nanoparticles on the Zn surface. Therefore, this could provide significant effect on the specific capacity. The columbic efficiencies of all samples are of 95-98% and operate with higher stability. The battery efficiency depends not only on the morphology of Zn deposits but also on the type used of electrolyte.



#### 4.4.4 The Zn with TiO<sub>2</sub> 5 g/L

Figures 65 a), b), c), and d) show the rate ability of the Zn with TiO<sub>2</sub> 5 g/L with current densities of 0.01, 0.02, 0.03, and 0.04 A/cm<sup>2</sup>, respectively, illustrating the rate ability of the battery from the 1<sup>st</sup> cycle to the 25<sup>th</sup> cycle. The figures also present charge & discharge specific capacity and columbic efficiency of all samples as shown in the figures. The columbic efficiencies of Zn with TiO<sub>2</sub> 5 g/L of all current densities are about 95-98% and operate with higher stability.

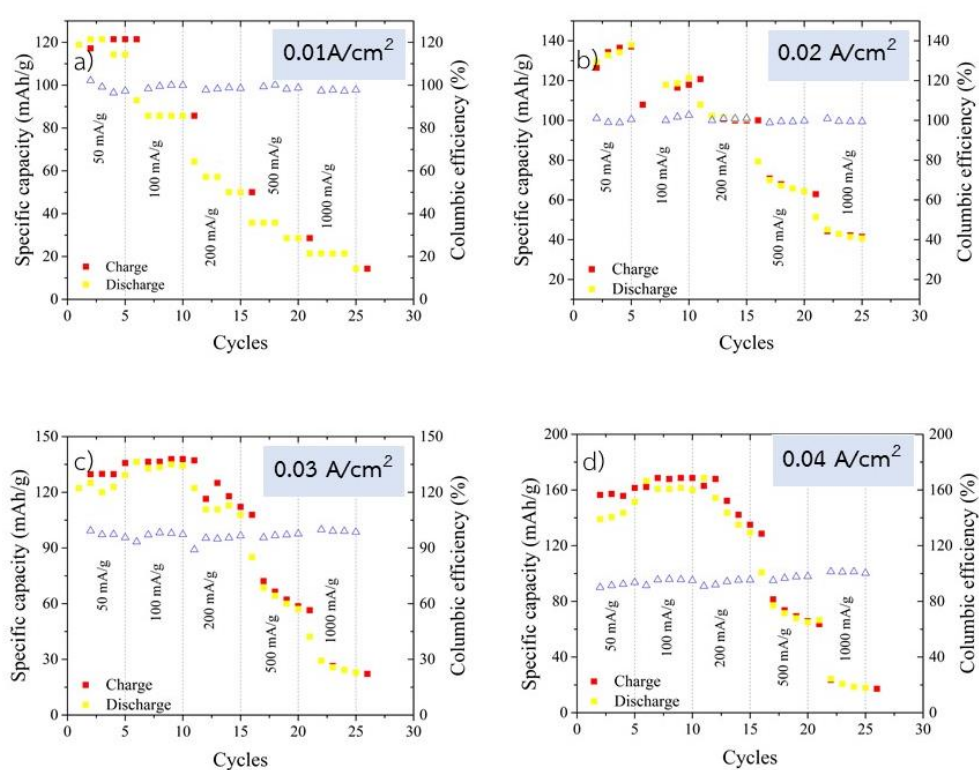


Figure 65 Rate ability of the Zn with TiO<sub>2</sub> 5 g/L at different current density

Figure 65 shows charge-discharge profile of Zn with TiO<sub>2</sub> 5 g/L with current densities of 0.01, 0.02, 0.03, and 0.04 A/cm<sup>2</sup>, respectively. The coin cells were tested at current density at 50mA/g in 1<sup>st</sup>-5<sup>th</sup> cycle under the lower and upper cut-off voltage between 0.6-1.7 V. The obtained results show open circuit voltage of freshly fabricated cells in table 13 and discharge specific capacity in table 14.

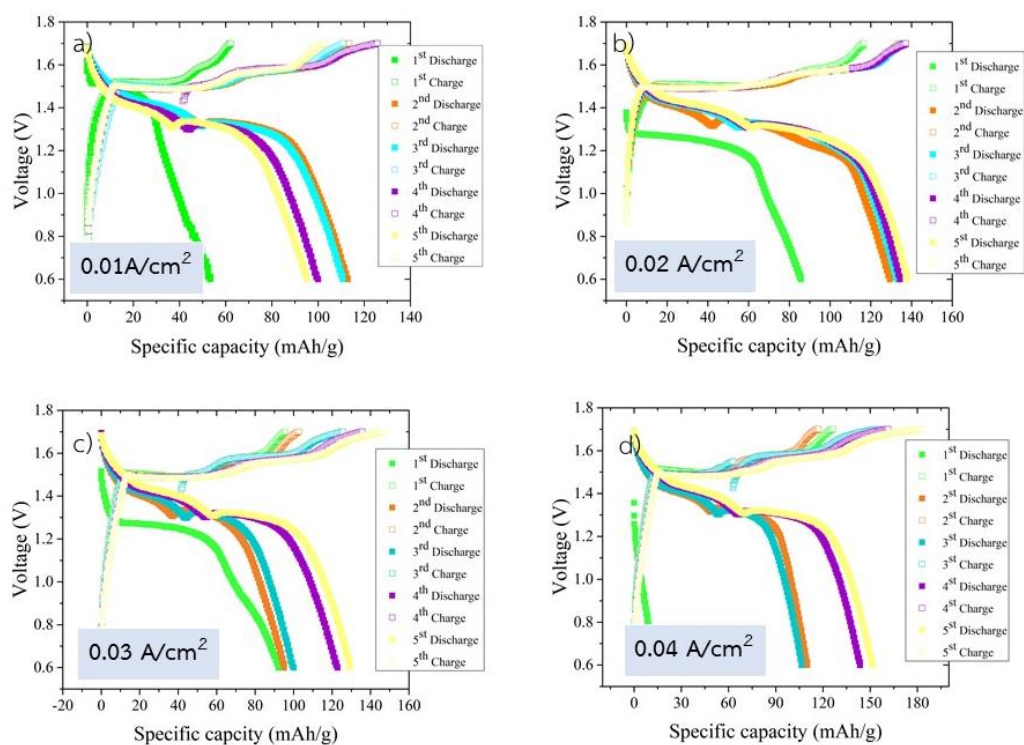


Figure 66 Charge-discharge profiles at 50 mA/g in 1<sup>st</sup>-5<sup>th</sup> cycles of the Zn with TiO<sub>2</sub> 5 g/L at different current densities

The battery provides an open-circuit voltage of the Zn with TiO<sub>2</sub> 5 g/L about 1.35-1.52 V as prepared. The voltage of coin cell will increase when the current density for electroplating increase but not very different as shown in table 13.

Table 13 Open circuit voltage of the Zn with TiO<sub>2</sub> 5 g/L

	Zn deposited with different current densities			
	0.01 A/cm <sup>2</sup>	0.02 A/cm <sup>2</sup>	0.03 A/cm <sup>2</sup>	0.04 A/cm <sup>2</sup>
Open circuit voltage	1.3904	1.3786	1.5154	1.3566

The discharge specific capacity of Zn with  $\text{TiO}_2$  5 g/L of all current densities were tested at current densities at 50mA/g in 1<sup>st</sup>-5<sup>th</sup> cycle, the result shows in table 14. The specific capacity increased slightly at 2<sup>nd</sup>-5<sup>th</sup> cycle due to electrolyte can be better adsorbed into the  $\text{MnO}_2$  cathode. When comparing results of different current densities, the specific capacity increased slightly when the current density for electroplating increased but not very different because the morphology was similar with the crystals are randomly size-distributed. The crystals shape layer and transform to a multilayer structure in Zn- $\text{TiO}_2$  composite coatings and has small amount and non-uniform distribution  $\text{TiO}_2$  nanoparticles on the Zn surface.

Table 14 The initial discharge specific capacity with current density at 50 mA/g of the Zn with  $\text{TiO}_2$  5 g/L

Cycles	Zn deposited with different current densities			
	0.01 A/cm <sup>2</sup>	0.02 A/cm <sup>2</sup>	0.03 A/cm <sup>2</sup>	0.04 A/cm <sup>2</sup>
1 <sup>st</sup>	53.85714	87.94221	92.14286	22.94328
2 <sup>nd</sup>	119.42857	129.28571	95	116
3 <sup>rd</sup>	118.94231	132.85714	101.85943	115.42857
4 <sup>th</sup>	101.28571	134.28571	122.85714	143.57143
5 <sup>th</sup>	98.83625	137.85714	129.28571	151.42857

Figure 67 shows charge-discharge profile in 1<sup>st</sup> cycle of Zn with  $\text{TiO}_2$  5 g/L all current densities. The coin cells were tested at various current densities of 50, 100, 200, 500, and 1000 mA/g under the lower and upper cut-off voltage between 0.6-1.7V. The obtained results are shown in table 15.

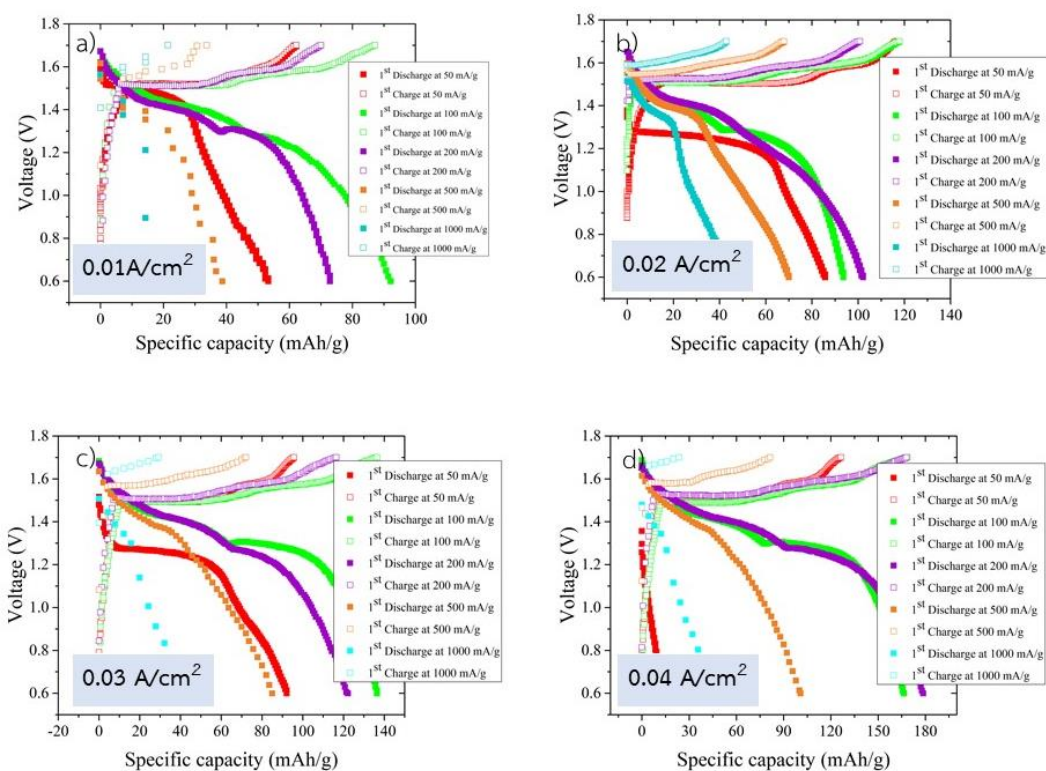


Figure 67 Charge-discharge profiles at various current densities of 50, 100, 200, 500, and 1000 mA/g of the Zn with  $\text{TiO}_2$  5 g/L at different current densities

Table 15 shows the discharge specific capacities of Zn with  $\text{TiO}_2$  5 g/L of all current densities, which were tested at various current densities of 50, 100, 200, 500, and 1000 mA/g, respectively. When increasing current density for testing, it was found that at 6<sup>th</sup>-25<sup>th</sup> cycles provided lower specific capacities than 1<sup>st</sup>- 5<sup>th</sup> cycles due to the  $\text{MnO}_2$  cathode had ZnO on the surface. Therefore, electrolyte could be reduced by being adsorbed into the  $\text{MnO}_2$  cathode. On the other hand, when comparing with this current density for depositing it was found that the specific capacity increased slightly when the current density for electroplating increased but not very different due to that the coating microstructure with randomly size-distribution crystals. The crystals shape layer and transformed to a multilayer structure in Zn- $\text{TiO}_2$  composite coatings and has small amount and non-uniform distribution  $\text{TiO}_2$  nanoparticles on the Zn surface.

Table 15 The initial discharge specific capacity at various current densities of 50, 100, 200, 500, and 1000 mA/g of the Zn with TiO<sub>2</sub> 5 g/L

Cycles	Zn deposited with different current densities			
	0.01 A/cm <sup>2</sup>	0.02 A/cm <sup>2</sup>	0.03 A/cm <sup>2</sup>	0.04 A/cm <sup>2</sup>
1 <sup>st</sup> (50 mA/g)	53.85714	87.94221	92.14286	22.94328
6 <sup>th</sup> (100 mA/g)	92.85714	108.94832	136.42857	166.42857
11 <sup>th</sup> (200 mA/g)	64.28571	102.14286	122.14286	168.57143
16 <sup>th</sup> (500 mA/g)	35.71429	70	85	100.71429
21 <sup>st</sup> (1000 mA/g)	21.42857	45	42.14286	66.42857

From the rate ability of the Zn with TiO<sub>2</sub> 5 g/L of all current densities (0.01-0.04 A/cm<sup>2</sup>) shows that increasing the current density for electroplating also increases slightly the specific capacity. This was due to the morphology of Zn electrode. At higher current density with higher wt% of Zn, which Zn<sup>+</sup> could insert into MnO<sub>2</sub> more than that of the lower current density. The coating layer were randomly size-distribution crystals. And transform to a multilayer structure in Zn-TiO<sub>2</sub> composite coatings and has small amount and non-uniform distribution TiO<sub>2</sub> nanoparticles on the Zn surface. Therefore, this could provide significant effect on the specific capacity. The columbic efficiencies of all samples are of 95-98% and operate with higher stability.

#### 4.4.5 The Zn with $\text{TiO}_2$ 10 g/L

Figures 68 a), b), c), and d) show the rate ability of the Zn with  $\text{TiO}_2$  10 g/L with current density of 0.01, 0.02, 0.03, and 0.04  $\text{A}/\text{cm}^2$ , respectively, illustrating the rate ability of the battery from the 1<sup>st</sup> cycle to the 25<sup>th</sup> cycle. The figures also present charge & discharge specific capacity and columbic efficiency of all samples as shown in the figures. The columbic efficiencies of Zn with  $\text{TiO}_2$  10 g/L of all current densities are about 95-98% and operate with higher stability.

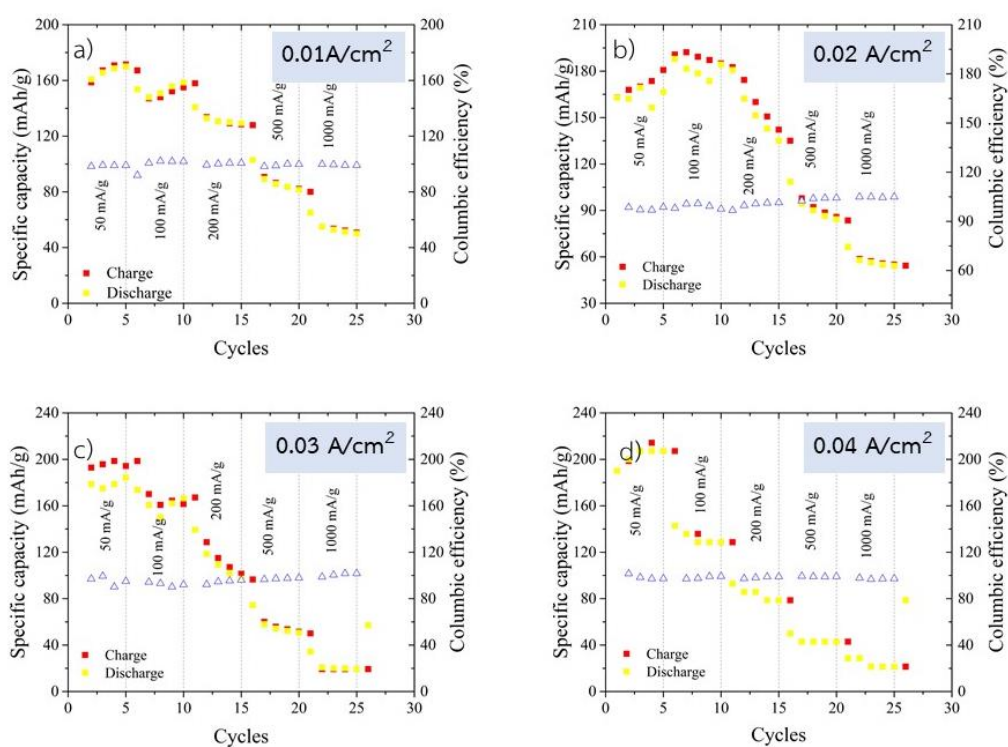


Figure 68 Rate ability of the Zn with  $\text{TiO}_2$  10 g/L at different current densities

Figure 69 shows charge-discharge profile of Zn with  $\text{TiO}_2$  10 g/L with current density of 0.01, 0.02, 0.03, and 0.04  $\text{A}/\text{cm}^2$ , respectively. The coin cells were tested at current density at 50mA/g in 1<sup>st</sup>-5<sup>th</sup> cycle under the lower and upper cut-off voltage between 0.6-1.7 V. The obtained results show open circuit voltage of freshly fabricated cells in table 16 and discharge specific capacity in table 17.



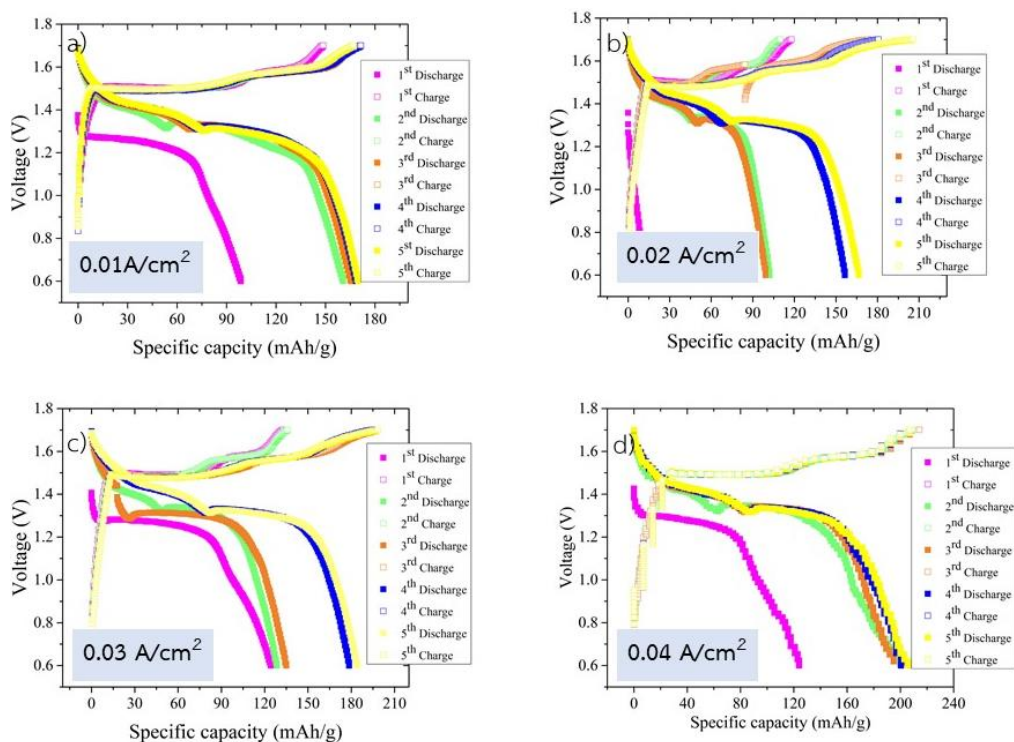


Figure 69 Charge-discharge profiles at 50 mA/g in 1<sup>st</sup>-5<sup>th</sup> cycles of the Zn with TiO<sub>2</sub> 10 g/L at different current densities

The battery provides an open-circuit voltage of the Zn with TiO<sub>2</sub> 10 g/L about 1.37-1.38 V as prepared. The voltage of coin cell will increase when the current density for electroplating increase but not very different as shown in table 16.

Table 16 Open circuit voltage of the Zn with TiO<sub>2</sub> 10 g/L

	Zn deposited with different current densities			
	0.01 A/cm <sup>2</sup>	0.02 A/cm <sup>2</sup>	0.03 A/cm <sup>2</sup>	0.04 A/cm <sup>2</sup>
Open circuit voltage	1.375	1.3573	1.4072	1.4267

The discharge specific capacities of Zn with  $\text{TiO}_2$  10 g/L of all current densities were tested at current densities at 50mA/g in 1<sup>st</sup>-5<sup>th</sup> cycle, the obtained results shown in table17. The specific capacity increased slightly at 2<sup>nd</sup>-5<sup>th</sup> cycle due to electrolyte can be better adsorbed into the  $\text{MnO}_2$  cathode. When comparing with different current densities, the specific capacity increased when the current density for electroplating increased due to that the coating microstructure with randomly size-distributed crystals. The crystals stacked together and transformed to a multilayer structure in Zn- $\text{TiO}_2$  composite coatings and samples all current densities exhibit uniform distribution  $\text{TiO}_2$  nanoparticles on the Zn surface.

Table 17 The initial discharge specific capacity with current density at 50 mA/g of the Zn with  $\text{TiO}_2$  10 g/L

Cycles	Zn deposited with different current densities			
	0.01 A/cm <sup>2</sup>	0.02 A/cm <sup>2</sup>	0.03 A/cm <sup>2</sup>	0.04 A/cm <sup>2</sup>
1 <sup>st</sup>	108.93842	16.85714	123.94827	126
2 <sup>nd</sup>	160.71429	99.14286	128.57143	200
3 <sup>rd</sup>	165.71429	103.28571	135	207.14286
4 <sup>th</sup>	168.57143	156.42857	178.57143	207.14286
5 <sup>th</sup>	170	166.42857	184.28571	207.14286

Figure 70 shows charge-discharge profile in 1<sup>st</sup> cycle of Zn with  $\text{TiO}_2$  10 g/L of all current densities. The coin cells were tested at various current densities of 50, 100, 200, 500, and 1000 mA/g under the lower and upper cut-off voltage between 0.6-1.7V. The obtain resulted are shown in table 18.



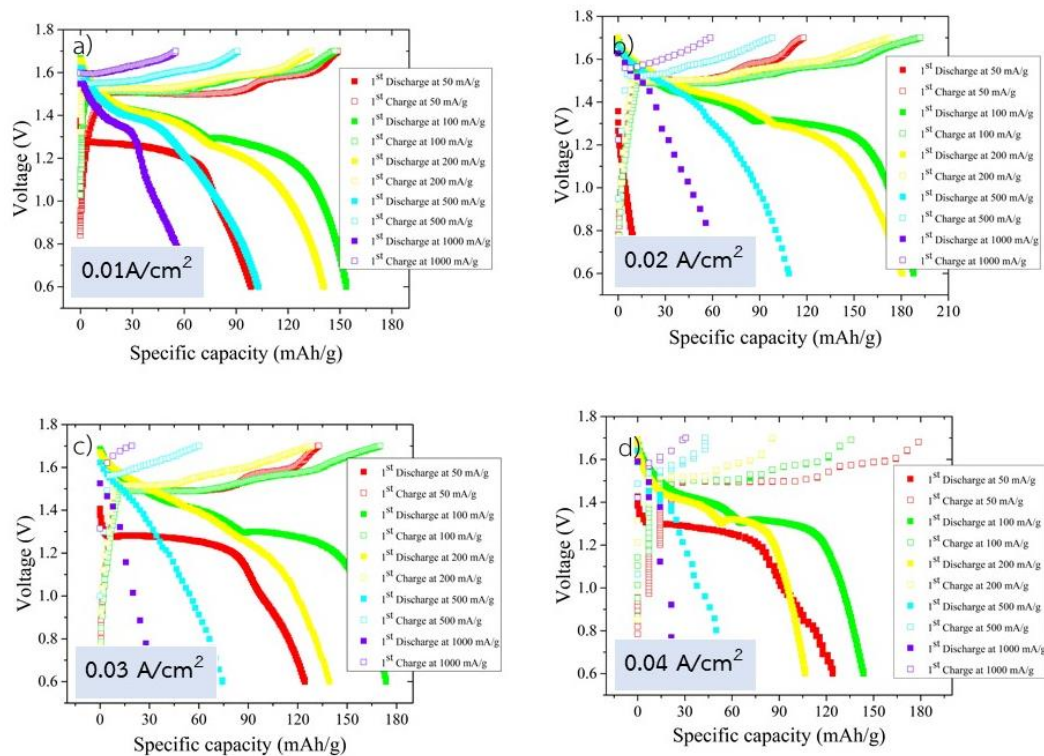


Figure 70 Charge-discharge profiles at various current densities of 50, 100, 200, 500, and 1000 mA/g of the Zn with  $\text{TiO}_2$  10 g/L at different current densities

Table 18 shows the discharge specific capacities of Zn with  $\text{TiO}_2$  10 g/L of all current densities. They were tested at various current densities of 50, 100, 200, 500, and 1000 mA/g, respectively. When increasing current density for testing, it was found that at 6<sup>th</sup>-25<sup>th</sup> cycles provided lower specific capacities than those of 1<sup>st</sup>- 5<sup>th</sup> cycles due to that the  $\text{MnO}_2$  cathode had ZnO on the surface. Therefore, electrolyte could be reduced by being adsorbed into the  $\text{MnO}_2$  cathode. On the other hand, when comparing with this current density for depositing it was found that the specific capacity increased slightly when the current density for electroplating increased but not very different due to the coating microstructure with randomly size-distribution crystals and crystals stacked and transformed to a multilayer structure in Zn- $\text{TiO}_2$  composite coating.

Table 18 The initial discharge specific capacity at various current densities of 50, 100, 200, 500, and 1000 mA/g of the Zn with TiO<sub>2</sub> 10 g/L

Cycles	Zn deposited with different current densities			
	0.01 A/cm <sup>2</sup>	0.02 A/cm <sup>2</sup>	0.03 A/cm <sup>2</sup>	0.04 A/cm <sup>2</sup>
1 <sup>st</sup> (50 mA/g)	108.93842	16.85714	123.94827	126
6 <sup>th</sup> (100 mA/g)	153.57143	187.85714	173.57143	142.85714
11 <sup>th</sup> (200 mA/g)	140.71429	180.71429	139.28571	117.85714
16 <sup>th</sup> (500 mA/g)	102.85714	108.57143	74.28571	57
21 <sup>st</sup> (1000 mA/g)	65	66.42857	34.28571	28.57143

From the rate ability of the Zn with TiO<sub>2</sub> 10 g/L of all current densities (0.01-0.04 A/cm<sup>2</sup>) shows that increasing the current density for electroplating also increases slightly the specific capacity. This was due to that morphology of Zn electrode. At higher current density with higher wt% of Zn, which Zn<sup>+</sup> could insert into MnO<sub>2</sub> more than that of the lower current density. The coating layer were randomly size-distribution crystals, stacked, and transformed to a multilayer structure in Zn-TiO<sub>2</sub> composite coatings and all samples exhibited uniform distribution TiO<sub>2</sub> nanoparticles on the Zn surface. Therefore, this could provide significant effect on the specific capacity. The columbic efficiencies of all samples are of 95-98% and operate with higher stability.

#### 4.5 Battery performance (cyclic ability)

The results of Zn plating and stripping of all samples at current density of  $0.02 \text{ A/cm}^2$  deposited via electroplating, show the stable properties. In this experiment, this current density was chosen to test the cyclic ability. The cycling tests of the battery were performed using a Zn ||  $\text{MnO}_2$  cell. In this cell, the prepared Zn electrode was used as the negative electrode whilst the prepared  $\text{MnO}_2$  was used as the positive. The test was conducted by discharging the battery until reaching the lower cutoff voltage of 0.6 V. Then charging was continued until reaching a higher cutoff voltage of 1.7 V. The cell was tested at constant current density of 200 mA/g for 500 cycles.

##### 4.5.1 The Zn without $\text{TiO}_2$

Figure 71 shows cyclic ability of the Zn without  $\text{TiO}_2$ , which was tested at current density of 200 mA/g. It illustrates the discharge specific capacity of this battery at about 80 mAh/g and could still be charged and be stable until 127<sup>th</sup> cycle. After 128<sup>th</sup> cycle, the discharge specific capacity is decreased and not stable until the end of the process due to the Zn electrode has some corrosion and dendrite formation on Zn surface.

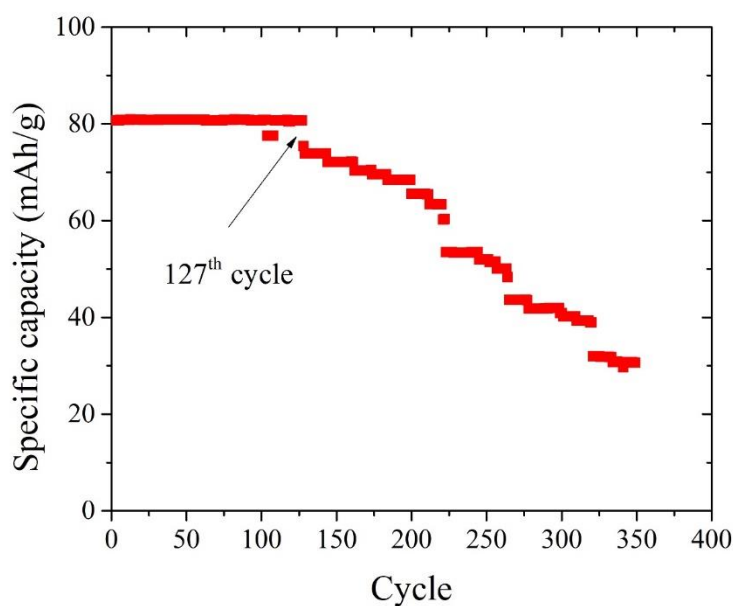


Figure 71 Cyclic ability of the Zn without  $\text{TiO}_2$

#### 4.5.2 The Zn with $\text{TiO}_2$ 1 g/L

Figure 72 shows cyclic ability of the Zn with  $\text{TiO}_2$  1 g/L, which was tested at current density of 200 mA/g. It illustrates the discharge specific capacity of this battery at about 87 mAh/g and could still be charged and be stable until 174<sup>th</sup> cycle. After 175<sup>th</sup> cycle, the discharge specific capacity is decreased and not stable until the end of the process due to that  $\text{TiO}_2$  nanoparticles on Zn electrode can reduce corrosion rate and dendrite formation on Zn surface. Therefore, it can be continued testing for longer time than that of the sample without  $\text{TiO}_2$ .

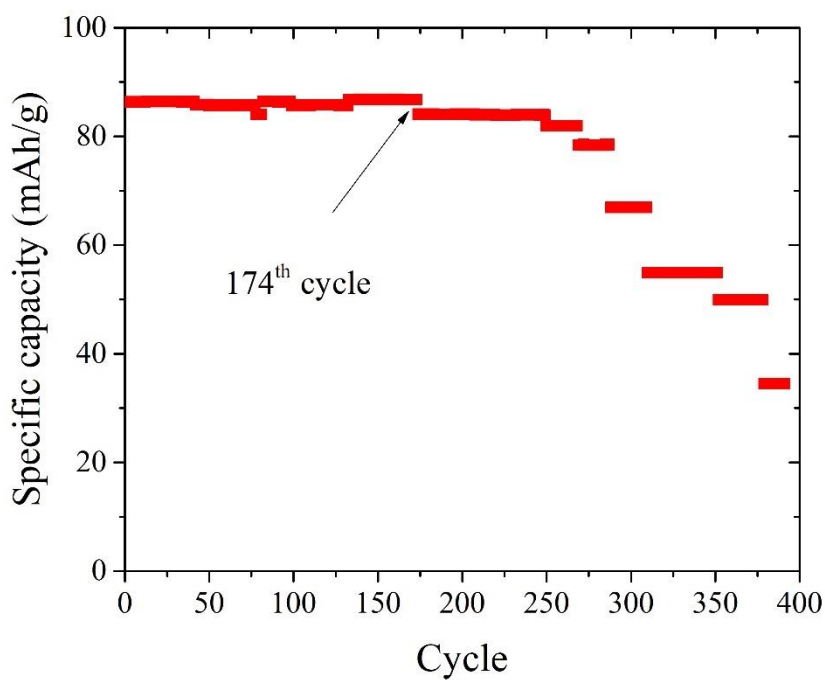


Figure 72 Cyclic ability of the Zn with  $\text{TiO}_2$  1 g/L

#### 4.5.3 The Zn with TiO<sub>2</sub> 3 g/L

Figure 73 shows cyclic ability of the Zn with TiO<sub>2</sub> 3 g/L, which was tested at current density of 200 mA/g. It illustrates the discharge specific capacity of this battery at about 94 mAh/g and could still be charged and be stable until 220<sup>th</sup> cycle. After 220<sup>th</sup> cycle, the discharge specific capacity is decreased and not stable until the end of the process. However, it has longer cycle life than that of the sample Zn with TiO<sub>2</sub> 1 g/L due to that Zn electrode has more TiO<sub>2</sub> nanoparticles which can reduce corrosion rate and dendrite formation on Zn surface. Therefore, it can be continued testing for longer time than that of the sample with TiO<sub>2</sub> 1 g/L.

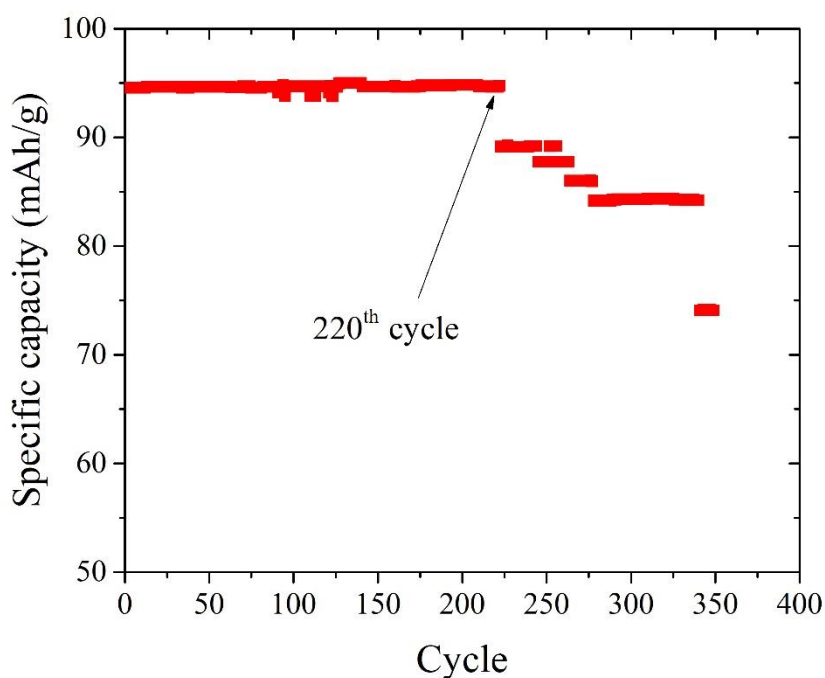


Figure 73 Cyclic ability of the Zn with TiO<sub>2</sub> 3 g/L

#### 4.5.4 The Zn with TiO<sub>2</sub> 5 g/L

Figure 74 shows cyclic ability of the Zn with TiO<sub>2</sub> 5 g/L, which was tested at current density of 200 mA/g. It illustrates the discharge specific capacity of this battery at about 148 mAh/g and could still be charged and be stable until 500<sup>th</sup> cycle until the end of the process due to Zn electrode has more TiO<sub>2</sub> nanoparticles which can reduce corrosion rate and dendrite formation on Zn surface. Therefore, it can be continued testing for longer time.

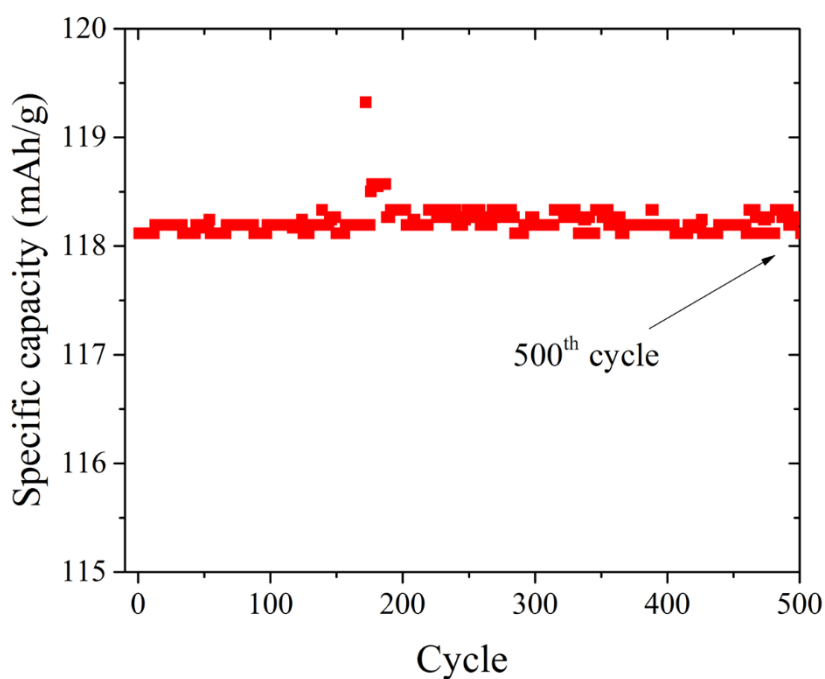


Figure 74 Cyclic ability of the Zn with TiO<sub>2</sub> 5 g/L

#### 4.5.5 The Zn with TiO<sub>2</sub> 10 g/L

Figure 75 shows cyclic ability of the Zn with TiO<sub>2</sub> 10 g/L, which was tested at current density of 200 mA/g. It illustrates the discharge specific capacity of this battery at about 148 mAh/g and could still be charged and be stable until 500<sup>th</sup> cycle until the end of the process due to Zn electrode has more TiO<sub>2</sub> nanoparticles which can reduce corrosion rate and dendrite formation on Zn surface. Therefore, it can be continued testing for longer time.

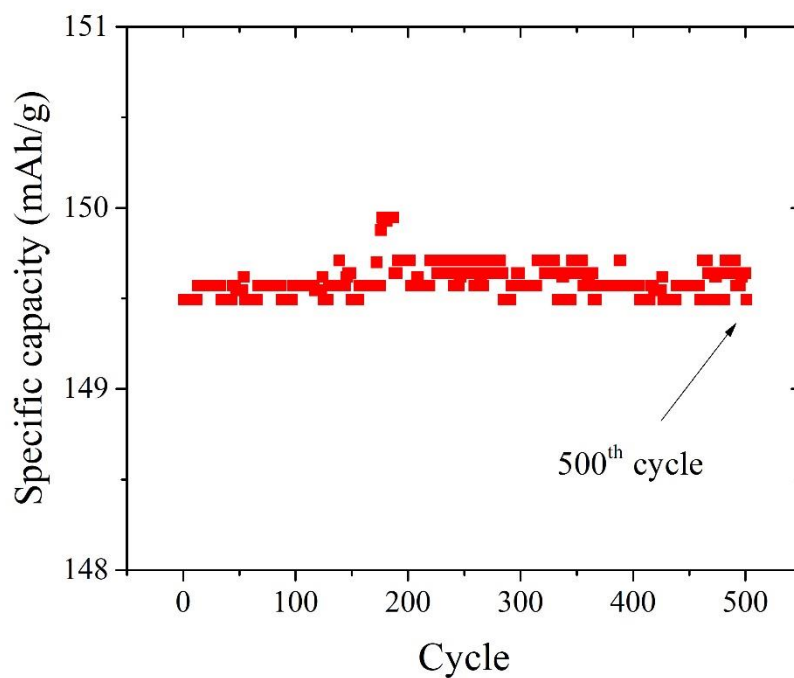


Figure 75 Cyclic ability of the Zn with TiO<sub>2</sub> 10 g/L

## 4.6 Microstructure Characterization after battery performance testing

### 4.6.1 Morphology and microstructure of Zn without $\text{TiO}_2$

The coin cells of Zn without  $\text{TiO}_2$  with all current densities were tested for battery performances at various current densities of 50, 100, 200, 500, and 1000 mA/g and long cycles. From the resulted, the specific capacity increased slightly when the current density for electroplating increased with no longer life cycles. They are not very different due to the current densities for depositing are similar. Therefore, after battery performance testing, it would be better to analysis morphology of Zn electrode again. The results exhibit shown non-uniform crystal of Zn layer and dendrite on the Zn surface as shown in figure 76. This might be due to that the shot circuit or corrosion could bring to shorter life cycle of this battery.

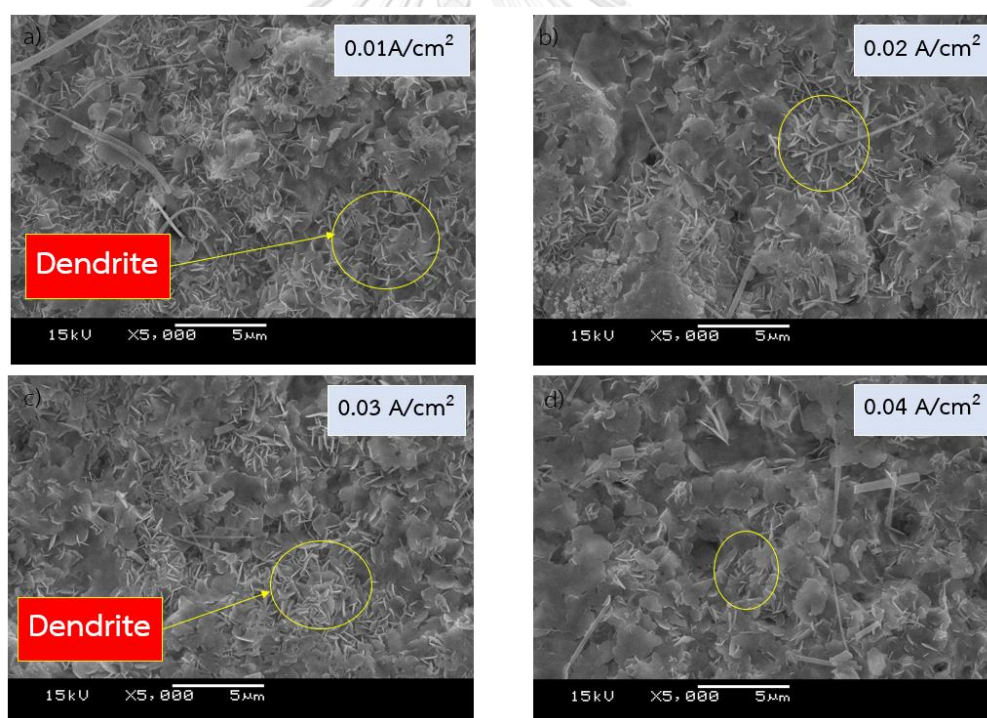


Figure 76 The Zn electrode sample of Zn without  $\text{TiO}_2$  after battery performance testing



#### 4.6.2 Morphology and microstructure of Zn with TiO<sub>2</sub> 10 g/L

The coin cells of Zn with TiO<sub>2</sub> 10 g/L with all current densities were tested for battery performances at various current densities of 50, 100, 200, 500, and 1000 mA/g and long cycles. From the resulted, the specific capacity increased slightly when the current density for electroplating increased with no longer life cycles. They are not very different due to the current densities for depositing are similar. Therefore, after battery performance testing, it would be better to analysis morphology of Zn electrode again. The results exhibit shown non-uniform crystal of Zn layer and small amount distribution TiO<sub>2</sub> nanoparticles on the Zn surface as shows in figure 77, This might be due to that increasing corrosion resistance on Zn electrode was increased, which could bring to the highest specific capacity and longest life cycle of this battery.

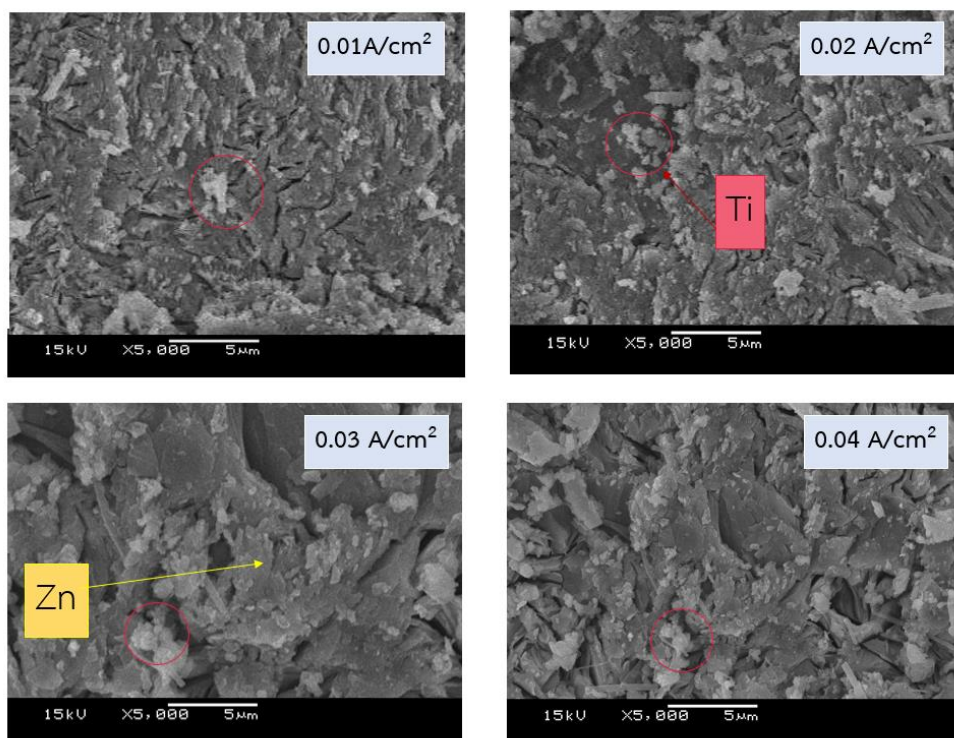


Figure 77 The Zn electrode sample of Zn with TiO<sub>2</sub> 10g/L after battery performance testing

## Chapter 5

### Conclusions

This research has objectives to prepare zinc with titanium dioxide (TiO<sub>2</sub>) particles coating on anode of zinc ion batteries via electrodeposition technique and to study the effect of electrodeposition parameters on the microstructure of zinc anode and battery performances. The research will focus on preparation parameters of zinc anode via electrodeposition by adding titanium dioxide nanoparticle (TiO<sub>2</sub>) in zinc electroplating solution. The effect of concentration of titanium dioxide (0, 1, 3, 5, and 10 g/L), the current density (0.01, 0.02, 0.03, and 0.04 A/cm<sup>2</sup>) and time (30 mins) were studied. The morphology and phase composition were analyzed by scanning electron microscope (SEM) and X-ray diffraction (XRD) respectively. The coin cell (CR2032) will be assembled for evaluating the electrochemical properties (CV and EIS) and battery performances (specific capacitance, and cyclic ability).

#### 5.1 Zn without TiO<sub>2</sub>

All samples show the coated microstructures with a non-uniform crystal distribution of Zn layer and the deposited particle size are smallest, as results shown in table19. The morphology had changed when the current density deposition was increased.

จุฬาลงกรณ์มหาวิทยาลัย  
CHULALONGKORN UNIVERSITY

*Table 19 Morphology of Zn without TiO<sub>2</sub>*

Current density	Morphology of Zn deposition	Grain size of Zn	wt% of Ti
0.01 A/cm <sup>2</sup>	non-uniform	2.18 μm	No
0.02 A/cm <sup>2</sup>	non-uniform	3.32 μm	No
0.03 A/cm <sup>2</sup>	non-uniform	3.36 μm	No
0.04 A/cm <sup>2</sup>	non-uniform	3.94 μm	No

From the battery performances of the Zn without TiO<sub>2</sub>, the results, are shown in tables 20-21 with all current densities (0.01-0.04 A/cm<sup>2</sup>), it was found that increasing the current density for electroplating can also increase slightly specific capacity due to that the morphology of Zn electrode at higher current density has higher wt% of Zn. Therefore, Zn<sup>+</sup> can insert into MnO<sub>2</sub> more than that of lower current density with non-uniform crystal of Zn layer, where current densities are not very different. Hence, this would not significantly affect to the specific capacity. The columbic efficiencies of all samples are about 90-98% and operate with higher stability. The battery efficiency depends not only on the morphology of Zn deposits but also on the type of electrolytes.

Table 20 The battery performances of the Zn without TiO<sub>2</sub> (1)

Current density	Polarization voltage	Open circuit voltage	Efficiency
0.01 A/cm <sup>2</sup>	-0.06 to +0.06 V	1.3725 V	90-98 %
0.02 A/cm <sup>2</sup>	-0.06 to +0.06 V	1.3818 V	
0.03 A/cm <sup>2</sup>	-0.06 to +0.06 V	1.3654 V	
0.04 A/cm <sup>2</sup>	-0.06 to +0.06 V	1.3741 V	

Table 21 The battery performances of the Zn without TiO<sub>2</sub> (2)

Current density	Specific capacity (mAh/g)					Cycle
	50mA/g	100 mA/g	200 mA/g	500 mA/g	1000 mA/g	
0.01 A/cm <sup>2</sup>	51	63.57143	57.14286	38.57143	26.42857	No
0.02 A/cm <sup>2</sup>	43.26	72.85714	60.71429	45.71429	29.28571	127
0.03 A/cm <sup>2</sup>	41.4	81.42857	59.28571	59.28571	42.85714	No
0.04 A/cm <sup>2</sup>	39.74	73.57143	66.42857	58.57143	60	No

In this condition, it could be summarized that the current density which is the most appropriate for deposition Zn without TiO<sub>2</sub> is at 0.04 A/cm<sup>2</sup> for providing the highest specific capacity with higher stability.

## 5.2 Zn with TiO<sub>2</sub> 1 g/L

At low current density of 0.01 A/cm<sup>2</sup>, samples show the coated microstructures with non-uniform crystal distribution. For higher current densities, (0.02-0.04 A/cm<sup>2</sup>) the morphology of Zn layer looks like flake-shape. The samples deposited with all current densities are found with less amount and non-uniform distribution of TiO<sub>2</sub> nanoparticles on the Zn surface, as the results shown in table 22.

Table 22 Morphology of Zn with TiO<sub>2</sub> 1 g/L

Current density	Morphology of Zn deposition	Grain size of Zn	wt% of Ti
0.01 A/cm <sup>2</sup>	non-uniform	3.2 μm	0.19
0.02 A/cm <sup>2</sup>	flakes	3.5 μm	0.22
0.03 A/cm <sup>2</sup>	flakes	4.4 μm	0.22
0.04 A/cm <sup>2</sup>	flakes	4.8 μm	0.3

From the battery performance of the Zn with TiO<sub>2</sub> 1 g/L, the results are shown in tables 23-24 with all current densities (0.01-0.04 A/cm<sup>2</sup>). It was found that increasing the current density for electroplating can also increase slightly specific capacity due to the morphology of Zn electrode with less TiO<sub>2</sub> nanoparticles on the Zn surface. Therefore, this provides insignificant affect to the specific capacity. The columbic efficiencies of all samples are about 93-98% and operate with higher stability.

Table 23 The battery performances of the Zn with TiO<sub>2</sub> 1 g/L (1)

Current density	Polarization voltage	Open circuit voltage	Efficiency
0.01 A/cm <sup>2</sup>	-0.05 to +0.05 V	1.0868 V	93-98 %
0.02 A/cm <sup>2</sup>	-0.05 to +0.05 V	1.3814 V	
0.03 A/cm <sup>2</sup>	-0.05 to +0.05 V	1.3799 V	
0.04 A/cm <sup>2</sup>	-0.06 to +0.06 V	1.3801 V	

Table 24 The battery performances of the Zn with TiO<sub>2</sub> 1 g/L (2)

Current density	Specific capacity (mAh/g)					Cycle
	50 mA/g	100 mA/g	200 mA/g	500 mA/g	1000 mA/g	
0.01 A/cm <sup>2</sup>	49.88432	78.57143	70.71429	45.71429	26.42857	No
0.02 A/cm <sup>2</sup>	54.14286	67.14286	53.57143	35.71429	22.85714	174
0.03 A/cm <sup>2</sup>	68.57143	72.85714	57.85714	36.42857	20.71429	No
0.04 A/cm <sup>2</sup>	63.45143	92.17914	84.17914	73.75057	33.03629	No

It could be summarized that the current density which is the most appropriate for deposition Zn with TiO<sub>2</sub> 1 g/L is at 0.04 A/cm<sup>2</sup> for providing the highest specific capacity with higher stability.

### 5.3 Zn with TiO<sub>2</sub> 3 g/L

At low current densities, (0.01-0.02 A/cm<sup>2</sup>), samples show the coated microstructures consisting the crystals with homogeneity and randomly size-distribution. The Zn crystals consists of layer as flake structure. Higher current densities (0.03-0.04 A/cm<sup>2</sup>) samples show the heterogeneous coated structures. Crystals tend to form hexagonal platelets. The samples of all current densities are with small amount and non-uniform distribution of TiO<sub>2</sub> nanoparticles on the Zn surface. The results are shown in table 25.

Table 25 Morphology of Zn with TiO<sub>2</sub> 3 g/L

Current density	Morphology of Zn deposition	Grain size of Zn	wt% of Ti
0.01 A/cm <sup>2</sup>	flakes	3.75 μm	0.41
0.02 A/cm <sup>2</sup>	flakes	5.12 μm	0.49
0.03 A/cm <sup>2</sup>	hexagonal platelets	8.54 μm	0.52
0.04 A/cm <sup>2</sup>	hexagonal platelets	10.2 μm	0.55

The results of the battery performances of the Zn with  $\text{TiO}_2$  3 g/L with all current densities (0.01-0.04  $\text{A}/\text{cm}^2$ ) are shown in tables 26-27. Increasing the current density for electroplating can also increase specific capacity due to that 1) morphology of Zn electrode at higher current density has higher wt% of Zn ( $\text{Zn}^+$  could insert into  $\text{MnO}_2$  more than lower current density). 2) The Zn crystal layer as flake structure tends to form hexagonal platelets and the Zn deposits transform to a multilayer structure with small amount and non-uniform distribution of  $\text{TiO}_2$  nanoparticles on the Zn surface. Therefore, they affect the specific capacity that is higher than Zn with  $\text{TiO}_2$  1 g/L.

Table 26 The battery performances of the Zn with  $\text{TiO}_2$  3 g/L (1)

Current density	Polarization voltage	Open circuit voltage	Efficiency
0.01 $\text{A}/\text{cm}^2$	-0.05 to +0.05 V	1.3811 V	95-99 %
0.02 $\text{A}/\text{cm}^2$	-0.04 to +0.04 V	1.1163 V	
0.03 $\text{A}/\text{cm}^2$	-0.04 to +0.04 V	1.3907 V	
0.04 $\text{A}/\text{cm}^2$	-0.05 to +0.05 V	1.3 V	

Table 27 The battery performances of the Zn with  $\text{TiO}_2$  3 g/L (2)

Current density	Specific capacity (mAh/g)					Cycle
	50 mA/g	100 mA/g	200 mA/g	500 mA/g	1000 mA/g	
0.01 $\text{A}/\text{cm}^2$	39.14286	81.42857	62	40.71429	28.42857	No
0.02 $\text{A}/\text{cm}^2$	18.47342	82.14286	65	43.57143	28.57143	220
0.03 $\text{A}/\text{cm}^2$	57.8773	104.28571	83.57143	55.71429	31.42857	No
0.04 $\text{A}/\text{cm}^2$	32.85714	114.28571	92.14286	59.28571	34.28571	No

In this condition, it could be summarized that the current density which is the most appropriate for deposition Zn with  $\text{TiO}_2$  3 g/L is at 0.04  $\text{A}/\text{cm}^2$  for providing the highest specific capacity with higher stability.

#### 5.4 Zn with TiO<sub>2</sub> 5 g/L

Samples with all current densities (0.01, 0.02, 0.03, and 0.04 A/cm<sup>2</sup>) show the coated microstructures with the randomly size-distributed crystals. The crystal layer transforms to a multilayer structure in Zn-TiO<sub>2</sub> composite. The samples with all current densities were in small amount and uniform distribution of TiO<sub>2</sub> nanoparticles on the Zn surface. The results are shown in table 28.

Table 28 Morphology of Zn with TiO<sub>2</sub> 5 g/L

Current density	Morphology of Zn deposition	Grain size of Zn	wt% of Ti
0.01 A/cm <sup>2</sup>	flakes	5.6 μm	0.8
0.02 A/cm <sup>2</sup>	flakes	5.8 μm	0.87
0.03 A/cm <sup>2</sup>	flakes	6.8 μm	0.88
0.04 A/cm <sup>2</sup>	flakes	7.1 μm	0.94

The results of the rate ability of the Zn with TiO<sub>2</sub> 5 g/L with all current densities (0.01-0.04 A/cm<sup>2</sup>) are shown in tables 29-30. Increasing the current density for electroplating can also increase specific capacity due to that 1) morphology of Zn electrode at higher current density has higher wt% of Zn (Zn<sup>+</sup> could insert into MnO<sub>2</sub> more than lower current density). 2) coated microstructures are randomly size-distributed crystals. The crystal layer transforms to a multilayer structure in Zn-TiO<sub>2</sub> composite coatings. They have amount and distribution of TiO<sub>2</sub> nanoparticles on the Zn surface more than those of Zn with TiO<sub>2</sub> 3 g/L. Therefore, in this condition, effect of higher concentration on the specific capacity is higher than those of Zn with TiO<sub>2</sub> 3 g/L. The columbic efficiencies of all samples are about 95-99% and operate with higher stability.

Table 29 The battery performances of the Zn with  $\text{TiO}_2$  5 g/L (1)

Current density	Polarization voltage	Open circuit voltage	Efficiency
0.01 A/cm <sup>2</sup>	-0.05 to +0.05 V	1.3904 V	95-99 %
0.02 A/cm <sup>2</sup>	-0.03 to +0.03 V	1.3786 V	
0.03 A/cm <sup>2</sup>	-0.03 to +0.03 V	1.5154 V	
0.04 A/cm <sup>2</sup>	-0.04 to +0.04 V	1.3566 V	

Table 30 The battery performances of the Zn with  $\text{TiO}_2$  5 g/L (2)

Current density	Specific capacity (mAh/g)					Cycle
	50 mA/g	100 mA/g	200 mA/g	500 mA/g	1000 mA/g	
0.01 A/cm <sup>2</sup>	53.85714	92.85714	64.28571	35.71429	21.42857	No
0.02 A/cm <sup>2</sup>	87.94221	108.94832	102.14286	70	45	500
0.03 A/cm <sup>2</sup>	92.14286	136.42857	122.14286	85	42.14286	No
0.04 A/cm <sup>2</sup>	22.94328	166.42857	168.57143	100.71429	66.42857	No

In this condition, it could be summarized that the current density which is the most appropriate for deposition Zn with  $\text{TiO}_2$  5 g/L is at 0.04 A/cm<sup>2</sup> for providing the highest specific capacity with higher stability.



### 5.5 Zn with TiO<sub>2</sub> 10 g/L

Samples with all current densities (0.01, 0.02, 0.03, and 0.04 A/cm<sup>2</sup>) show the coated microstructures with the randomly size-distributed crystals. The crystals layer transforms to a multilayer structure in Zn-TiO<sub>2</sub> composite coatings. Samples with all current densities exhibit uniform distribution of TiO<sub>2</sub> nanoparticles on the Zn surface. The results are shown in table 31.

*Table 31 Morphology of Zn with TiO<sub>2</sub> 10 g/L*

Current density	Morphology of Zn deposition	Grain size of Zn	wt% of Ti
0.01 A/cm <sup>2</sup>	stacked	5.4	2.24
0.02 A/cm <sup>2</sup>	stacked	6.8	2.47
0.03 A/cm <sup>2</sup>	stacked	7.9	2.61
0.04 A/cm <sup>2</sup>	stacked	8.3	2.83

The results of the rate ability of the Zn with TiO<sub>2</sub> 10 g/L with all current densities (0.01-0.04 A/cm<sup>2</sup>) are shown in tables 32-33. Increasing the current density for electroplating also increased specific capacity due to that 1) morphology of Zn electrode at higher current density has higher wt% of Zn (Zn<sup>+</sup> can insert into MnO<sub>2</sub> more than that of lower current density). 2) coated microstructures are randomly size-distributed crystals. The crystals stack and transform to a multilayer structure in Zn-TiO<sub>2</sub> composite coatings. Samples with all current densities exhibit uniform distribution of TiO<sub>2</sub> nanoparticles on the Zn surface. Therefore, they could affect to the specific capacity higher than those of Zn with TiO<sub>2</sub> 5 g/L.

Table 32 The battery performances of the Zn with TiO<sub>2</sub> 10 g/L (1)

Current density	Polarization voltage	Open circuit voltage	Efficiency
0.01 A/cm <sup>2</sup>	-0.03 to +0.03 V	1.375 V	95-99 %
0.02 A/cm <sup>2</sup>	-0.03 to +0.03 V	1.3573 V	
0.03 A/cm <sup>2</sup>	-0.03 to +0.03 V	1.4072 V	
0.04 A/cm <sup>2</sup>	-0.04 to +0.04 V	1.4267 V	

Table 33 The battery performances of the Zn with TiO<sub>2</sub> 10 g/L (2)

Current density	Specific capacity (mAh/g)					Cycle
	50 mA/g	100 mA/g	200 mA/g	500 mA/g	1000 mA/g	
0.01 A/cm <sup>2</sup>	108.93842	153.57143	140.71429	102.85714	65	No
0.02 A/cm <sup>2</sup>	16.85714	187.85714	180.71429	108.57143	66.42857	500
0.03 A/cm <sup>2</sup>	123.94827	173.57143	139.28571	74.28571	34.28571	No
0.04 A/cm <sup>2</sup>	126	142.85714	117.85714	57	28.57143	No

In this condition, it could be summarized that the current density, which is the most appropriate for deposition Zn with TiO<sub>2</sub> 10 g/L is at 0.04 A/cm<sup>2</sup> for providing the highest specific capacity with higher stability.

Finally, it could be concluded that increasing both concentration of TiO<sub>2</sub> in electrolyte and current density for electroplating can strongly influence to the morphology of composite deposits of zinc electrode. This required morphology can provide higher performance and lifetime of battery. The Zn electrodes prepared under the condition were tested and found to have columbic efficiencies in the range of 95-99% and operate with higher stability. For further development of Zn ion battery to have higher specific capacity, cyclability and stability, the batteries should be made from inexpensive, readily available and environmentally friendly materials.

## REFERENCES

1. Guo, J., et al., *Zinc-ion batteries: Materials, mechanisms, and applications*. Materials Science and Engineering R Reports, 2018. **135**: p. 58-84.
2. Ming, J., et al., *Zinc-ion batteries: Materials, mechanisms, and applications*. Materials Science and Engineering: R: Reports, 2019. **135**: p. 58-84.
3. Fang, G., et al., *Recent Advances in Aqueous Zinc-Ion Batteries*. ACS Energy Letters, 2018. **3**(10): p. 2480-2501.
4. Pistoia, G., *Battery Categories and Types*. 2009. p. 17-73.
5. Nitta, N., et al., *Li-ion battery materials: present and future*. Materials Today, 2015. **18**(5): p. 252-264.
6. Song, M., et al., *Recent Advances in Zn-Ion Batteries*. 2018. **28**(41): p. 1802564.
7. Verma, V., et al., *Progress in Rechargeable Aqueous Zinc- and Aluminum-Ion Battery Electrodes: Challenges and Outlook*. 2019. **3**(1): p. 1800111.
8. Sun, K.E.K., et al., *Suppression of Dendrite Formation and Corrosion on Zinc Anode of Secondary Aqueous Batteries*. ACS Applied Materials & Interfaces, 2017. **9**(11): p. 9681-9687.
9. Lee, S.-M., et al., *Improvement in self-discharge of Zn anode by applying surface modification for Zn-air batteries with high energy density*. Journal of Power Sources, 2013. **227**: p. 177-184.
10. Praveen, B.M. and T.V. Venkatesha, *Electrodeposition and properties of Zn-nanosized TiO<sub>2</sub> composite coatings*. Applied Surface Science, 2008. **254**(8): p. 2418-2424.
11. Kordesch, K., *Electrochemical Energy Storage*, in *Comprehensive Treatise of Electrochemistry: Volume 3: Electrochemical Energy Conversion and Storage*, J.O.M. Bockris, et al., Editors. 1981, Springer US: Boston, MA. p. 123-190.
12. Viswanathan, B., *Chapter 12 - Batteries*, in *Energy Sources*, B. Viswanathan, Editor. 2017, Elsevier: Amsterdam. p. 263-313.
13. Xu, C., et al., *Secondary batteries with multivalent ions for energy storage*. Scientific Reports, 2015. **5**: p. 14120.

14. Hoang, T.K.A., et al., *Corrosion chemistry and protection of zinc & zinc alloys by polymer-containing materials for potential use in rechargeable aqueous batteries*. RSC Advances, 2015. **5**(52): p. 41677-41691.
15. Higashi, S., et al., *Avoiding short circuits from zinc metal dendrites in anode by backside-plating configuration*. Nature Communications, 2016. **7**: p. 11801.
16. Shoji, T., M. Hishinuma, and T.J.J.o.A.E. Yamamoto, *Zinc-manganese dioxide galvanic cell using zinc sulphate as electrolyte. Rechargeability of the cell*. 1988. **18**(4): p. 521-526.
17. Xu, C., et al., *Energetic Zinc Ion Chemistry: The Rechargeable Zinc Ion Battery*. 2012. **51**(4): p. 933-935.
18. Zhang, N., et al., *Cation-Deficient Spinel ZnMn<sub>2</sub>O<sub>4</sub> Cathode in Zn(CF<sub>3</sub>SO<sub>3</sub>)<sub>2</sub> Electrolyte for Rechargeable Aqueous Zn-Ion Battery*. Journal of the American Chemical Society, 2016. **138**(39): p. 12894-12901.
19. Han, S.-D., et al., *Mechanism of Zn Insertion into Nanostructured  $\delta$ -MnO<sub>2</sub>: A Nonaqueous Rechargeable Zn Metal Battery*. Chemistry of Materials, 2017. **29**(11): p. 4874-4884.
20. Hu, P., et al., *Zn/V<sub>2</sub>O<sub>5</sub> Aqueous Hybrid-Ion Battery with High Voltage Platform and Long Cycle Life*. ACS Applied Materials & Interfaces, 2017. **9**(49): p. 42717-42722.
21. Liu, Z., G. Pulletikurthi, and F. Endres, *A Prussian Blue/Zinc Secondary Battery with a Bio-Ionic Liquid–Water Mixture as Electrolyte*. ACS Applied Materials & Interfaces, 2016. **8**(19): p. 12158-12164.
22. Chae, M.S., et al., *Electrochemical Zinc-Ion Intercalation Properties and Crystal Structures of ZnMo<sub>6</sub>S<sub>8</sub> and Zn<sub>2</sub>Mo<sub>6</sub>S<sub>8</sub> Chevrel Phases in Aqueous Electrolytes*. Inorganic Chemistry, 2016. **55**(7): p. 3294-3301.
23. Munteniță, C., et al., *Functional surfaces modified with gelatin and TiO<sub>2</sub> nanoparticles*. Vol. 55. 2018. 258-262.
24. Sun, K.E.K., *Synthesis of Novel Zinc Anode via Electroplating for Rechargeable Hybrid Aqueous Batteries*. 2016, UWSpace.
25. Ullah, D.S., et al., *Electrodeposited Zinc Electrodes for High Current Zn/AgO*

- Bipolar Batteries*. Vol. 6. 2011.
26. Alias, N. and A.A. Mohamad, *Morphology study of electrodeposited zinc from zinc sulfate solutions as anode for zinc-air and zinc-carbon batteries*. Journal of King Saud University - Engineering Sciences, 2015. **27**(1): p. 43-48.
27. Deguchi, T., et al., *Rapid electroplating of photocatalytically highly active TiO<sub>2</sub>Zn nanocomposite films on steel*. Vol. 36. 2001. 4723-4729.
28. Fustes, J., A. Gomes, and M.I. Pereira, *Electrodeposition of Zn-TiO<sub>2</sub> nanocomposite films—effect of bath composition*. Vol. 12. 2008. 1435-1443.
29. Benea, L. and E. Dănilă, *Development of Electrodeposited Zn/nano-TiO<sub>2</sub> Composite Coatings with Enhanced Corrosion Performance*. IOP Conference Series: Materials Science and Engineering, 2017. **209**: p. 012014.



## VITA

**NAME** Kittima Lolupiman

**DATE OF BIRTH** 26 October 1992

**PLACE OF BIRTH** Nakhonpathom

**INSTITUTIONS ATTENDED** Bachelor of Science and Technology in Materials Science  
at Thammasat University in 2016

**HOME ADDRESS** 415/1 M.3 T.donyaihom A.muang Nakhonpathom 73000

